Implementation of the novel high-throughput Fungal Isolation one step Device method FIND and secondary metabolite extraction from the isolate *Heydenia* cf. *alpina*

Dissertation
zur
Erlangung des Doktorgrades (Dr. rer. nat.)
der
Mathematisch-Naturwissenschaftlichen Fakultät
der
Rheinischen Friedrich-Wilhelms-Universität Bonn

vorgelegt von
Benjamin Libor
aus
Bottrop

Bonn 2020

Angefertigt mit Genehmigung der Mathematisch-Naturwissenschaftlichen Fakultät der
Rheinischen Friedrich-Wilhelms-Universität Bonn

1. Gutachterin : Prof. Dr. Gabriele M. König
2. Gutachter : Prof. Dr. Till F. Schäberle

Tag der Promotion: 04.05.2021
Erscheinungsjahr: 2021

Vorveröffentlichungen der Dissertation/In Advance Publications of the Dissertation

Teilergebnisse aus dieser Arbeit wurden mit Genehmigung der Mathematisch-Naturwissenschaftlichen Fakultät, vertreten durch die Mentorin/Betreuerin der Arbeit, in folgenden Beiträgen vorab veröffentlicht:

Parts of this study have been published in advance by permission of the Mathematisch-Naturwissenschaftlichen Fakultät, represented by the supervisor of this study:

Publikationen/Research Papers

Libor B., Harms H., Kehraus S., Eguereva E., König G. M., Isolation of fungi using the diffusion chamber device FIND. *Beilstein J. Org. Chem.* 2019, *15,* 2191-2203. doi:10.3762/bjoc.15.216

Tagungsbeiträge/Research Presentations

Libor B., Harms H., Eguereva E., König G. M., Isolation studies on marine derived fungi using the diffusion chamber device. Short talk presented at the 2nd International Conference of Marine Fungal Natural Products (MaFNaP), June 27th–29th, 2017, Kiel, Germany.

Libor B., Harms H., Kehraus S., Eguereva E., König G. M., Isolation of marine-derived fungi using the diffusion chamber device FIND. Poster talk presented at the XVI International Symposium on Marine Natural Products and XV European Congress on Marine Natural Products joint meeting (MaNaPro & ECMNP), September 1st–5th, 2019, Peniche, Portugal.

Acknowledgments

A particular debt of gratitude is owed to my supervisor Prof. Dr. Gabriele M. König, who offered me the opportunity to work on an exciting and satisfying project, independently, but always guided by her experience and encouraged by her curiosity. I am especially thankful for the right words at the right time, for always being there for everyone and never giving up on anyone.

I want to thank Prof. Dr. Till Schäberle for officiating as second referee.

I also thank Prof. Dr. Gerd Bendas and Prof. Dr. Heike Wägele for participating in the examination committee.

I thank:

Dr. S. Kehraus for his indispensable analytical knowledge, proofreading parts of this dissertation and sharing educational thoughts on life.

Dr. Max Crüsemann for the collection and analysis of HR-LC-MS and Tandem-MS data, as well as the introduction to GNPS based molecular networking.

Dr. Raphael Reher for introduction to the SMART 2.0 system and his patient support. I thank him for his caring and inspirational attitude and for all the good times.

Dr. Alexander Bogdanov for sharing his experience in GNPS molecular networking, Haute Cuisine and community pharmacy.

Ekaterina Egereva for recording LC-MS spectra, performing disk diffusion assays and all fungi-related work from cultivation to extraction.

Dr. Peter Hufendiek for introducing me into fungal natural product research.

Dr. Henrik Harms for diffusion chamber-related works, e.g., development, sampling and execution of experiments.

Paul Barac for taking me under his wing on my very first days at the department showing me the tricks of fungal natural product chemistry, sharing fungal isolates and working on projects together.

Tobias Benkel for the performance of the cell viability and DMR assays and especially for his coassistance in the course ´Pharmaceutical Biology III´.

Fayrouz El-Maddah for her feedback on questions regarding fungi, sharing the office, providing me with fruit salad, invitations with violin lessons for her son and more fruit salad.

Ralf Schröder for all the administrative questions.

Dr. Christel Drewke for her great management of the course ´Pharmaceutical Biology III´ and the unforgettable time in the assistant office.

Cora Hertzer for being my PhD twin sister, working through our time at the institute together, and for introducing me to climbing and surfing.

Cornelia Hermes for performing the DM at our weekly DSA meetings and for participating at our MTG sessions.

Dr. René Richarz for being on the same wavelength, hilarious comments and deep lunch conversations.

Julian Zeiner for being the best apprentice for the position of an assistant in the course ´Pharmaceutical Biology III´ and a worthy successor.

Thomas Kögler for all the IT-based questions and the prompt solutions.

Nils Böhringer, Wiebke Hanke, Daniel Wirtz, Guadalupe Soto Zarazúa, Anna Krome and Emilia Goralski for a wonderful atmosphere at the department.

Special thanks go to my beloved friends, too many to be mentioned separately, but truly supporting, compassiante and sympathetic.

My warm thanks go to my family who were always excited about any progress, understanding in stressful periods and always supporting in any circumstances. They forged me into the persona I am today: curios, ambitious, caring - characteristics I adopted from them, which was the greatest gift.

I thank my wife Nina for the infinite joy she is providing me with, the unforgettable time we are spending together and her ability to ignite the fire in me to achieve my goals.

Abbreviations

°C	degrees Celsius
1D	one dimensional
2D	two dimensional
$[\alpha]_D^T$	specific rotator power, sodium D-line (589 nm); T: temperature
α	optical rotation
δ	NMR chemical shifts [ppm]
λ	wavelength [nm]
ε	molar absorption coefficient
µ	micro (10^{-6})
µg	10^{-6} gram
µl	10^{-6} litre
µM	10^{-6} molar, micromolar (=10^{-6} mol L^{-1})
ν	wave number [cm^{-1}]
Ac	acetone
AHBA	3-amino-5-hydroxybenzoic acid
AIDS	acquired immune deficiency syndrome
ASW	artificial seawater
BMS	biomalt salt
BGC	Biosynthetic gene cluster
br	broad (in connection with NMR data)
c	concentration
C_{18}	C-18 modified silica gel
Ca^{+2}	calcium ion
$CaCl_2$	calcium chloride
calcd	calculated
cDNA	complementary deoxyribonucleic acid
cf.	confer [lat.], compared to
CO_2	carbon dioxide
CoA	coenzyme A
conc.	concentration
COSY	correlated spectroscopy
cm	10^{-2} metre
d	doublet (in connection with NMR data)
dd	doublet of doublet (in connection with NMR data)
Da	Dalton
DAD	diode array detector
DCM	dichloromethane
DEPT	distortionless enhancement by polarization transfer
DKP	diketopiperazine
dm	10^{-1} metre
DMAPP	dimethylallyl diphosphate
DMR	dynamic mass redistribution
DMSO	dimethylsulfoxide
EA	ethylacetate
e.g.	exempli gratia [lat.] or example given (for example)
EI	electron ionization
ESI	electron spray ionization
et al.	et alli [lat.]; and others

EtOAc	ethylacetate
EtOH	ethanol
FDA	food and drug administration
Fr	fraction
g	gram
GI	growth inhibition
GPCR	G protein-coupled receptor
GPP	geranyl diphosphate
h	hour
H_3BO_4	boric acid
HCl	hydrochloric acid
HEK	human embryonic kidney
HMBC	heteronuclear multiple-bond correlation
HMG-CoA	3-hydoxy-3-methylglutaryl-CoA
HPLC	high performance liquid chromatography
HR	high resolution
HSQC	heteronuclear single quantum correlation
H_2O	water
i.e.	id est [lat.]; that is
IL-2	interleukin 2
IPP	Isopentenyl diphosphate
IR	infrared
J	spin-spin coupling constant [Hz]
KBr	potassium bromide
KCl	potassium chloride
l	cell length
L	liter
LC	liquid chromatography
m	metre
m	multiplet (in connection with NMR)
m/z	mass-to-charge ratio (in connection with mass spectrometry)
Me	methyl
MeOH	methanol
mg	10^{-3} gram
$MgCl_2$	magnesium chloride
MHz	megahertz
min	minute
mL	10^{-3} litres
mm	10^{-3} metres
mM	10^{-3} molar, millimolar ($=10^{-3}$ mol L^{-1})
MRSA	methicillin resistant *Staphylococcus aureus*
MS	mass spectrometry
MVA	mevalonic acid
N	normality
NaCl	sodium chloride
$NaHCO_3$	sodium bicarbonate
Na_2SO_4	sodium sulfate
n.d.	not detectable
NFAT	nuclear factor of activated T-cells

ng	10^{-9} gram
NH_4Ac	ammonium acetate
nm	10^{-9} metre
N-Me	N-methyl
NMR	nuclear magnetic resonance spectroscopy
no	number
NOE	nuclear Overhauser effect
NOESY	nuclear Overhauser effect spectroscopy
NP	normal phase (in connection to chromatography)
NRPS	non-ribosomal peptide synthase
NSCLC	non-small cell lung cancer
OSMAC	one strain many compounds
p-	para
PBP	penicillin binding protein
PDA	photodiode array
PE	petroleum ether
PEP	phosphoenolpyruvate
PGPR	plant growth promoting rhizobacteria
pH	potentia hydrogenii
PKS	polyketide synthase
ppm	part per million
PPP	pentose phosphate pathway
PTX	pertussis toxin
qC	quaternary carbon
ROESY	rotating frame Overhauser effect spectroscopy
RP	reversed phase (in connection with chromatography)
rpm	revolutions per minute
RT	room temperature
s	singlet (in connection with NMR data)
SAR	structure activity relationship
sec	second
Si	silica gel
sp.	species
spp.	species (plural)
$SrCl_2$	strontium chloride
t	triplet (in connection with NMR data)
t_R	retention time
TE	thioestrase
TLC	thin layer chromatography
U-	uniformely
USD	United States dollar
UV	ultraviolet
VIS	visible
VLC	vacuum liquid chromatography
v/v	volume for volume
WG	working group
w/v	mass for volume

Table of content

1 Introduction 1

1.1 The role of fungal natural products in therapy 1

1.2 Methods for the isolation of fungi 1

1.2.1 Standard isolation methods 3

1.3 Fungal specialised metabolites 17

1.3.1 Fungal polyketides 17

1.3.2 Fungal terpenoids 19

1.3.3 Fungal peptides 21

1.3.4 Fungal metabolites of mixed biosynthetic origin 23

1.4 Terpenoids with bergamotene skeleton structure and their bioactivities 25

2 Scope of the present study 32

Course of study 33

3 Materials and Methods (General procedures) 34

3.1 FIND 34

3.1.1 Device specifications 34

3.1.2 Find procedure 34

3.2 Cultivation and extraction 37

3.2.1 Culture media 37

3.2.2 Pre-cultures 40

3.2.3 Main culture 40

3.2.4 Extraction 41

3.2.5 Taxonomic identification of strains 41

3.2.6 Salt dependency experiments 41

3.3 Chromatography 43

3.3.1 Thin Layer Chromatoraphy (TLC) 43

3.3.2 Vacuum Liquid Chromatography (VLC) 43

3.3.3 High-Performance Liquid Chromatography (HPLC) 43

3.4 Structure elucidation 44

3.4.1 NMR spectroscopy 44

3.4.2 Mass Spectrometry (MS) 45

3.4.3 Optical rotation 45

3.4.4 UV measurements 46

3.4.5 IR spectroscopy 47

3.4.6 CD spectroscopy 47

3.5 Bioinformatic tools 47

3.5.1 Molecular networking 47

3.5.2 SMART 48

3.6 Biological testing 48

3.6.1 Agar diffusion assay 48

3.6.2 Disk diffusion assay 50

3.6.3 Label-free dynamic mass redistribution (DMR) assay for HEK293 cell lines 51

3.6.4 Cell viability 52

3.7 Chemicals and other materials 53

3.7.1 Chemicals 53

3.7.2 Cell culture 54

4 Results 56

4.1 FIND procedure 56

4.2 Isolation of terrestrial and marine-derived fungi via FIND 57

4.3 Salinity dependency studies on C. allicinum and H. cf. alpina 65

4.4 OSMAC approach for the culturing of Emericellopsis cf. minima 67

4.5 Growth quality and psychrotolerance, OSMAC approach and bioinformatic analysis of Heydenia cf. alpina 69

4.5.1 Determination of growth quality under OSMAC conditions and psychrotolerance 72

4.5.2 Bioactivity of extracts from different media 74

4.5.3 Visualisation and dereplication of natural products from extracts using bioinformatic tools – example *Heydenia* cf. *alpina* 76

4.5.4 Evaluation of the OSMAC approach on extracts of *H.* cf. *alpina* 94

4.6 Structure elucidation of novel sesquiterpenoids isolated from the main culture (BMS) extract of H. cf. alpina 824 98

4.7 Structure elucidation of compounds isolated from the main culture (BMS) extract of H. cf. alpina 824 108

4.8 Biological activity of metabolites produced by fungal strains isolated by the FIND technology..... 113

4.9 Structure elucidation via SMART of compounds 1 using NMR spectra of the main culture (BMS) extract 118

5 Concluding remarks 122

6 Summary..... 127

7 References 131

8 Appendix..... 157

1 Introduction

1.1 The role of fungal natural products in therapy

Fungi contributed several blockbusters [1] (therapeutic drugs with projected annual sales of 1 billion USD or more) to the pharmaceutical industry and play a prominent role as lead structures in drug discovery [2]. Fungi are an impressive group of microorganisms in this respect, due to the high structural diversity of their rich secondary metabolism [3]. Generally, fungal metabolites were shown to have antiviral, cytotoxic, antineoplastic, cardiovascular, anti-inflammatory, immune-modulating, and anticancer activities [4]. This broad field of bioactivities make fungal natural products an irreplaceable source for medical treatment of humans.

1.2 Methods for the isolation of fungi

Isolation of axenic fungal strains from environmental samples is a key element in many fields, including basic science, drug discovery and treatment of fungal infections [5]. In mycology, it is necessary to obtain fungi in pure culture to investigate their morphology, collect genomic data and to ultimately make a taxonomic decision [6]. Such results are the basis for identifications of fungi in medicine, agriculture, food and beverage analytics and scientific research. It is of major importance to identify fungi isolated from human tissue to gather information on the pathogenicity of the individual organisms, as well as on the appropriate drug therapy [7]. Similarly, pathogens threatening harvests of vegetables, fruits, and herbs have to be identified by analysis of the infested material to protect the latter by appropriate fungicides [8].

Fungi are ubiquitous and natural decomposers of organic material. What is a blessing outside of human habitats can be a curse when fungi infiltrate the living space, freshwater supplies or

stored food [9]. Moulds decomposing wooden furniture or hangings can harm the respiratory health of inhabitants by the production of spores and their release into the air [10]. Consumption of spoiled food or water from contaminated water piping can lead to intoxications by mycotoxins, specialised fungal metabolites for defence against predators and competitors [11]. Identification of those fungi and their preferred living conditions can help to prevent decay of housings by adjusting room temperature and moisture, or coating of walls and furniture with inaccessible materials as well as development of sterilisation procedures, predicting of storage conditions, conservation precautions and expiring time for food and beverages, as well as filter and material composition of water supply vessels.

In contrast to mycotoxins, fungi also produce specialised metabolites, which are considered beneficial for human health issues [12]. With the isolation of penicillin from *Penicillium notatum* in the late 1930s, the development of the first antibiotic successfully revolutionised drug therapy [13]. This period in time is called the antibiotic era and the use of substances killing all kinds of bacteria in infected patients saved millions of lives [14]. Not surprisingly, fungi got in the focus of natural product researchers and contributed numerous lead structures for drug development [15]. In order to obtain pure cultures of a target organism for natural product isolation, methods for the isolation from all kinds of environmental locations and samples were developed and modified [16]. In the following, a comprehensive list of methods for the isolation of fungi is presented, containing the state of the art as well as innovations and future perspectives.

1.2.1 Standard isolation methods

Direct isolation

The easiest way to isolate fungi is to simply collect them straight from their environment by cutting the entire or parts of the macroscopic fruiting body in case of mushroom producing strains, or by scraping the whole or parts of the macroscopic mycelium of mould producing strains [17]. This method is limited to visible material of the fungus of interest, which presupposes excellent growth conditions and is rarely found in nature or easily accessible habitats [18]. In fact, fungi inhabit mostly inaccessible regions like soils, narrow clefts or the insides of living and dead organic materials, e.g. endophytic or parasitic fungi [19]. Often their presence can only be determined indirectly by their odour (*Tuber* spp.) or the release of spores [20]. A useful tool for direct isolation is the moist chamber, where a sample of interest can be kept moist for several weeks and in which growth and sporulation of moulds inhabiting the sample are induced [21]. Glass containers, e.g. Petri dishes, are covered with absorbent materials, e.g. cotton, paper, cloth, sterile sand, soil or moss, one or several layers of filter paper are placed on top of it to create a surface, and the sample material is stored on this surface, on which the fungus will eventually grow hyphae or eject spores, which can be transferred onto isolation media [22].

Direct plating

Direct plating is mainly used for bioburden testing [23]. In the pharmaceutical and food industries ingredients and process steps have clearly defined limits of contamination. To determine the quantitative and qualitative bioburden, direct plating is used on solid or liquid samples [24]. The whole or a portion of the solid sample is put on an agar plate (or alternatively dipped into an appropriate nutrient solution) containing nutrients, unprocessed or

after blending. If the sample is a fluid or was blended for homogenisation, it is spread uniformly across the agar plate using a spreader and therefore called *spread plate method* [25]. Alternatively, the sample is put into the empty Petri dish, and the cooled agar medium is poured over the sample. This is called the *pour plate method* [26]. The fungi start growing from the material and mycelium can be transferred to cultivation plates as soon as visible. To prevent the growth of bacteria, antibiotics should be added to the isolation medium [27]. For bioburden experiments, airborne fungi are the organisms of interest, therefore Sabouraud agar containing antibiotics is used as a standard medium [28]. Fungal spores typically found in room air are very often fast-growing fungi, which might not depict the real a vast composition of fungal material in a given sample. In order to slow down fast-growing fungi, to simultaneously stain slow-growing fungi and to inhibit the growth of bacteria, e.g. actinomycetes the dye “rose Bengal” (4,5,6,7-tetrachloro-2',4',5',7'-tetraiodofluorescein) can be added to agar media. In fact, dichloran rose bengal chloramphenicol (DRBC) agar was found to be superior in terms of both, enumeration of fungal colonies and number of different genera isolated from air samples [29]. Cooke Rose Bengal Agar or Martin’s rose agar both, contain “rose Bengal” in addition to chloramphenicol and streptomycin, respectively, as the combination of two antibiotics was found to be more effective than only a single one [30].

Outside of the field of bioburden testing, fungi found on the surface of a sample are considered contaminants, if the fungi of interest are located inside of the sample, e.g. endophytic fungi from plant material or keratinolytic fungi from human tissues. To determine those fungi, that are obligately associated with the sample, surface sterilisation is necessary to avoid contaminants [31]. The choice of the surface disinfectant depends on the sample material. For inorganic or artificial materials, 70% ethanol can be used. However, this is

extremely toxic to plants [32]. Hypochlorites and hydrogen peroxides are used for plants in concentrations of around 3% and 30%, respectively [33].

In conclusion, direct plating is the method of choice for the determination of fungal contaminants. It can be used to isolate fungi that are associated with certain tissues after surface sterilisation. In natural product discovery, it is crucial to associate isolated compounds with the real producer. The drawback of this method is that it favours fast-growing fungi that overgrow the plates and suppress growth of slow-growing and specialised organisms.

Dilution plating

Dilution plating is used on a regular basis in environmental microbiology for the determination of Colony Forming Units (CFU), in order to evaluate the fertility of soil samples, which is linked to a high abundance of microorganisms [34]. To do so, a defined fraction of the soil sample is suspended in deionised water or 0.85% NaCl solution (Ringer solution), agitated manually and/or exposed to ultrasonication to detach microorganisms from soil particles [35]. Abundances of fungi in soil range between 10^5 – 10^6 g^{-1} [36], therefore the suspension is diluted several times with deionised water or Ringer solution to obtain a dilution containing a countable number of microorganisms, that will grow into individual discrete colonies [37]. These dilutions are processed in the same way as described above under *pour plate method*. After solidification of the agar, the plates are incubated, e.g. for a week, upside down to prevent condensation drops from falling onto the agar surface [38]. The fungal colonies will easily grow through the agar to reach the surface, can be counted and the abundance in the original sample can be extrapolated under the assumption that each colony derived from a single organism. For cell counts, the moisture content should be considered when abundances are calculated [39]. It is not surprsingly that this method can also be used to

isolate fungi, as it results in viable and discrete colonies. A commonly used variant in natural product discovery is the dilution-to-extinction method, where the dilution step is repeated until only a single cell of a microorganism is present in a given solution. A drawback of the dilution plating method is the high amount of insufficient plates that are either overgrown or not containing colonies at all.

Single spore isolation

Single spore isolation is used mainly in morphological identification of fungi, especially in anamorph-teleomorph classifications [40]. In order to determine the taxonomy of an isolate, pure cultures must be obtained, which is ensured by collecting representative reproductive structures, e.g. spore-producing structures or spores. Although several aspects of morphology must be considered, the most specific feature of a species lies in the anatomy of the produced spores [41]. Procedures for single spore isolation are simple and can be performed with basic laboratory equipment [42]. In general, spore-producing structures are surface sterilized, dissected from the sample material using very thin equipment, e.g. insect needles, glass needles pulled from Pasteur pipettes or micro tool needles and observed under the microscope. Spore suspensions are then prepared according to fruiting bodies, e.g. closed, cup-shaped, etc. For the preparation of the suspensions, the protocol by Zhang et al should be used, which modified the commonly used method by Choi et al and reduces contamination significantly [43].

In the case of basidiomycetes, the reproductive structures can be cut from the gills of the fruiting body and single spore isolation is performed by execution of the spore drop method, where the cut-out material is fixed to the lid of a petri dish usually containing water agar. The petri dish is then closed and stored in an incubator. As soon as the basidia are mature, they

will fall onto the agar, discharged by the Bullers drop, a fluid generated by condensed water from humid air. Subsequently they are analysed under the microscope and can be transferred to a cultivation plate of suitable nutrition level [44].

For ascospore producing strains the spore ejection method is applicable where an ascomata containing sample is placed onto an agar plate in such a way, that the ascomata face the surface of the agar [45]. The plate is stored upright (on the side) in the incubator and the ascospores are ejected across the plate when mature. Again, spores are checked under the microscope and transferred onto cultivation plates for germination. In natural product isolation from fungi, basidiomycetes and, especially, ascomycetes are the most frequently investigated phylae, which explains the advances being made in this method. The major drawback of this isolation method is the need of visible material of the fungus. In addition, fruiting bodies or at least asci or spores must be present, where the latter two can be hard to find under the microscope.

Selective isolation

Sometimes a specific species, a genus or a certain class of fungi are in the focus of interest. This is especially the case regarding pathogenic fungi from plants, animals or humans [46]. For the identification of the pathogen that causes the disease in beforementioned organisms, the completeness of the microbiome from infested sample tissue is negligible [47]. Therefore, it is necessary to oppress the growth of the “by-catch”, i.e. fungi also growing under otherwise same culture conditions, and favour only those conditions suitable for the fungus of interest. This can be achieved by the composition of the nutrients in the cultivation media, adjustment of the culture conditions, addition of substances to the culture media that inhibit certain microorganisms, or combinations of all three [48].

The lack of easily utilisable carbon or nitrogen sources in a culture medium, for instance, can be selective towards fungi with specialised digestion enzymes or germination of spores containing high reserve materials, i.e. carbohydrates, lipids, or proteins. Spores of *Monilinia fructicola,* for example, did not germinate when cultured without the addition of carbohydrates, e.g. dextrose, galactose, sucrose [49] and spores of *Glomerella cingulata* additionally needed nitrogen, phosphorus, magnesium and sulfur for initiation of the germination processes [50].

In all organisms, enzymes are responsible for the transformation of nutrients into essential building blocks necessary for vital processes. These enzymes have a certain thermal optimum, stop their activity by falling below a minimum threshold or denature and become inactive if temperatures rise above a critical value [51]. The majority of fungi grow well at moderate temperatures between 15 to 25°C. Psychrophilic fungi in a sample can, therefore, be separated from others by culturing them at temperatures around 0°C [52]. Most fungi are not able to grow cultures at 37°C, three noteworthy exceptions are *Cryptococcus neoformans, Histoplasma capsulatum,* and *Aspergillus fumigatus*, where the former is routinely isolated from bird excrement, whereas the latter two can be found in lung tissue of immunodeficient humans, causing mycoses. To survive at the average body temperature of birds and mammals of 37°C ± 1°C fungi developed mechanisms such as thermotolerant proteins. In *A. fumigatus* the gene *cgrA* was shown to play a key role in temperature-dependent ribosome synthesis. A Δ*cgrA* mutant showed no difference in growth rates compared to the wild type at 25°C, whereas growth rates of the wild type was increased threefold and stagnated in the mutant [53]. Temperature has even influence on the morphology of *H. capsulatum*, as it grows as a saprobic filamentous mould at room temperature, i.e. in soil, and changes to a parasitic yeast like appearance at body temperature, i.e. in human lung tissue [54]. The denaturation of

enzymes by increasing temperatures is counteracted by so-called heat shock proteins, which initiate the production of chaperons, stabilising the heat-sensitive peptides [55]. Apart from temperature also moisture content of the culture material and humidity during cultivation, levels of oxygen and carbon dioxide, presence or absence of light and other conditions affect germination and growth rates [56].

Another possibility to prioritise the growth of certain fungi lies in the use of additives to the culture medium, that inhibit growth of generalists. The simplest additives are acids or bases to adjust the pH. Rousk et al. analysed the occurrence of microbes in a soil strip of decreasing pH from 8.3 to 4.0. Tolerance was observed towards higher pH however, significant growth inhibition was observed at acidic levels below 4.5. This may have two ecological reasons, the first one is the increase of available aluminium, the second is the low abundance of plants at low pH and therefore a decrease in carbon source from roots [57]. However, extremophiles are found in both acidic (pH<3) as well as alkaline (pH>8) natural and anthropogenic regions [58].

To inhibit the growth of microbes apart from fungi, i.e. actinomycetes and other bacteria, antibiotics are added to the culture media. Special caution is required regarding the choice of the antibiotic, as it should not affect the growth of desired fungi. Streptomycin and chloramphenicol are standard antibiotic agents used in selective isolation and were shown to inhibit certain fungal species although mostly when used in very high concentrations [59,60]. Also antifungals can be added to selectively inhibit growth of fungi and at the same time obtain strains that lack commonly addressed targets or are otherwise insensitive, as it is the case in some entomopathogenic fungi when treated with cycloheximide, which is highly active against a large number of yeasts, except those pathogenic for vertebrates and insects [61].

In general, additives can be numerous and vary in type, function, and tolerance to different fungal classes. Addition of salts, heavy metals, or antifungals can lead to the isolation of marine adapted or halotolerant, heavy metal tolerant or drug-resistant species, respectively [62-64]. In natural product discovery selective isolation is a good way to cultivate fungi from specific groups of interest; a circumstance that is also the major drawback of this method, as only a very limited spectrum of fungi are portrayed and the requirements for the isolates can be extreme and result in low recovery rates.

Baiting methods

Baiting is a special type of the beforementioned selective isolation, where the substrate is very specific and only specialised fungi are able to utilise it as a nutrient source [65]. Baiting is commonly used for the isolation of phyto-, entomo-, zoo-, and anthropopathogenic fungi by using the respective target tissues as baits. For their saprophytic (better: saprotrophic) counterparts the respective detritus or dead material is used instead [66]. In general, the bait is placed into the environment of interest, or a sample is collected and processed in the laboratory. In the first case, after colonization of fungi on the bait, it can be transferred to the laboratory, surface sterilised and the fungal material can be cultivated using appropriate isolation medium. In the second case, a sample of interest is placed into a sterile petri dish with the bait buried inside or placed beside, on top or under the sample according to the material used [67]. One example of baiting in the field is placement of sterilised wooden panels into the water column and transfer of the ascomata of marine saprotrophs onto isolation medium [68]. More often, baiting is performed on sediment or water samples in the laboratory [69].

For the isolation of plant-pathogenic fungi from soil, the sample is placed into a petri dish and the bait, in this case, a piece of the plant, is placed on top of the soil, and the dish is incubated at room temperature. The pathogen will grow into the plant tissue and can be isolated on a sterile petri dish containing isolation medium [70], e.g. *Thielaviopsis basicola* can be isolated easily using one of its preferred hosts, carrot. Carrot disks are dipped into the soil and transferred into a petri dish containing a sterile wet filter paper to provide moisture [71].

Baiting on moving targets, i.e. insect larvae, is a bit more challenging, as contact of the bait with the soil sample must be assured. If the bait burrowed into the soil, no additional treatment of the dish is necessary, when it is avoiding the soil by webbing or climbing the walls of the dish, inversion of the plate after appropriate time intervals is recommended [72]. After the infection of the larvae transfer of the dead or euthanised bodies onto agar plates leads to cultures of the entomopathogenic fungi.

In order to isolate zoopathogenic fungi or dermatophytes, the mouse injection technique is used frequently, where a diluted soil suspension is injected into the host via the tail vein. After infection with the fungi, the affected tissue is transferred onto cultivation plates for isolation [73]. Phytiosis is a fungal infection caused by the oomycete *Phytium insidiosum* and can lead to serious ocular, cutaneous or arterial diseases in humans and animals [74]. *P. insidiosum* is a plant-pathogen occurring in warm wet climates which explains its opportunistic behaviour in vertebrates and can be baited from affected tissue using water cultures with grass or water lily incubated at body temperature [75]. All beforementioned examples can also be performed using the respective dead organic material, i.e. plant litter or dead wood, insect corpses or shed exoskeletons, bird feathers or horns, human hair or nails. Human hair is used as bait on a regular basis for the isolation of keratinophilic fungi which are important decomposers in nature, but can cause infections of the skin or the nails [76].

In summary, baiting is a great tool for the isolation of very specific fungal groups using compact equipment and indispensable in interdisciplinary diagnostics of pathogens. In natural product discovery, this allows the isolation of taxonomically, thus chemically related species.

Table 1.1 Advantages and disadvantages of state-of-the-art methods for the isolation of fungi

Method of isolation	Advantages	Disadvantages
Direct isolation Fungal material is directly taken from nature and cultivated	+ Straight forward method + Time-saving + Little effort	– Very rare event – Visible material necessary – High chances of mixed cultures – Expert knowledge of fungal morphology needed
Direct plating Sample is placed in growth media, and individual fungi that develop are separated	+ Easy to handle method + Fast procedure + Little material necessary	– Initially always mixed cultures – Favours fast-growing fungi – Passaging and purification are very time consuming – Slow-growing fungi are extremely hard to isolate
Dilution plating Environmental suspension is diluted serially, then cultivated on plates	+ Moderate effort and technologies necessary + Suitable for enumeration of organisms in sample + Discrete colonies	– High use of materials – High number of unusable agar plates, because of insufficient dilution – Direct interaction between cultures can prevent growth

Method of isolation	Advantages	Disadvantages
Single spore isolation Isolation of fungal strains from specific spores	+ Pure cultures + Moderate effort and technologies necessary	– Visible material necessary – Reproductive structures indispensable – Expert knowledge of fungal morphology needed
Selective isolation Specific cultivation conditions are used to obtain certain fungi preferably	+ Isolation of fungi showing specific features + Isolation of specialised specimen + Little material necessary	– Very limited range of isolated fungal cultures – Expert knowledge for choice of culture condition – High effort to oppress growth of undesired organisms
Baiting Host material or preferred organic matter is used to isolate associated strains	+ Time-consuming + High selectivity towards specialised specimen	– Very limited range of isolated fungal cultures – High effort and specific material necessary – Expert knowledge about bait is necessary

Concluding remarks

Generally speaking, much effort has been put into the invention, modification and specialisation of methods for the isolation of fungi (See Table 1.1). This circumstance underlines the importance of isolation techniques for fungi in all fields of human life, especially in natural product research. The isolation and cultivation of known and well-examined species has been advanced, is routinely performed and can be undertaken in various ways from different sample types. The problem, however, is the isolation of rare and undescribed fungal cultures species. Among them, strains that withstand pathogens by the

development of defensive strategies, e.g. antimicrobial compounds, are of special interest in natural product chemistry. The only way to utilise those compounds in therapy is the isolation and cultivation of the producing strain under laboratory conditions. Therefore, tools to access slow-growing, highly specialised strains, that under circumstances are heavily depending on their environment, are desperately needed.

Regardless of the isolation method used, or how optimal the culture conditions are in view of medium composition, pH and temperature, the majority of microorganisms will not grow into cultures on plates, even when their presence was observed under the microscope beforehand. The first person to discover this phenomenon was Austrian scientist Heinrich Winterberg in 1898 [77], only about a decade after the invention of the petri dish by the titan of microbiology Robert Koch and his colleague Julius Richard Petri. Many scientists agreed with his findings, such as Razumov [78], who observed this discrepancy also in water samples. It was Staley and Konopka who gave this phenomenon the telling name *great plate count anomaly* [79]. Per definitionem a cultured species is one that grows under laboratory conditions [80] and only a fraction of all the different species in an environmental sample, that can be observed under the microscope, i.e. <2%, can be recovered and cultured on growth medium [81].

The reasons for that phenomenon are manyfold and concern physical as well as chemical growth conditions. All efforts to mimic environmental conditions failed, and certain organisms did not grow cultures when diluted to extinction and spread on plates [82]. Coculturing was a promising step in the right direction and conclusions were drawn that the interaction between microorganisms played an important part in signalling and growth factor exchange [83].

Concerning bacteria, Epstein and Lewis transferred the culture step within the process of microorganism isolation into the field, this way hoping to provide all crucial factors. They designed the diffusion chamber, where microorganisms, i.e. actinomycetes, were trapped inside of a small agar plate (33 mm in diameter) sandwiched between semipermeable membranes. The pore size of the membranes was chosen large enough to let molecules pass, this way providing vital growth factors from the respective environments, but small enough to prevent growth of mycelium out of the diffusion chamber and at the same time blocking out other microorganisms, keeping the diffusion chamber free from contaminants [84]. Promising first results led to the high throughput version of the diffusion chamber, the iChip. This device comprised hundreds of those diffusion chamber prototypes in a single tool by reducing the size of each chamber to the fraction (1mm in diameter) of the original one. Recovery rates of up to 50% were achieved compared to a maximum of 14% on Petri dishes, and numerous undescribed species were isolated [85].

Among them, *Eleftheria terrae* caught the most attention, as it not only belonged to an undescribed bacterial genus but also produced a substance named teixobactin, which shows promising antimicrobial activity with no detectable resistances in respective serial passaging assays using sub-MIC concentrations [86]. Teixobactin targets hitherto untargeted structures in cell wall synthesis, a not yet identified part of lipid II (Liu et al. suggest the pyrophosphate-MurNAc moiety as the minimal motif for stable binding, see Figure 1.1 red part), as well as to the wall teichoic acid (WTA) precursor lipid III (undecaprenyl-PP-GlcNAc) [87] (see Figure 1.1). It is not surprising, that hitherto uncultured species hold the potential for the production of novel compounds, as they could not be isolated before and their natural products could, at the most, be anticipated by genome mining [88]. Growing microorganisms in large scales is the crucial step in natural product isolation, and therefore the diffusion chamber technology

was an important step to shed light on the *dark matter* of microorganisms, unknown species, probably producing desperately needed compounds for drug development. An aim of this thesis was to transfer the iChip technology to the isolation of fungi (see Chapter 4.2).

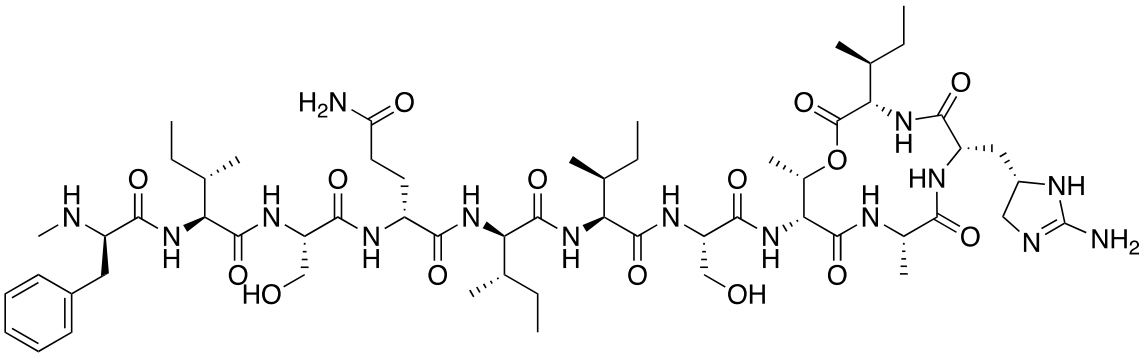

Teixobactin

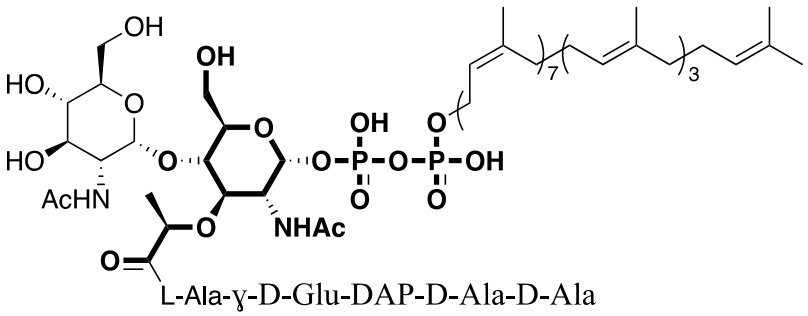

Lipid II

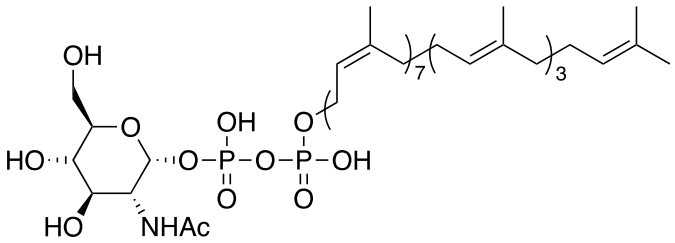

Lipid III

Figure 1.1 Teixobactin, isolated from *E. terrae* and its binding targets in peptidoglycan synthesis lipid II and lipid III; in bold: putative minimal motif of Lipid II necessary for stable binding [87].

1.3 Fungal specialised metabolites

1.3.1 Fungal polyketides

Secondary metabolites, like polyketides, are produced by multiple enzymes, organised in pathways [89]. These enzymes can either consist of individual proteins (e.g. free-standing condensation domain) or as part of proteins that belong to a multi-enzyme complex (e.g. ketoreductase as part of a polyketide synthase, PKS) [90]. Genes encoding these proteins are often chromosomal and arranged in biosynthetic gene clusters (BGC), frequently within only a few thousand base pairs [91]. Expression of these genes is regulated by environmental influences, which suggests secondary metabolite production as a reaction to ecological threats [92].

An example is the polyketide melanin, which is a natural pigment found primarily in spores or hyphae and known to protect the organism from cell damages caused by UV radiation and by quenching free radicals [93]. As in many polyketide syntheses, that of melanin starts with the endogenous precursor molecule malonyl-coenzyme A (malonyl-CoA) bound to the acyl carrier protein domain (ACP domain) of the first module, which is elongated by condensation of following malonyl-CoA molecules via the keto synthase domain (KS domain) of the module. This newly synthesised polyketide is altered by modifying domains and thus the molecules receive their specific properties, e.g. functional groups, halogenations, cyclisations. After all modification steps within the PKS, the molecule is released by the thioesterase domain (TE domain) for further alteration by other enzymes or for its final purpose within or outside of the organism. In the case of melanin, the polyketide chain undergoes several ketoreductions along with two cyclisation steps to yield 1,3,6,8-tetrahydroxynaphthalene (1,3,6,8-THN). After release from the PKS, 1,3,6,8-THN is further modified by enzymes to yield 1,8- dihydroxynaphthalene, which is ultimately polymerised to melanin [93]. Fungi

living in areas of intense UV radiation, e.g. Antarctic and equatorial regions, mountain ranges and deserts, therefore, developed dark septa. As these specimens share this common characteristic, they are classified as dark septate fungi (DSF). They play an important role in natural product isolation [94].

Environmental threats are not only of physical nature but also other organisms can be harmful and defence strategies are needed to survive attacks by predators, competitors or parasites. Microorganisms outnumber all other living organisms manifold, so competition for space and nutrients is especially contested. Fungi developed secondary metabolites with antiviral, antiprotozoal, antibacterial and even antifungal activities [95]. Some of these bioactivities are of medicinal interest. A prominent polyketide with antifungal activity is griseofulvin, which was isolated from *Penicillium aethiopicum* and was the first oral antifungal drug [96]. Belonging to the globally best-selling drugs, statins, i.e. lovastatin, isolated from *Aspergillus terreus*, are polyketides with cholesterin lowering effects [96].

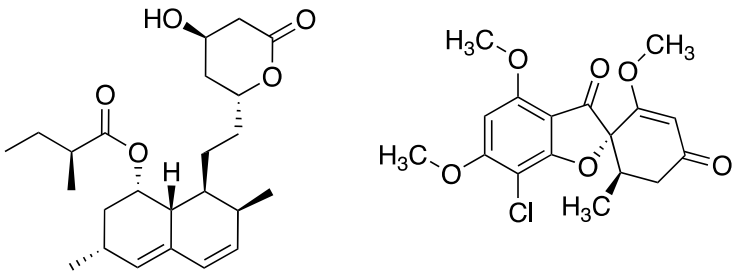

Figure 1.2 The fungal polyketides lovastatin and griseofulvin, which are used as drugs.

1.3.2 Fungal terpenoids

With more than 80000 known structures, isoprenoids form the largest group of natural products [98]. Plants and fungi represent the biggest producers of isoprenoids among eukaryotes [99]. In contrast to that, isoprenoids are rarely isolated from prokaryotes, with the exception of actinomycetes [100]. Isoprenoids or terpenes are produced by the respective organisms by sequential head-to-tail condensation of the precursor molecules dimethylallyl pyrophosphate (DMAPP) and isopentenyl pyrophosphate (IPP), derived from acetate in the cytosolic mevalonate (MVA) pathway. In the 1990s an alternative pathway was discovered that is used by eubacteria, green algae, and higher plants for synthesis of the same C_5 building blocks, in this case from D-glyceraldehyde 3-phosphate and pyruvate via the production of 1-deoxy-D-xylulose 5-phosphate (DXP), which is then reductively isomerised to 2-C-methyl-D-erythritol 4-phosphate (MEP). Therefore, the latter is called MEP pathway [101].

Terpene synthases are classified as class I or class II, depending on the first step of the catalytic reaction cascade [102]. The formation of highly reactive resonance stabilised carbocationic intermediates is performed by the heterolytic cleavage of the diphosphate ester bond (class I), or protonation of the enzymatic substrate (class II) [103]. The number of possible isomers exponentially increases with the number of carbons in a terpenoid structure. Considering only monoterpenes Tian, Poulter, and Jacobson predicted 18758 possible carbocations by computational methods, that resulted in 123093 hypothetical linear, monocyclic or bicyclic compounds. These hypothetical cyclic monoterpenes have been grouped into 74 skeleton types, of which five were found already in natural products [104]. For sesquiterpenes, the amount increases manyfold, and the number of hypothetical structures assumes astronomical proportions. Energetic aspects of chemical properties in a molecule and enzymatic reactions, constrained geometrical flexibility, as well as the instability of certain

hypothetical cations, limit the number of known skeletons [102]. Additionally, species-specific alterations, e.g. functional groups, heteroatoms, cyclisations, lead to an uncountable amount of hypothetical natural products for scientists to discover [105].

Terpenes are categorised by their number of C-atoms, where a structure containing ten carbons is called monoterpene, whereas structures containing 5, 15, 20, 25, 30, 35 and 40 carbons are named hemiterpenes, sesquiterpenes, diterpenes, sesterterpenes, triterpenes, sesquaterpenes and tetraterpenes, respectively. Higher multiples are called polyterpenes, i.e. rubber from *Hevea brasiliensis*. If molecules fall out of the classification mentioned above by missing one or more C-atoms, the prefix *nor*- is used to emphasise the irregularity in nomenclature, i.e. trinor-bergamotene derivative xylariterpenoid E (C12) missing three carbons to be categorized as sesquiterpene [106] (see Figure 1.3). Fusidic acid, first isolated from *Fusidium coccineum,* serves as an example for a 29-nor protostane triterpenoid (see Figure 1.3) [107]. Among 18 known compounds, it is the representative molecule of the fusidane-type antibiotics, together with helvolic acid and cephalosporin P_1 [108]. Fusidic acid shows excellent inhibitory activity against Gram-positive bacteria and its sodium salt is used as a topical antibiotic in the treatment of skin infections, e.g. impetigo, or in combination with betamethasone or hydrocortisone in the treatment of atopic dermatitis [109,110]. The pharmacological target of fusidic acid is the bacterial ribosome, preventing pathogens from peptide elongation [111]. As a steroid antibiotic the structure of fusidic acid resembles the one of lanosterol, a key compound in the production of animal and fungal steroid secondary metabolites. In this respect, it could be proven that *F. coccineum* utilises squalene as a precursor in the production of fusidic acid, similarily to the biosynthesis of lanosterol and related derivatives [112, 113].

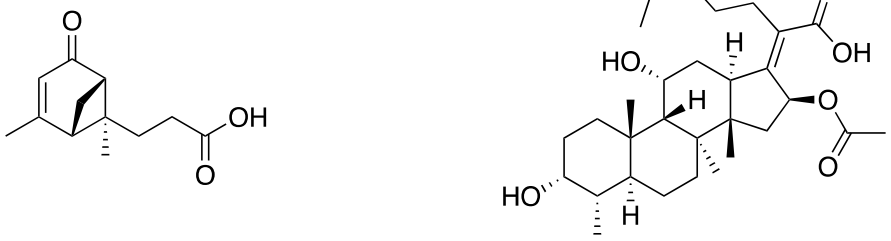

Xylariterpenoid E

Fusidic acid

Figure 1.3 Fungal-derived trinor sesquiterpene xylariterpenoid E and 29-nor protostane triterpenoid fusidic acid

1.3.3 Fungal peptides

Fungal peptides played a fundamental role in early drug discovery [114]. Not only was a natural product isolated from a *Penicillium* sp. the first antibiotic in history, i.e. penicillin G, it was also a peptide [115]. Production of peptides in fungi is performed in two mechanistically different ways. Fungal peptides are assembled either through ribosomal gene translation, i.e. production of the infamous amatoxins and phalloidins [116] or by non-ribosomal peptide synthetases (NRPS), where the latter pathway is described for most of the isolated fungal peptides [117]. Similarily to PKS mentioned before, NRPS can be classified as megaenzymes, consisting of specialised modules capable of peptide chain formation by condensation of amino acids. Each module further comprises several catalytic domains. Of these, the adenylation-domain (A-domain) is responsible for selection, activation and transfer of the respective building block to the peptidyl carrier protein (PCP-domain). The function of the PCP-domain is the tethering of the product to the enzyme. At the condensation domain (C-domain), the condensation reaction is catalysed, and the peptide bond formation takes place [118].

Additional structural diversity is driven by auxiliary domains, which add new or alter existing features of a non-ribosomal peptide. Typical auxiliary domains are epimerization domains (E-domains), which allow the incorporation of D-amino acids and therefore lead to an improvement in the proteolytic stability of the peptide [119], N-methylation domains (N-Mt-domain) and methylation domains (Mt domain) for addition of methyl groups to the respective atoms, as well as oxidation (Ox-domain) and reduction (R-domain) domains for introduction of thiazoles, oxazoles or thiazolidines, oxazolidines, respectively [120]. In contrast to bacterial NRPS, where a TE-domain catalyses release and/or cyclisation of the peptides, in fungi, a condensation-like domain (C_T-domain) performs the macrocyclisation reaction.

Fungal cyclic peptides can be classified depending on the type of linkage present in the final molecule [121]. Homodetic peptides show only regular peptide bonds, i.e. the immunosuppressant ciclosporin A, whereas heterodetic cyclic peptides incorporate other covalent bonding types, e.g. lactone bonds like in the octadepsipeptide PF1022A, whose semisynthetic derivative emodepside is used as an anthelmintic veterinary agent, currently in phase II for the use in humans [122]. Complex cyclic peptides combine both types of linkages and can, e.g. be found in bicyclic peptides [123].

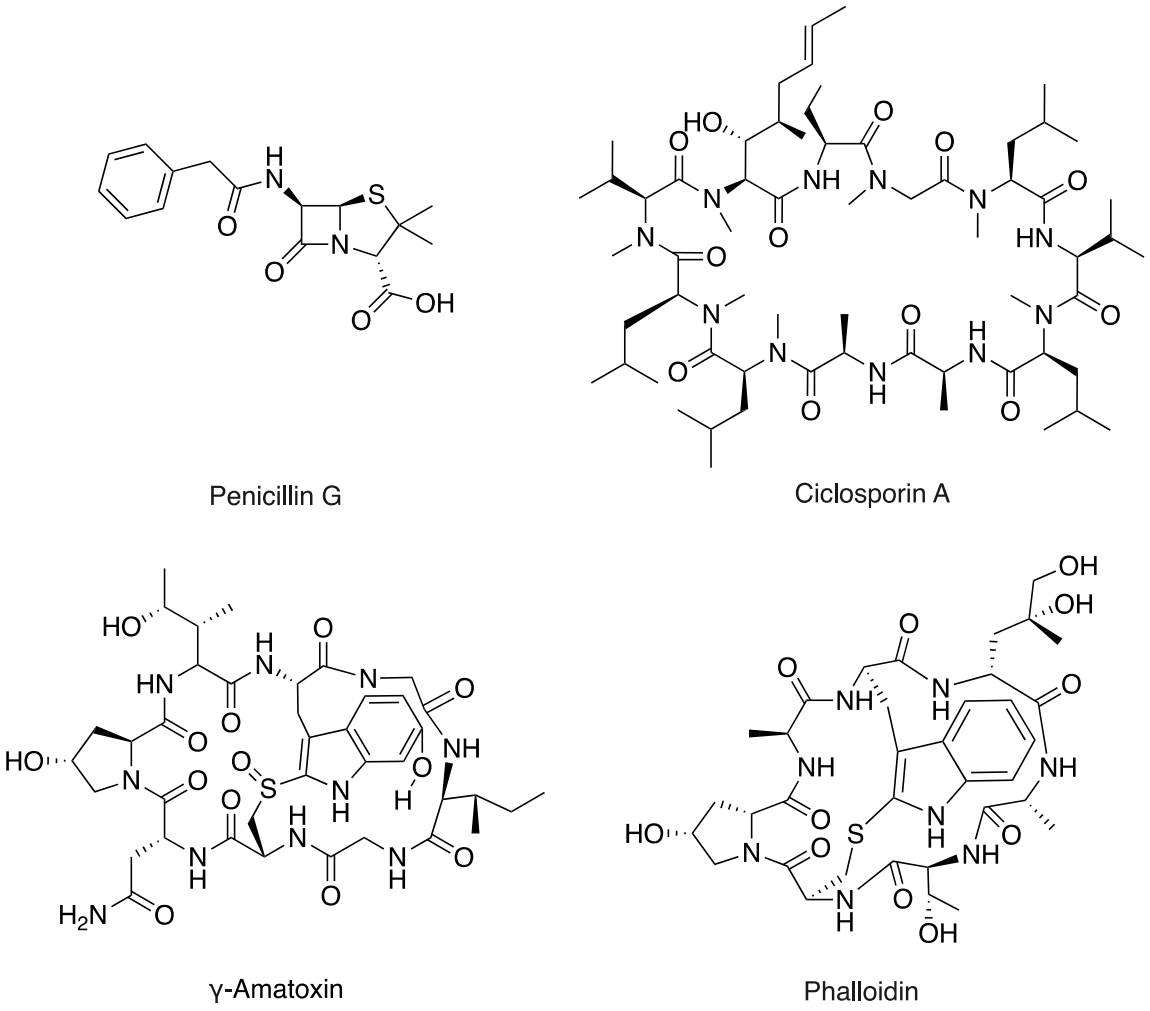

Figure 1.4 Non-ribosomally synthesised fungal peptides, e.g. penicillin G and ciclosporin A; Ribosomally synthesised fungal peptides, e.g. ɣ-amatoxin and phalloidin.

1.3.4 Fungal metabolites of mixed biosynthetic origin

Categorising secondary metabolites by their biosynthetic origin allows to assemble groups of structurally related compounds, predict features of similar structures and to draw conclusions on taxonomic similarities of the respective host organisms [124-126]. In nature, patterns can be found on a regular basis, but many times exceptions from the rule are observed, which is the case when two or more metabolic pathways are combined. For specialised metabolites that do not solely use one of the synthetic pathways described above, the term *mixed biosynthetic origin* is applied [127].

A molecule in which terpenoid parts of varying levels of complexity are attached to moieties originated from another biosynthetic pathway, e.g. PKS, ribosomal or non-ribosomal peptides, are called hybrid isoprenoids (HI) in general [128]. To be more precise, the combination of polyketide and terpenoid features in a single molecule is called meroterpene. An example of a fungal meroterpene is the immunosuppressant drug mycophenolic acid, which is biosynthetically comprised of an acetate-derived phthalide nucleus and a terpenoid side chain [129].

For metabolites that show both polyketide as well as peptide moieties, the term polyketide peptide hybrid natural products is used, where the ochratoxins isolated from *Aspergillus ochraceus* suit as a prominent example. Biosynthetically, they are pentaketides resembling dihydrocoumarins, where a beta-phenylalanine is attached via a peptide bond.

The combination of terpenes and peptides is rather rare, and no special term describes such structures. Fumitremorgin B, first isolated from *A. fumigatus* is an example of a peptide hybrid isoprenoid [130, 131].

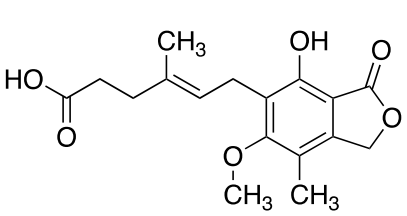

Mycophenolic acid

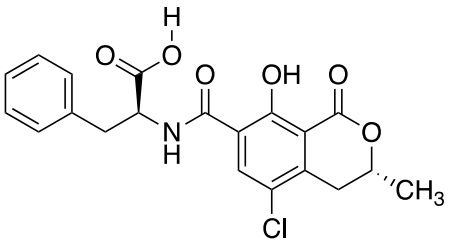

Ochratoxin A

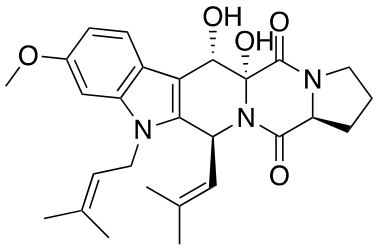

Fumitremorgin B

Figure 1.5 Fungal meroterpene mycophenolic acid, polyketide peptide hybrid ochratoxin A and prenylated cyclic peptide fumitremorgin B.

1.4 Terpenoids with bergamotene skeleton structure and their bioactivities

Since this thesis deals with terpenoids having a bergamotene skeleton, the structural diversity and biological activity of this group of compounds shall be discussed. Assigning trivial names to recurring structural motives categorises similar compounds into groups, that share the same carbon skeleton. An important sesquiterpene skeleton is the bergamotene, probably named after the hybrid plant *Citrus bergamia*, known as bergamot orange [132]. Natural compounds containing this carbon skeleton were reported in both plants, e.g. *Cyperus articulans*, *Lepidolaena clavigera*, *Lycopersicon hirsutum*, *Tanacetum vulgare*, *Tinospora cordifolia* and fungi, e.g. *Ampulliferina sp.*, *Ampulliferina*-like sp., *Aspergillus fumigatus*, *Cytospora* sp., *Graphostroma* sp., *Massarina tunicata*, *Paraconiothyrium brasiliense*, *Paraconiothyrium sporulosum*, *Penicillium expansum*, *Podospora decipiens*, *Xylariaceae* sp., as well as soft

corals of the genus *Gorgonia* [104, 133-139]. The environmental role of secondary metabolites showing this specific motif ranges from insect pheromones to growth factors in plants to bioactive agents against pathogens [140-145]. Figure 1.6 gives an overview of the impressive diversity in bergamotene, incorporating sesquiterpenes across various species.

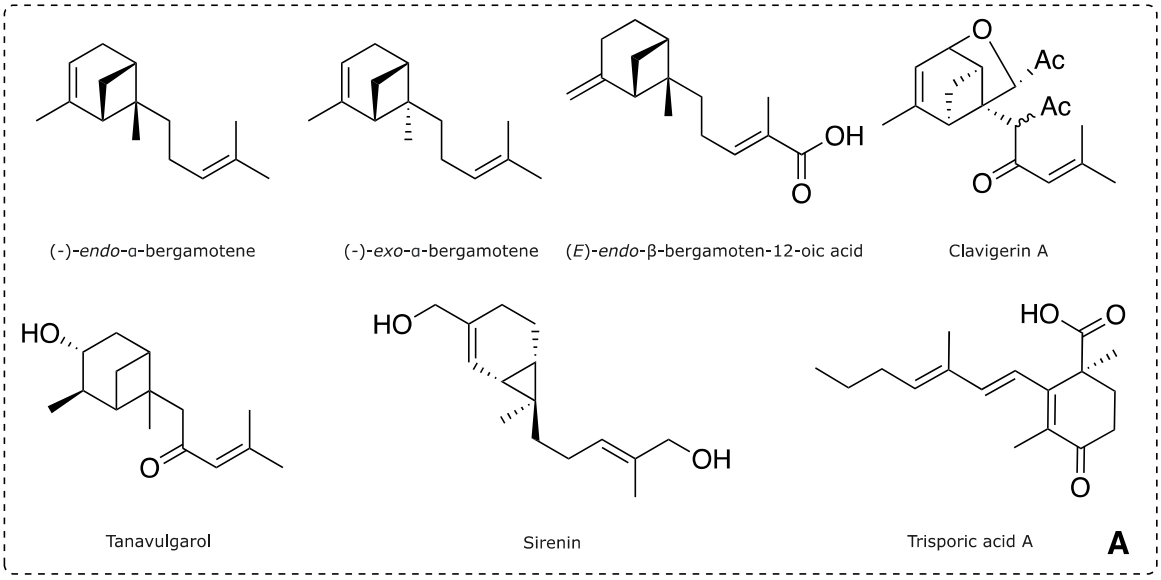

Figure 1.6 Several sesquiterpenes incorporating the bergamotene backbone, arrayed according to their ecological role; A: pheromonal activities; B: plant growth regulatory activities; C: Antimicrobial, antineoplastic and anti-inflammatory activities.

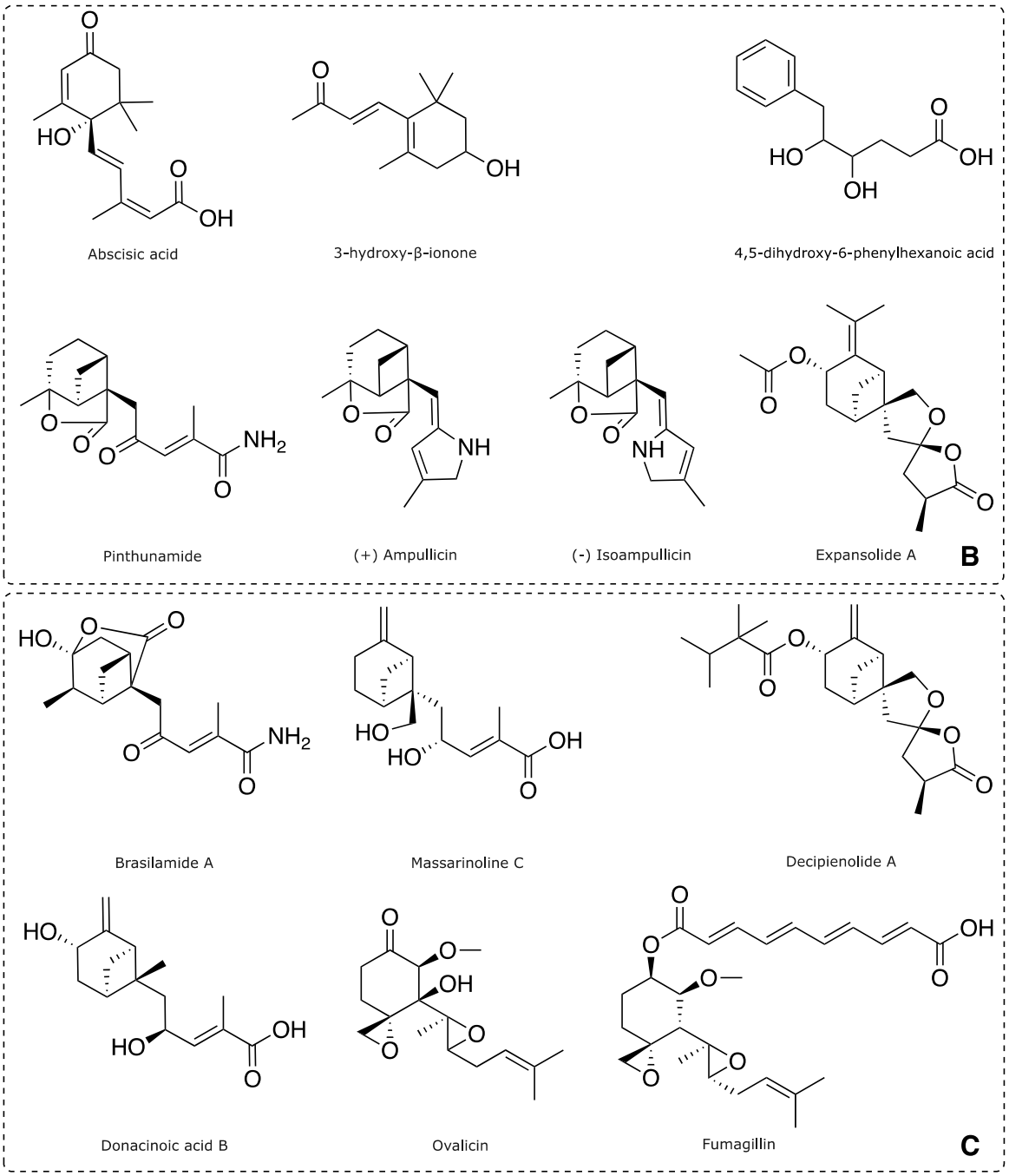

Figure 1.6 Continued

Pheromonal activities

The most basic members of the bergamotene class of sesquiterpenes are the constitutional isomers α-bergamotene and β-bergamotene, which each exist in an endo- and an exoisomeric form. Nevertheless, both isomers play crucial roles in pheromone interactions between plants and insects. The monocot *Zea mays* emits these volatile hydrocarbons after a herbivore attack, alongside a cassette of structurally closely related compounds, e.g. 7-epi-sesquithujene, sesquisabinene A, to lure predators of the attacking pests [146]. Female winged ectoparasitic wasps, e.g. *Melittobia digitate*, are highly susceptible to those compounds, especially to exo-α-bergamotene, anticipating wingless males; instead, they are left with their prey, liberating the plant from its vermins [147]. The closely related chemical constituent (*E*)-endo-β-bergamoten-12-oic acid was found to be both attractant, as well as repellent in *Lycopersicon hirsutum*, depending on the pest colonizing it. Present in the trichomes of the leaves it served as an oviposition stimulant to the moth *Heliothis zea* in *Lycopersicon hirsutum* LA 1777 [138]. On the other hand, (*E*)-endo-β-bergamoten-12-oic acid showed repellent activity against arthropod mites. In fact, *L. hirsutum* is highly resistant to arthropod herbivores, thanks to its capability of bergamotene-class sesquiterpenoid production [148]. The liverwort *Lepidolaena clavigera*, endemic to New Zealand, utilises the insect repellent activity of the bergamotene motif by production of polyoxygenated bergamotene sesquiterpenes [oxST] with an unusual 7-oxatricyclo[4.3.0.$0^{3,9}$]nonane ring system, namely clavigerins [144]. Clavigerins A-C showed antifeedant activity against carpet beetle larvae *Anthrenocerus australis*, and clothes moth larvae *Tineola bisselliella*, comparable to the commercial pesticide azadirachtrin, which is originally a natural product [149]. Another oxST with a bergamotene skeleton is tanavulgarol, which is a component of the insect repellent essential oils of *Tanacteum vulgare* [150]. Bark beetles, e.g. *Ips pini* use monoterpenes (MT) as aggregating

pheromones in order to propagate on newly infested host trees and oxygenated monoterpenes (oxMT) as anti aggregating pheromones when it comes to imbalances in reproductive partners or insufficient space. Pteromalid parasitic wasps oviposit on the beetle's larvae and locate them through those emitted oxMT [151]. Strategies developed by fungi to attract insects for vectored spore dispersal, or as hosts, in the case of endosymbiotic or parasitic species, comprise mimicking these pheromones [152,153]. An example is the production of volatiles in ophiostomatoid fungi, e.g. *Ophiostoma ips*, in order to attract the predator of its host, *Ips pini*, for dissemination [154]. For sexual reproduction in fungi a compound with a 1-hydroxy-2-methlypentenoic side chain and a bicyclo[4.2.1] ring system, called sirenin, plays an important part. This compound, resembling bergamotene very closely, was the first discovered fungal sex hormone. It is produced by female gametangia and attracts the male gametes of the genus *Allomyces* [155]. A second terpenoid hormone, trisporic acid, was discovered years later, also showing a similar structure, although its biosynthetic origin is the tetraterpene β-carotene [156].

Plant growth regulatory activities

Natural compounds with bergamotene skeleton not only affect the hormone system of insects and fungi, but they also play a major role in the growth regulation of plants. The fact, that bergamotene sesquiterpenoids resemble endogenous hormones, e.g. abscisic acid and 3-hydroxy-ß-ionone, and exogenous growth stimulators, e.g. 4,5-dihydroxy-6-phenylhexanoic acid, responsible in the plant growth regulating system, is one of the key element of their specialised bioactivity [157]. The plant metabolite abscisic acid shows ambivalent potency in root growth stimulation, depending on other factors, e.g. water stress. 4,5-dihydroxy-6-phenylhexanoic acid, isolated from the bacterium *Erwinia quercina*, induced the rapid development of lateral roots in carrots directly [158]. The root growth in lettuce was also

induced by the fungal metabolites pinthunamide, ampullicin and isoampullicin, bergamotene derivatives, isolated from an *Ampulliferina*-like strain [141,142]. On the contrary, the endogenous plant metabolite 3-hydroxy-ß-ionone inhibits root growth from shoots under unfavourable conditions [159]. Root growth inhibitory activities were also determined for the fungal bergamotene sesquiterpenes expansolides, isolated from *Penicillium expansum*, in respective elioted wheat coleoptile assays [160]. In the expansolides, the sidechain is cyclised into two five-membered heterocyclic rings, making it less flexible [161]. Interfering with plant growth processes is a powerful tool for fungi associated with plants, e.g. endophytes, symbionts or saprotrophs, to alter living conditions to their own favour, benefit from improved host defence against environmental stresses, or compete for living space and natural resources, respectively [162].

Antimicrobial, antineoplastic and anti-inflammatory activities

Natural products isolated from fungi with bergamotene structure were tested regarding their pharmacological activity by various laboratories. These compounds were found to be active against microbial pathogens, ranging from viruses to bacteria and fungi. Derivatives with an amide functional group, so-called brasilamides, isolated from the plant endophytic fungi *Paraconiothyrium brasiliense,* were tested for inhibitory effects on HIV-1 replication in C8166 cells, expressing moderate activity [163]. Massarinolins, produced by the aquatic fungus *Massarina tunicata,* showed activity in disk diffusion assays against *Bacillus subtilis* (ATCC 6051) and *Staphylococcus aureus* (ATCC 29213) [164]. For the decipienolides, found in *Podospora decipiens* and structurally closely related to the beforementioned expansolides, weak antimicrobial activity against *B. subtilis* was observed [165]. *Montagnula donacina*, an edible mushroom, provided four bergamotene type sesquiterpenes, of which two resembled bergamotenoic acid. Of those two donacinoic acids, donacinoic acid B exhibited weak

inhibitory activity against *S. aureus* subsp. *aureus* [166]. Ovalicin and fumagillin, bergamotane derivatives without a four-membered ring, isolated from *Pseudorotium ovalis* and *Aspergillus fumigatus*, respectively, were shown to have antimicrobial activities [167,168]. Both compounds were broadly effective against microsporidia, single-celled, obligately intracellular parasites, belonging to the class of atypical fungi, whereas fumagillin was found to be less toxic in vivo [169]. Ovalicin, additionally, showed immunosuppressive activities in mice, treated with sheep red cells [167]. In fact, both compounds, ovalicin and fumagillin, are very potent inhibitors of angiogenesis, and the latter was chosen for drug development [170]. The xylariterpenoids, isolated from a *Xylaria* sp., showed inflammatory activity in RAW 264.7 macrophages [104].

This comprehensive literature search on bergamotene type sesquiterpenes from natural sources, with special interest in fungi, expresses the wide variety in structure and bioactivities of this class of specialised metabolites. Isolation, structure elucidation and bioactivity testing of bergamotene type sesquiterpenes is, therefore, a fruitful task and an important step to an advanced understanding of their functions in nature, and in order to access them in drug development.

2 Scope of the present study

Fungi contributed to drug development in an extraordinary manner which resulted in live-saving therapeutic agents. Novel natural compounds bear the potential of becoming lead structures in drug discovery and therefore reducing the number of untreatable diseases. The chances of isolating novel compounds increase significantly when screening a hitherto unexamined species and even more when examining a to date unidentified species. With 150 000 species named and classified, it was suggested that 95% of fungi to date remain unknown [171]. These so-called dark matter fungi (DMF) are a promising source for novel compounds [172-175], and their isolation and culture is one of the keys to finding new pharmacological agents. Many approaches were made from sampling in remote or extreme locations to adjustment of the isolation medium and growth conditions to find rare and underexamined colonies. In this study, an isolation method was developed that allows the isolation of hundreds of fungal strains in a single step, and the incubation of these organisms under their preferred growth conditions in the environment the sample was originally taken from. This way slow-growing fungi or to date uncultured fungi can be isolated.

As a result of the isolation procedure, 12 different filamentous fungi were obtained, their taxonomy was identified by DNA sequencing as well as microscopical analysis and their antimicrobial activities and secondary metabolite production was screened. According to those results the strain 824 *Heydenia* cf. *alpina* was elected for an in-depth investigation. Literature search confirmed that no chemical investigation was performed on any species within this genus. Furthermore, the *Heydenia* cf. *alpina* belongs to the phylum Ascomycota, the largest fungal phylum, whose members include the well known *Penicillium* and *Aspergillus* spp. extensively studied for their medicinal and disease-causing properties. They are the most frequent producers of natural products, including the penicillin antibiotics and

the cholesterol-lowering drug lovastatin. All of the reasons mentioned above make strain 824 an exceptional candidate for natural product research.

Course of study

The first part of the study has the aim to develop an isolation method for filamentous fungi from four different sample sites. After adjustment of the sample concentration, successful isolation of axenic cultures is anticipated.

The focus of the second part of the study is the intensive investigation of the metabolome of *Heydenia* cf. *alpina*, a marine adapted filamentous fungal strain obtained during the first part of the study and showing promising results in prospective screenings, using chromatographic (HPLC, VLC) and spectroscopic (CD, IR, MS, NMR, UV) methods and ultimately isolation and structure elucidation of novel compounds.

The third and last part focuses on the effect of different culture conditions on the metabolome of certain isolated strains using latest technological approaches, i.e. HRMS based dereplication (GNPS) and deep learning NMR guided structure elucidation (SMART), and the evaluation of the biological activities of the isolated compounds.

3 Materials and Methods (General procedures)

3.1 FIND

3.1.1 Device specifications

The device was crafted from polyoxymethylene by the technical staff of the Helmholtz-Institute for Radiation- and Nuclear Physics, Nussallee 14-16, 53115 Bonn. The central plate (127 mm by 92 mm by 1 mm) and the two symmetrical upper and lower plates, the latter with screw threads, contain 96 through-holes 2 mm in diameter arranged in an 8 by 12 grid in a way that it perfectly aligns with the wells of a 96 well plate. The array of through-holes can be covered by one 142 mm polycarbonate membrane filter with a pore size of 0.03 micron (Sterlitech corp., Kent, WA). The device is sealed by six hex bolts size M3.

3.1.2 Find procedure

For experiment 1, 5 mL of soil (Falcon tube) was diluted in 45 mL of sterile-filtered NaCl 0.85% solution (Ringer solution). This solution underwent manual agitation for 10 minutes and ultrasonication using a Bandelin Sonorex at 100% amplitude (35 kHz) two times for 5 seconds to detach cells from sample surfaces. After centrifugation using a Thermo Scientific Heraeus Multifuge X1R at 130 gravities for 5 minutes, cell counting was performed on the supernatant using a Neubauer Improved or Thoma chamber on an Olympus BX51 polarizing microscope at 100x magnification, and the abundance of bacteria was calculated by counting bacterial cells in all 25 medium squares of the central large square or all 16 medium squares of one of the large square, respectively. With Neubauer Improved chambers the supernatant was exchanged three times, for Thoma chambers, three different large squares were counted. All the cells within each medium square (totally) together with those that are over the top and right sides of the square (even partially) were considered inside of a square. Mean cell counts

were calculated and converted into concentrations by multiplying cell counts with the reciprocal value of the volume of a small square in L, considering possible dilution steps. For experiment 2 and 3, samples were treated alike, but instead of a Ringer's solution, seawater from the respective sampling site was used. For experiment 4, only seawater was used.

With the calculated abundances 2 x 10^{13} as well as 7 x 10^{9}, 13 x 10^{9} and 8 x 10^{9} bacterial cells/L for experiments 1 - 4, respectively volumes between 10 and 50 mL of the solutions were taken according to the corresponding assumed bacteria-to-fungi ratios of the given sample type. These volumes, *e.g.* 16, 24 and 42 mL respectively, were then added to a volume of FAM solution to obtain a concentration of 320.000 fungal parts per litre.

For experiment 4, 500 mL portions of a 10 L sample were poured through a sieve with a mesh size of 35 (0,5 mm) onto Whatman filter paper disks 602H with a pore size of 2 µm attached to a Büchner funnel. The funnel was put onto a 2 L suction bottle which was connected to a KNF Neuberger N811 KN.18 vacuum pump that provided negative pressure in the bottle and therefore ensured filtration of the sample portions. The residues on the filter paper disks (5 mL) were resuspended in 5 mL autoclaved sea sample and also mixed with 15 mL warm FAM solution resulting in a concentration of approximately 320 000 fungal parts/L. The prepared FAM solutions containing the corresponding samples were homogenized by stirring, and the central plate was dipped into it. The desired target concentration is necessary to allow only one fungal part per through hole in the central plate. As the agar solidifies, the specimen is trapped in the chamber. A semipermeable polycarbonate membrane filter was attached to both sides of the central plate. The upper and lower parts of the FIND were connected to each other with six M3 hex bolt screws, sandwiching the central plate with the attached membranes between them. To ensure the devices seal commercial aquarium safe and antifungal-less silicone (Soudal) was applied to the edges of the device. The silicone was given time to dry,

and the device was inserted into a tank containing 40 L of soil for experiment 1, 2 L of seawater and sediment for experiment 2, 20 L of seawater and sediment for experiment 3 and seawater for experiment 4. An aquarium powerhead provided water current for simulation, oxygenation and distribution purposes for experiments 2-4. Evaporated tank water was replaced by autoclaved deionized water for experiments 2-4, and the soil in experiment 1 was watered with autoclaved deionized water every two days.

After four weeks of incubation inside of the tank, the device was removed, rinsed with autoclaved deionized water to remove sediment and soil and opened under a laminar airflow cabinet to transfer each agar plug to a corresponding agar plate for cultivation. For transfer into 96 well plates, a Boekel replica plater was used to punch all agar plugs from the central plate into the corresponding wells containing liquid FAM medium. For transfer onto agar plates, autoclaved wooden toothpicks were used to pick each agar plug from the central plate manually and streak them onto agar plates. The plates were stored in a Memmert BE500 incubator at 25 °C for four weeks.

3.2 Cultivation and extraction

3.2.1 Culture media

Table 3.1 Artificial Seawater (ASW)

Ingredient	[g] or [mL]
KBr	0.10
NaCl	23.48
$MgClx6H_2O$	10.61
$CaCl_2x2H_2O$	1.47
KCl	0.66
$SrCl_2x6H_2O$	0.04
Na_2SO_4	3.92
$NaHCO_3$	0.19
H_3BO_3	0.03
Water	1000

Table 3.2 FIND agar medium (FAM)

Ingredient	[g] or [mL]
Casamino acids	0.05
Fish peptone	0.025
Agar	15
0.9% NaCl solution / seawater	1000
Penicillin G (sterile filtered)	0.25
Streptomycin (sterile filtered)	0.25

Table 3.3 Biomalt Salt medium (BMS): 20 g L^{-1} biomalt extract, 15 g L^{-1} agar (for solid medium)

Ingredient	[g] or [mL]
Biomalt extract	20
Agar	15
ASW	1000

Table 3.4 Biomalt medium (BM)

Ingredient	[g] or [mL]
Biomalt extract	20
Agar	15
Water	1000

Table 3.5 Sabboraud Dextrose Agar (SDA), pH 5.6

Ingredient	[g] or [mL]
Mycological peptone (enzymatic digest of casein and animal tissues)	10
Dextrose	40
Agar	15
Water	1000

Table 3.6 Synthetic Nutrient-poor Agar (SNA), pH 5.6

Ingredient	[g] or [mL]
KH_2PO_4	1
KNO_3	1
$MgSO_4x7H_2O$	0.5
KCl	0.5
Glucose	0.2
Sucrose	0.2
Water	1000

Table 3.7 Gesteinsmehl Agar (GMA)

Ingredient	[g] or [mL]
Urgesteinsmehl (powdered rock)	150
Agar	0.2
Water	50

Table 3.8 Tenellin Medium (TE)

Ingredient	[g] or [mL]
Mannitol	50
KNO_3	5
KH_2PO_4	1
Agar	15
Water	1000

Table 3.9 Pharmamedium (BPM)

Ingredient	[g] or [mL]
Glucose	20
Organic soy flour	10
Pharmamedia	10
$(NH_4)_2SO_4$	1
$CaCO_3$	10
Glycerol	20
Agar	15
Water	1000

3.2.2 Pre-cultures

First pre-culture (solid): fungal strain was inoculated on BMS agar Petri-dishes and incubated at 25°C for 4 weeks.

Second pre-culture (liquid): from the first pre-culture, a seed inoculum was used to inoculate 1 L Erlenmeyer flasks (3 flasks) each containing 300 ml of liquid BMS media. Liquid pre-cultures were shaken at 121 rpm at 25°C for ten days.

3.2.3 Main culture

From the previous liquid pre-culture, liquid seed inoculums were aseptically transferred to Fernbach flasks (5 ml for each flask) containing 250 ml BMS agar media and incubated at room temperature for 30 days.

3.2.4 Extraction

At the end of the cultivation period (30 days), the homogenized fungal biomass and cultivation media were exhaustively extracted with ethyl acetate and concentrated under vacuum (using vacuum rotatory evaporator, 40°C) to yield the crude extract.

3.2.5 Taxonomic identification of strains

Sequencing of the obtained isolates from the FIND experiments was performed by P. Massart and C. Decock at the Belgium coordinated collections of microorganisms (BCCM/IHEM, Brussels) by extracting DNA using their usual protocols and genomic DNA extraction kits and generation of partial sequences of DNA loci using standard primers of ITS1, ITS2, ITS4, 5.8S, RPBII, tef1α and β-tubulin. Digitalized and formatted DNA sequences were compared to reference sequences using BLASTn. ID% of the ITS regions was used to identify each strain. If multiple strains came into question, the ID% of other gene sequences were taken into consideration to find the best match. Additionally, macromorphology was examined by colony observation using a Leica MZ6 stereomicroscope (Leica, Wetzlar, Germany) and micromorphology was examined with an Olympus BX51 polarizing microscope (Olympus, Shinjuku, Japan) by analysis of conidia and mycelium to support the bioinformatic suggestions.

3.2.6 Salt dependency experiments

Artificial seawater was used for the preparations of the agar plates. The stock solution (see Table 3.10) equals 35‰ salinity.

Table 3.10 Artificial Seawater

Ingredient	[g] or [mL]
NaCl	23.48
$MgCl_2 \cdot 6H_2O$	10.61
Na_2SO_4	3.92
$CaCl_2 \cdot 2H_2O$	1.47
KCl	0.66
$NaHCO_3$	0.19
KBr	0.1
$SrCl_2$	0.04
H_3BO_3	0.03

Dilutions with 7, 14, 21 and 28 ‰ water were achieved by adding deionized water to portions containing 480, 360, 240, 120 mL of the stock solutions, respectively, to obtain 600 mL each. For the 0 ‰ medium, 600 mL deionized water was used. 20 mg biomalt and 15 mg agar per litre were added to the solutions and pH was adjusted at 7 by adding NaOH/HCl. After autoclaving for 20 minutes at 121 °C using an H+P Varioklav autoclave, 100 mL of cooled agar solution was poured into Petri dishes 130 mm in diameter. Agar plugs (1 cm^2) cut from pure Petri dish cultures of *Cladosporium allicinum* and *Heydenia* cf. *alpina* were transferred onto the centre of the prepared agar plates. The experiment was performed in triplicates for each salinity level at room temperature (21°C).

3.3 Chromatography

3.3.1 Thin Layer Chromatoraphy (TLC)

Standard chromatograms of extracts and fractions were developed on either TLC aluminum sheets silica gel 60 F_{254} (Merck) as stationary phase using a petroleum ether/acetone mixture in different concentrations or TLC aluminum sheets RP-18 F_{254} (Merck) as stationary phase using a methanol/water mixture in different concentrations, both at room temperature under saturated conditions. Chromatogram detection was accomplished under UV light (λ 254 nm and 366 nm) and using vanillin-sulphuric acid spraying reagent (0.5 g vanillin dissolved in a mixture of 85 ml methanol, 10 ml acetic acid and 5 ml sulphuric acid, TLC plates heated at 100°C after spraying).

3.3.2 Vacuum Liquid Chromatography (VLC)

VLC was used for crude extract fractionation using Bakerbond spe Octadecyl C18 disposable extraction columns. Prepacked plastic columns (dimensions 3 x 1.5 cm) were equilibrated under vacuum using methanol. One gradient solvent system of increasing polarity was used for sample elution, starting with 25% methanol to 50% methanol to 75% to 100% methanol yielding four fractions (1-4). Fractions were collected and concentrated under vacuum (using vacuum rotatory evaporator, 40°C). Fractions 2 and 3 were then subjected to the beforementioned VLC system to yield four subfractions each (2.1-2.4 and 3.1-3.4).

3.3.3 High-Performance Liquid Chromatography (HPLC)

HPLC was performed on a Waters HPLC system equipped with a 1525µ binary pump, a 2998 PDA detector, Breeze 2 software and a Rheodyne 7725i injection system. A Macherey-Nagel Nucleoshell C18 column (250 mm x 4.6 mm; 5 µm), Nucleodur PolarTec column (250 mm x

4.6 mm; 5 µm), Pyramid C18 column (250 mm x 4.6 mm; 5 µm) and Phenomenex Kinetex C18 column (250 mm x 4.6 mm; 5µm) as well as a Phenomenex Aqua C18 column (250 mm x 10 mm; 5µm) were used.

3.4 Structure elucidation

The chemical structures of the isolated compounds were established using one dimensional and two-dimensional NMR techniques along with MS methods. Additional structural information was provided from optical rotation measurements, CD, UV and IR spectroscopy. Database and literature search using MarinLit database®, AntiBase database® and Scifinder database® was performed to determine the novelty of the isolated compounds.

3.4.1 NMR spectroscopy

All NMR spectra were recorded in acetone-d_6 or methanol-d_4 referenced to residual solvent signals with resonances at $\delta_{H/C}$ 2.04/29.8 and $\delta_{H/C}$ 3.35/49.0 respectively, using either a Bruker Avance 300 DPX spectrometer operating at 300 MHz (^{1}H) and 75 MHz (^{13}C) or a Bruker Avance 500 DRX spectrometer operating at 500 MHz (^{1}H) and 125 MHz (^{13}C) and a Bruker Ascend 600 spectrometer operating at 600 MHz (^{1}H) and 150 MHz (^{13}C). Spectra were processed using Bruker Topspin1.3 software, as well as Mestrenova version 8.0.1- 10878 (Mestrelab Research S.L.). ChemSketch version 11.02 (ACD/Labs 2012) was used to compare characteristic chemical shifts of isolated compounds to calculated values. The following NMR experiments: ^{1}H, ^{13}C, DEPT 135, ^{1}H-^{1}H COSY, ^{1}H-^{13}C direct correlation (HSQC), ^{1}H-^{13}C long-range correlation (HMBC) and ^{1}H-^{1}H ROESY, were performed for structural assignment. From DEPT experiments, multiplicity of carbons could be deduced. Additionally, HSQC spectra were used for SMART experiments.

3.4.2 Mass Spectrometry (MS)

HPLC-MS measurements were conducted by E. Egereva (Department of Pharmaceutical Biology, University of Bonn, Germany), employing an Agilent 1100 Series HPLC including DAD, with RP C_{18} column (Macherey Nagel Nucleodur 100, 125 x 2 mm, 5µm) and a 2 mmol NH_4Ac buffered methanol/water gradient elution system (flow rate 0.25 ml min^{-1}), starting from 10% to 100% MeOH over a 20 min period, then isocratic for 10 min. The HPLC system was coupled with an API 2000, Triple Quadrupole LC/MS/MS, Applied Biosystems/MDS Sciex and an ESI source. Samples were dissolved in MeOH (1 mg ml^{-1}) prior to injection.

HRESIMS measurements were conducted by M. Crüsemann (Department of Pharmaceutical Biology, University of Bonn, Germany) using a Bruker Daltonik MicrOTOF-Q II mass spectrometer with an ESI-source coupled to an HPLC Dionex Ultimate 3000 (Thermo Scientific) and a EC10/2 Nucleoshell C18 2.7 µm column (Macherey-Nagel) was used. The column temperature was set to 25°C. MS data were acquired over a range from 100-3000 *m/z* in positive mode. Auto MS/MS fragmentation was achieved with rising collision energy (35-50 keV over a gradient from 500-2000 *m/z*) with a frequency of 4 Hz for all ions over a threshold of 100. HPLC started with 90 % H_2O containing 0.1% HOAc. The gradient starts after 1 min ending up with 100% acetonitrile (0.1% acetic acid) in 20 min. The flow was set to 0.3 mL/min. 5 µL per sample solution (1mg/mL) was injected for each run.

3.4.3 Optical rotation

Optical rotations were measured on a Jasco DIP 140 polarimeter (1 dm, 1 cm^3 cell) operating at wavelength λ=589 nm corresponding to the sodium D line at room temperature. Specific optical rotation $[\alpha]_D^T$ was calculated pursuant to:

$$[\alpha]_D^T = \frac{100 \times \alpha}{c \times l}$$

T: temperature [°C]

D: sodium D line at λ=589 nm

c: concentration [g/100 ml]

l: cell length [dm]

α: optical rotation

Compounds were dissolved in methanol, and the average optical rotation α was based on at least 10 measurements.

3.4.4 UV measurements

UV spectra were obtained using a Perkin Elmer Lambda 40 UV/Vis spectrometer with UV WinLab Version 2.80.03 software, using 1.0 cm quartz cell. The molar absorption coefficient ε was determined in accordance with the Lambert-Beer-Law:

$$A = \varepsilon \times c \times b \Longleftrightarrow \varepsilon = A/(c \times b)$$

ε: molar absorption coefficient [L/mol×cm]

A: absorption at peak maximum

c: concentration [mol L^{-1}]

b: layer thickness of solution [cm]

3.4.5 IR spectroscopy

IR spectra were recorded as film using Perkin Elmer FT-IR Spectrum BX spectrometer, with Spectrum v3.01 software.

3.4.6 CD spectroscopy

ECD spectra were taken on a Jasco J-810 CD spectropolarimeter. The CD (circular dichroism) is measured as ellipticity Θ (in mdeg, millidegrees) and subsequently converted into the molar ellipticity $[\Theta]_M$ and finally into Δε in accordance with the following equation:

$$[\Theta]_M = \Theta \cdot M / 10 \cdot C \cdot d$$

$[\Theta]_M$ = molar ellipticity [degrees · cm^2/dmol]; Θ = ellipticity [degrees]; Mr = molecular weight (g/mol); C = concentration (mg/ml); D = path length (0.1 cm)

Results presented as Δε =[θ]M / 3300

3.5 Bioinformatic tools

3.5.1 Molecular networking

The ethylacetate extracts from cultures of *H.* cf. *alpina* on BM, BMS, SDA, SNA and GMA medium and at 4°C and 25°C, respectively, were analysed with HR-ESI MS/MS. Data files were exported to .mzxml format, and then uploaded to CCMS (ccms.ucsd.edu). A molecular network was created using the online workflow at GNPS (gnps.ucsd.edu). The data were filtered by removing all MS/MS peaks within +/- 17 Da of the precursor *m/z*. MS/MS spectra were window filtered by choosing only the top 6 peaks in the +/- 50 Da window throughout the spectrum. The data was then clustered with MS-Cluster with a parent mass tolerance of 0.02 Da and an MS/MS fragment ion tolerance of 0.02 Da to create consensus spectra.

Further, consensus spectra that contained less than 2 spectra were discarded. A network was then created where edges were filtered to have a cosine score above 0.7 and more than 6 matched peaks. Further edges between two nodes were kept in the network if and only if each of the nodes appeared in each other's respective top 10 most similar nodes. The spectra in the network were then searched against GNPS' spectral libraries. The library spectra were filtered in the same manner as the input data. All matches kept between network spectra and library spectra were required to have a score above 0.7 and at least 6 matched peaks. Results were visualized in Cytoscape 3.4.0 (www.cytoscape.org).

3.5.2 SMART

^{1}H-^{13}C-HSQC experiments for extracts of fungal cultures, as well as fractions thereof, were performed on a Bruker Avance 300 DPX spectrometer operating at 300 MHz (^{1}H) and 75 MHz (^{13}C). Samples were solved in MeOD and spectra processed in Mestrenova version 8.0.1 - 10878 (Mestrelab Research S.L.). Peak lists were prepared and uploaded to the SMART online interface (https://smart.ucsd.edu/classic).

3.6 Biological testing

3.6.1 Agar diffusion assay

Culture plates (5% sheep blood Columbia agar, BD) were overlaid with 3 mL tryptic soy soft agar, inoculated with TSB (Tryptic soy broth, Oxoid) growth suspension of the bacteria to be tested. Compounds were diluted to a concentration of 1mg/mL (Syringomycin 0.5 mg ml^{-1}) with DMSO, and 3 µL of this dilution were placed on the surface of the agar. Compounds diffuse into the agar, and the size of the inhibition zone was measured after 24 hours incubation at 37 °C.

Table 3.11 Bacterial and yeast strains used to assess antimicrobial activity.

Strain	Number
methicillin-sensitive *Staphylococcus aureus* (MSSA)	5185
methicillin-sensitive *Staphylococcus aureus* (MSSA)	I-11574
methicillin-resistant *Staphylococcus aureus* (MRSA)	LT-1334
methicillin-resistant *Staphylococcus aureus* (MRSA)	LT-1338
methicillin-resistant *Staphylococcus epidermidis* (MRSE)	LT-1324
Candida albicans	I-11301
Candida albicans	I-11134
Citrobacter freundii	I-11090
Klebsiella pneumoniae subsp. *ozeanae*	I-10910
Enterococcus faecium	I-11305b
Enterococcus faecium	I-11054
Escherichia coli	I-11276b
Escherichia coli	O-19592
Stenotrophomonas maltophilia	O-16451
Stenotrophomonas maltophilia	I-10717
Pseudomonas aeruginosa	I-10968

Table 3.9 Continued

Strain	Number
coagulase-negative *Staphylococci* (KNS)	I-10925
Staphylococcus simulans	22
Micrococcus luteus	ATCC 4698
Mycobacterium smegmatis	ATCC 70084
Bacillus subtilis	168
Bacillus megaterium	ATCC 13632
Arthrobacter crystallopoietes	DSM 20117
Listeria welchimeri	DSM 20650
Bacillus cereus	Va167198
Corynebacterium xerosis	
Staphylococcus aureus	133
Staphylococcus aureus	

3.6.2 Disk diffusion assay

Antimicrobial tests of isolated compounds were performed by Ekaterina Egereva (Department for Pharmaceutical Biology, University of Bonn, Germany) following the method described by Schulz et al [176]. The bacteria *Bacillus megaterium* and *Escherichia coli* were used as representatives for Gram-positive and Gram-negative bacteria. *Microbotryum violaceum* (Basidiomycete), *Eurotium rubrum* (Ascomycete), and *Mycotypha microspora* (Zygomycete) were used as fungal test organisms.

Raw extracts were dissolved in MeOH to give a concentration of 1 mg/mL per test sample. 50 µL (equivalent to 50 µg) of each solution was pipetted onto sterile filter disks (diameter: 9 mm, Carl Roth GmbH+Co. KG, KA08.1) which was then placed onto the appropriate agar medium and sprayed with a suspension of the test organism. Growth media, preparation of spraying suspensions and conditions of incubation were carried out according to Schulz et al [176]. For tested samples, a growth inhibition zone ≥ 3 mm and/or a complete inhibition ≥ 1 mm, measured from the edge of the filter disk, were regarded as a positive result. Growth inhibition was defined as follows: growth of the appropriate test organism was significantly inhibited compared to a negative control; total inhibition: no growth at all in the appropriate zone. Benzylpenicillin (1 mg ml^{-1} MeOH), streptomycin (1 mg ml^{-1} MeOH) and miconazole (0.5 mg ml^{-1} DCM) were used as positive controls.

3.6.3 Label-free dynamic mass redistribution (DMR) assay for HEK293 cell lines

Dynamic mass redistribution measurements were performed using the Epic® reader (Corning®). 18-24 hours prior to the assay, 30 µl/well of cell suspension were seeded into fibronectin-coated 384-well Epic® biosensor microplates to reach 18 kc/well. Cells were spun down shortly (800 rpm, 10 s). The cells in the microplates were left to grow to a monolayer overnight at 37°C and 5% CO_2. The following day, cells were washed twice with assay buffer. Since DMSO intrinsically evokes a DMR response, the buffer was formulated to contain the same percentage of DMSO as the corresponding compound solutions to help avoid artefacts. During washing, a manifold was used to aspirate medium from the wells. Afterwards, assay buffer was added to a total of 30 µl/well. The prepared plate was loaded onto the DMR reader located in a 37°C incubator and equilibrated for 1 h. In the meantime, compounds were diluted and pipetted into storage plates. The solutions were prepared 4x or 5x over their final concentration, respective to performance of measurement in agonist (single

addition á 10 µl) or antagonist (two additions á 10 µl) mode. To provide enough surplus for the liquid handling system, 25 µL per well were supplied. The prepared compound plates were stored with lids at 37°C. For the Epic® reader to recognize the cell-occupied areas, the cell plate was aligned to the camera within the reader using the Epic® Aligner tool. Subsequently, the measurement was launched using the Epic® Imager software. A baseline was recorded for 300 s, prior to compound addition with the CyBi® Selma, which was also kept in a 37°C environment. The measurement continued for up to 7000 s. Finally, data were transformed using the Transform table to column macro and subsequently copied into Prism. All optical DMR recordings were buffer corrected.

3.6.4 Cell viability

This assay was carried out by Tobias Benkel (working group of Prof. Kostenis, Department for Pharmaceutical Biology, University of Bonn, Germany). HEK293 cells were seeded into a PDL-coated 96-well plate (25.000/well) and allowed to settle for 2 hours prior to addition of the compounds (solubilized in water). After incubating for 22 hours, CellTiter Blue reagent (Promega) has been added. After another 2 hours of incubation, the fluorescence has been detected using FlexStation 3 (Molecular Devices), and data were expressed as percentage of cell viability relative to DMSO control (the cytotoxic anticancer drug etoposide was used as a positive control).

3.7 Chemicals and other materials

3.7.1 Chemicals

Table 3.12 Chemicals used for experiments.

Chemical	Trader
Acetone-d_6	Deutero GmbH (Kastellaun, Germany)
Acetonitrile HPLC grade	VWR International (France)
Boric acid	Roth (Karlsruhe, Germany)
Calcium chloride dihydrate	Sigma-Aldrich (Steinheim, Germany)
Chloroform-d_1	Deutero GmbH (Kastellaun, Germany)
Deuterium oxide	Deutero GmbH (Kastellaun, Germany)
DCM (pure, anhydrous)	Roth (Karlsruhe, Germany)
HPLC- grade water	Bernd Kraft GmbH (Duisburg, Germany)
Magnesium chloride hexahydrate	Merck (Darmstadt, Germany)
Methanol-d_4 (99.8 %)	Deutero GmbH (Kastellaun, Germany)
Methanol (hyper grade for LC/MS)	Merck (Darmstadt, Germany)

Table 3.10 Continued

Chemical	Trader
Methanol (HPLC gradient grade)	Bernd Kraft GmbH (Duisburg, Germany)
Potassium bromide	Sigma-Aldrich (Steinheim, Germany)
Potassium chloride	Sigma-Aldrich (Steinheim, Germany)
Sodium chloride	Roth (Karlsruhe, Germany)
Sodium bicarbonate	Merck (Darmstadt, Germany)
Sodium sulfate	Sigma-Aldrich (Steinheim, Germany)
Strontium chloride	Roth (Karlsruhe, Germany)
Trifluoroacetic acid (TFA) 99.9%	Roth (Karlsruhe, Germany)

3.7.2 Cell culture

Cell culture conditions

Mammalian cell lines were cultivated in an incubator at 37°C in an atmosphere of 5% CO_2 and 96% humidity. All cell culture media and solutions were warmed to 37°C before use. Passaging of cells Cells were passaged according to their growth rate, about 2-4 times per week. Under laminar airflow conditions, medium was removed, cells were washed with PBS, and trypsin was added to cover the cell surface in a thin layer. PDL-treated flasks required the use of higher concentrated trypsin (0.25%). When cells were fully detached, the trypsinisation was stopped by addition of medium. The desired amount of detached cells was either replated or transferred to a new flask and supplied with fresh medium.

Cell counting

To determine the number of cells in suspension, cells were counted in the Neubauer counting chamber. To this end, a given cell suspension was homogenized by vortexing prior to pipetting 10 µl into the area between a coverslip and the counting plate. The amount was determined as cell density [cells/ml] = count x dilution factor x 10^4.

4 Results

Preface

Portions of this chapter were previously published as Libor B., Harms H., Kehraus S., Eguereva E., König G. M., Isolation of fungi using the diffusion chamber device FIND. *Beilstein J. Org. Chem.* 2019*, 15,* 2191-2203. doi:10.3762/bjoc.15.216*, and have been reproduced with permission. Copyright is held by* Beilstein Journal of Organic Chemistry.

4.1 FIND procedure

Inspired by the approach of Epstein et al. we developed the Fungal one step IsolatioN Device (FIND), in order to obtain axenic cultures of rare and underexamined filamentous fungi, as several tries before with the iChip were not successful. Apart from terrestrial soil probes, we focused on the marine habitat, probing sediment and seawater samples for the presence of fungi. For the isolation of fungal strains from terrestrial and aquatic environments a device was constructed, i.e. FIND, that is similar to the one described by Epstein et al. for "unculturable" bacteria [135]. For the FIND we adjusted the isolation procedure and technical features, e.g. the dimensions of the through holes utilized as growing chambers, to fungi. The FIND protocol now suits fungal physiology and the prevalence of fungi in different habitats. In general, the FIND technology is a multi-chambered micro agar plate. After inoculation, the device is placed back into the original natural environment of sample collection, to ensure favourable growth conditions for specific fungi. Inoculation is performed in only one step and thus suitable for high throughput approaches. Figure 4.1 illustrates the FIND, consisting of merely three plastic parts crafted from polyoxymethylene, which are solid and durable enough for use in most natural environments. The central plate is a thin plastic board with 96 through holes that function as compartments, capable of holding inoculated agar plugs.

Semipermeable membranes are attached to both sides of this plate, this way covering the through holes and preventing contamination by other microbes. These membranes, at the same time, permit diffusion of nutrients and growth factors from the environment through the feeding pores of the upper and lower plates. This way slow-growing fungi or to date uncultured fungi can be isolated.

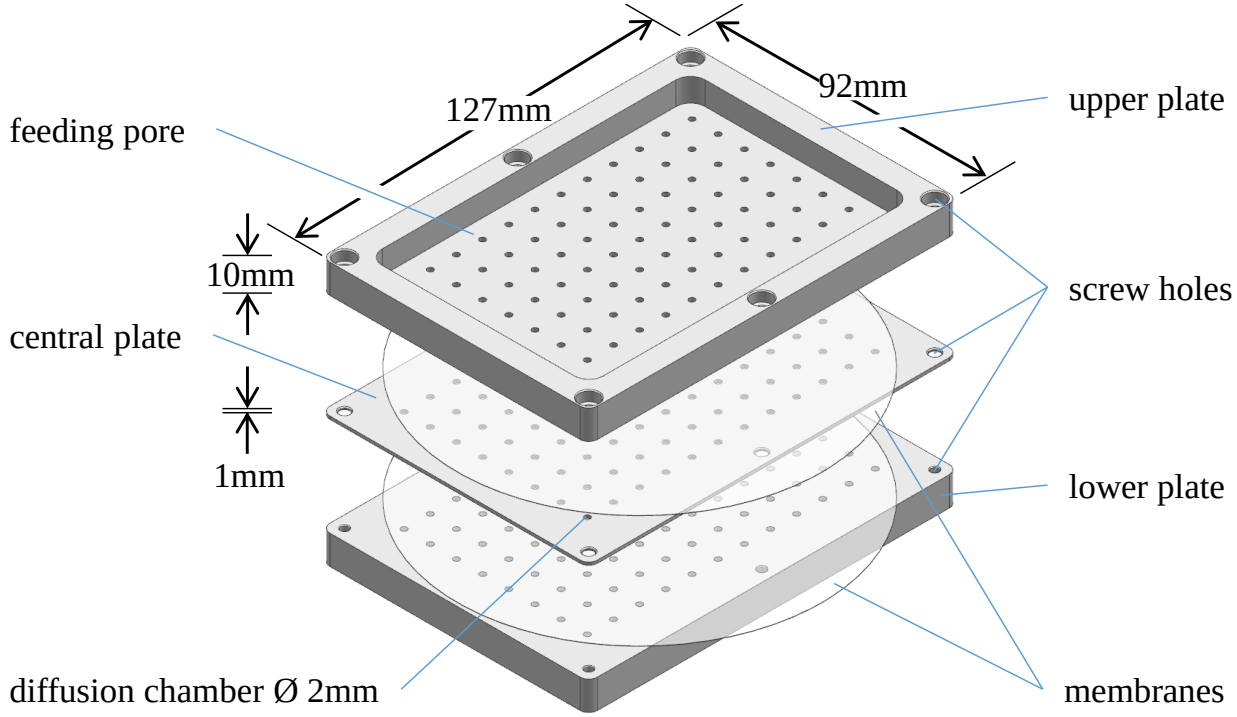

Figure 4.1 Design and functional parts of the FIND technology.

4.2 Isolation of terrestrial and marine-derived fungi via FIND

To test the FIND technology, we used samples from terrestrial and marine environments, i.e., soil from Wuppertal, Germany (experiment 1), marine sediments from the Aegean Sea, Greece (experiment 2), brackish soil samples from the Schlei region around Kappeln,

Germany (experiment 3), and seawater samples from Katwijk aan Zee, Netherlands (experiment 4).

Adjustment of the sample concentration (i.e., number of fungal parts per volume), which is crucial for the success of a FIND experiment, has to take the abundance of fungal parts, i.e., hyphae, mycelial fragments or spores in the collected environmental samples into account. Ideally, for incubation one fungal part per through hole should be present. Thus, for the here presented FIND with 96 through-holes each with a volume of 3×10^{-3} mL, a concentration of 320 000 fungal parts/L must be reached in the agar solution, with which the central plate is loaded. The number of fungi in a given volume of a sample is experimentally hard to determine. We thus counted bacterial cells and applied the ratio of bacteria-to-fungi, which is described in the literature for most environments, to estimate suitable dilution or concentration steps in our experiments. Figure 4.2 illustrates each individual step of a FIND experiment.

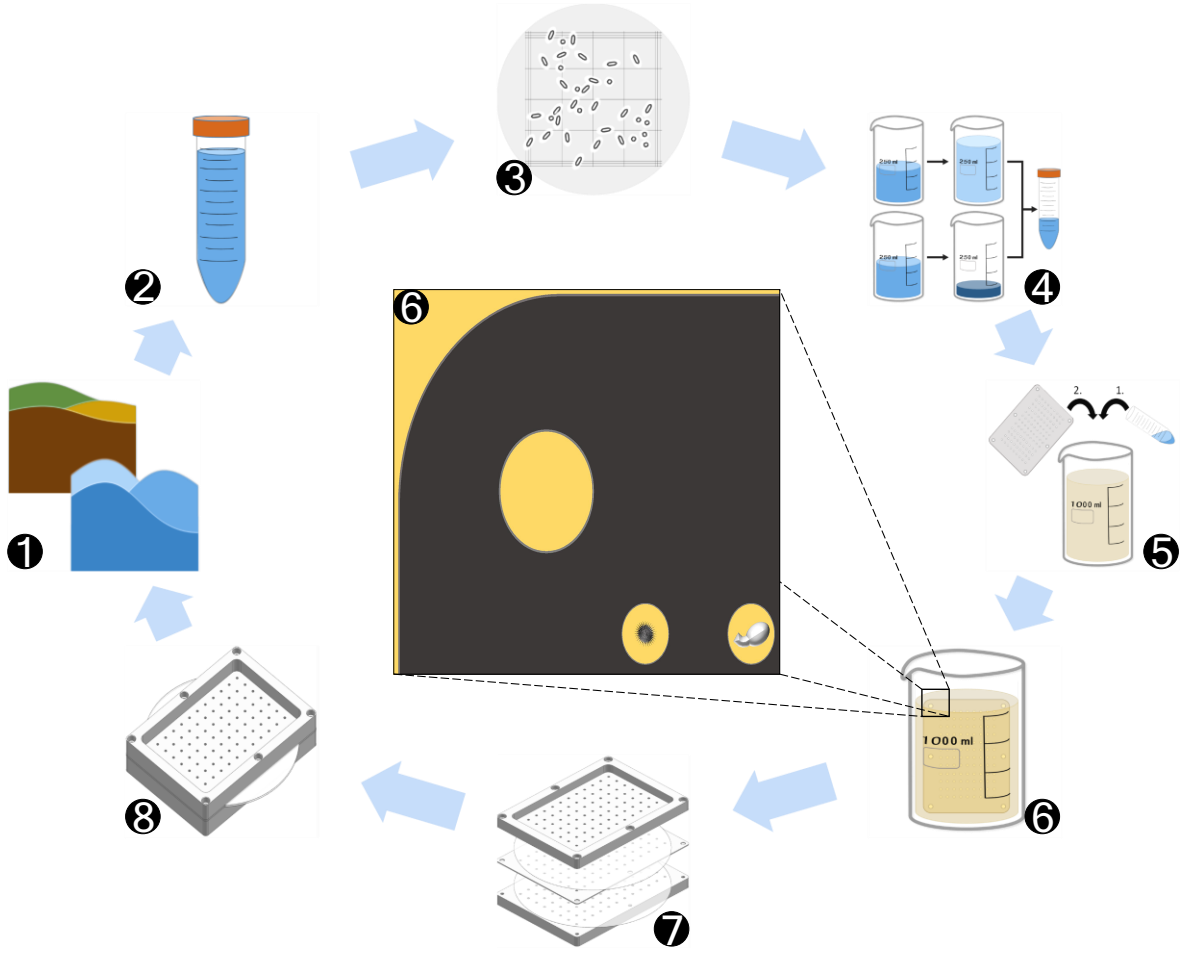

Figure 4.2 Isolation of fungal strains with the FIND technology. 1. Collection of terrestrial or marine sample. 2. Sample preparations. 3. Determination of the number of microbial cells. 4/5. Dilution or concentration of the sample and merging with molten agar. 6. Adjustment of the concentration of fungal parts in such a way that on average, one fungal part is finally placed in one growing chamber. 7. Attachment of semipermeable membranes to the central plate and sealing with upper and lower plates. 8. Placement of the loaded and assembled device into the original environment for incubation.

For experiment 1 (terrestrial soil sample), a small volume of soil was treated with a sterile-filtered isotonic NaCl solution [177,178]. After centrifugation cell counting was performed on the supernatant using a Neubauer Improved or Thoma chamber [179] to determine the abundance of bacterial cells. For our soil sample, $2 \pm 0.25 \times 10^{13}$ bacteria/L were determined. For experiment 2 (marine sediment) and 3 (brackish water sediment), samples were treated alike, but instead of a NaCl solution, seawater from the respective sampling site was used. For experiment 4 (seawater), seawater was analysed directly. The extant abundances of bacterial

cells/L in experiments 2, 3 and 4 were found to be $7 \pm 0.7 \times 10^9$, $13 \pm 5 \times 10^9$ and $8 \pm 0.8 \times 10^9$ bacterial cells/L, respectively.

The samples were then diluted, concentrated or used undiluted according to the bacteria-to-fungi ratio, in order to ultimately reach an approximate target concentration of 320 000 fungal parts/L. Literature documented a bacteria-to-fungi ratio as 10^3 to 1 for terrestrial soil [180]. Thus, the sample from Wuppertal (experiment 1) was diluted sequentially to a concentration of 2×10^{10} bacterial cells/L, which should be equivalent to 2×10^7fungal parts/L, and 16 mL of this solution were necessary to be added to one litre of agar solution to obtain the required target concentration.

For marine sediment samples (experiments 2 and 3), in general, the bacteria-to-fungi ratio was hardly known. Thus, we applied the ratio described for terrestrial soil samples, i.e., 10^3 to 1. With abundances of 7×10^9 and 13×10^9 bacterial cells/L concentrations of 7×10^6 and 13×10^6 fungal parts/L, respectively, were assumed. The samples were thus used undiluted and 42 and 24 mL, respectively, were added to one litre of agar solution to obtain the required target concentration. Using this ratio, in our experiments, however, we had hardly any success (apart from one fungal isolate, i.e., *Cladosporium allicinum* and *Heydenia* cf. *alpina* from samples 2 and 3, respectively). Obviously in these experiments the concentration of fungal parts was too low, and thus we addressed this question in experiment 4 more carefully.

Abundances of around 1000 fungi/L seawater were documented for samples from the North Sea [181,182]. Considering this information, we performed experiment 4 on the assumption of an abundance of 1000 fungi/L, which required fungal cells of 8 L of seawater in a volume of 25 mL agar solution in step 5 of the FIND procedure. Since our bacterial count on this unprocessed seawater sample had revealed an abundance of 8×10^9 cells per L, we ourselves

calculated a bacteria-to-fungi ratio of around 10^7 to 1 for subsurface samples from littoral areas of the North Sea. This is in accordance to literature reports for surface slick and subsurface samples from littoral areas of Florida, where ratios of 10^5 to 1 and higher were determined [183].

Vacuum filtration of the marine water sample (10 L) from Katwijk aan Zee/North Sea through paper disks with a pore size of approx. 2 µm, i.e., wide enough to let pass bacteria, but small enough to concentrate fungal spores and mycelia in the filter cake, was performed. Around 5 mL of filter cake was resuspended in another 5 mL of sterile seawater and mixed with 15 mL agar solution.

In summary, the diluted sample from experiment 1, the undiluted solutions from experiments 2 and 3, and the concentrated, resuspended seawater solution from experiment 4 were each mixed with a warm agar preparation, containing a minimal nutrient medium and antibiotics (experiment 1: amino acids/peptone, antibiotics; experiments 2–4: ditto, but in seawater) to yield the desired concentration of roughly 320 000 fungal parts/L. Then, the central plate of FIND (Figure 4.1) was lowered into these preparations to fill each chamber with an agar solution, containing in average one fungal part. As the agar solidified, the fungal spore or mycelium was trapped in the chamber and separated from other ones, e.g., competing organisms. Semipermeable membranes were attached to both sides of the central plate and the device was sealed with the upper and lower parts and fixed with screws. To guarantee that the device was sealed properly, commercial aquarium safe silicone without antifungal additive was applied to the edges. All materials and tools were sterilized by autoclaving or surface disinfection and the procedure was performed under the laminar airflow cabinet.

The sample-loaded and sealed device was then inserted into an appropriate container with 40 L of the original soil for experiment 1, seawater and sediment from the collection sites for experiments 2 and 3, whereas for experiment 4 (seawater) 20 L of seawater from the sample site were used to mimic environmental conditions of the corresponding sample sites.

At this stage the trapped organisms are separated from each other, but connected to their original environment via semipermeable membranes. This way the fungal seeds are provided with growth factors exclusively found in their natural habitat. The device was incubated for four weeks. Deionized water was applied to the soil of experiment 1 every two days. An aquarium water pump provided water current simulation and evaporated tank water was replaced by autoclaved deionized water in experiments 2–4.After incubation, the device was removed from the tanks, rinsed with autoclaved deionized water to remove sediment and soil and opened under a laminar airflow cabinet. Each agar plug was transferred to a corresponding agar plate for cultivation. The agar plates contained the same minimal nutrient medium as the agar solution into which the central plate was dipped earlier. Alternatively, a stamp can be used to punch all agar plugs simultaneously into the wells of a 96 well plate. Fermentation on agar plates was performed in an incubator at 25 °C for another four weeks. Morphology of the axenic colonies was then analysed microscopically, and their taxonomy was additionally identified by DNA sequencing.

In total, experiments 1–4 led to 76 fungal isolates (41 fungi in experiment 1, 1 fungus in experiment 2, 1 fungus in experiment 3 and 33 fungi in experiment 4). All fungal cultures were obtained in single isolation steps directly via the FIND procedure and found to be axenic. From experiment 1, 39 isolates were microscopically identified as belonging to genera common in soil, e.g., *Fusarium, Penicillium* or *Trichoderma* and thus were not further processed. The addition of antibiotics prevented bacterial contamination in all marine

samples. However, a few antibiotic-resistant strains were isolated from soil but also not further processed. One isolate from experiment 4 was found to belong to the genus *Cladosporium*, and therefore was also not considered further. The remaining 36 isolates were identified at least to the genus level (Table 4.1). The pooled results from comparison (BLAST) of DNA sequences (ITS1, ITS2, 18S, 5.8S, 28S, RPBII, tef1α and β-tubulin) with reference sequences deposited in public databases (GenBank) and microscopical analysis of morphological characteristics, identified 12 ascomycetes from 12 different genera. Except for *Scopulariopsis brevicaulis* (25 isolates), all strains were encountered only once, due to the ideally adjusted microbial concentration and homogenisation of the sample material. Nine of those 12 different isolates could be identified to species level, whereas for the remaining three (*Cadophora* sp., *Chrysosporium* sp., *Leucothecium* sp.) no species could be assigned. In the case of fungi of the genus *Cadophora*, genetic information for all 25 hitherto described species (MycoBank) are deposited in GenBank. As the alignments of our sequences with the best matching ones of a cultured species, e.g., *C. orchidicola* reached only 97% identity in BLAST, it can be assumed that our isolate is an undescribed species, as it shows 99% identity with sequences of an undescribed species (Table 4.1). For the 116 legitimate species of *Chrysosporium*, BLAST of our sequences revealed 99% identity with reference sequences of *Ch. submersum*. Unfortunately, sequences for only 33 *Chrysosporium* species are available as reference sequences, and thus no identification on the species level could be achieved. Interestingly, the sequence of our isolated *Leucothecium* species is 100% identical to the reference sequence of an uncultured fungus isolated from cotton in 2014 and seems to be closely related to the type species *L. emdenii*, which is one of only two known species among *Leucothecium*. Most of the isolates obtained in our experiments belong to the Sordariomycetes, the by far biggest class of ascomycetes, and to the Dothideomycetes. Some of our cultures, however, are from less examined classes, e.g., Eurotiomycetes and

Leotiomycetes. Only *Chaetomium globosum* aggr. comes into consideration as a common air mould.

Table 4.1 Fungal taxa obtained by four FIND experiments and identified by sequence comparison with the best BLASTn match within the NCBI GenBank database.

Species/genus [GenBank accession number]	ID%	Number of bp analysed	Taxonomic Class
Clonostachys rosea (Link:Fries) Schroers et al.[1] [KT323182]	99[a]	506	Sordariomycetes
Ilyonectria europaea A. Cabral, Rego &Crous[1] [JF735294]	100[b]	531	Sordariomycetes
Cladosporium allicinum (Fries) Bensch, U. Braun & Crous[2] [MH118272; MH567104]	100[c]; 100[d]	511; 241	Dothideomycetes
Heydenia cf. alpina[3] [KF574887]	100[a]	549	incertae sedis
Alternaria armoraciae E.G. Simmons & G.F. Hill[4] [KC584638]	100[d]	236	Dothideomycetes
Auxarthron cfr. *umbrinum* (Boudin) G.F. Orr & Plunkett[4] [MH857026]	99[b]	509	Eurotiomycetes
Cadophora sp.[4] [FJ820724; KF636777]	99[b];99[e]	552; 999	Leotiomycetes
Chaetomium globosum aggr.[4] [MH644079; MG890100]	100[f]; 100[g]	380; 585	Sordariomycetes
Chrysosporium sp.[4] [MF939600]	99[h]	538	Eurotiomycetes
Leucothecium sp.[4] [LT608439]	100[i]	200	Sordariomycetes
Metarhizium carneum (Duché & R. Heim) Kepler, S.A. Rehner & Humber[4] [MH864783]	100[b]	624	Sordariomycetes
Scopulariopsis brevicaulis Bainier[4] [LM652465]	100[b]	609	Sordariomycetes

[1]Eskesberg, Wuppertal (DE), soil sample, [2]Aegean Sea (GR), marine sediment, [3]Kappeln (DE), brackish water sediment, [4]Katwijk aan Zee (NL), seawater

[a]18S rRNA gene, ITS1, 5.8S rRNA gene, ITS2, [b]18S rRNA gene, ITS1, 5.8S rRNA gene, ITS2, 28S rRNA gene, [c]ITS1, 5.8S rRNA gene, ITS2, [d]tef1α, [e]28S rRNA, [f]β-tubulin, [g]RPBII, [h]ITS1, 5.8S rRNA gene, ITS2 and 28S rRNA gene, [i]ITS2

4.3 Salinity dependency studies on *C. allicinum* and *H.* cf. *alpina*

In a next series of experiments, we set out to shed light on the halotolerance of our isolates from experiments 2 and 3 by testing their salt tolerance or dependency. Thus, we analysed the growth behaviour of *Cladosporium allicinum* and *Heydenia* cf. *alpina* on agar plates containing growth medium of increasing salinity from 0–35‰ (seawater has a salinity of approx. 35‰). As outcome, the diameter of radial growth was measured after 14 days. All experiments were performed in triplicate on 130 mm agar plates containing bio malt agar medium.

For the isolate from the Mediterranean Sea (experiment 2), i.e., *C. allicinum*, our results showed optimal growth conditions at 35‰ salinity, i.e., a diameter of 107 ± 2 mm was reached. Only poor growth of 54 ± 1 to 89 ± 1 mm was observed at levels of salinity of 14‰ and below (see Figure 4.3).

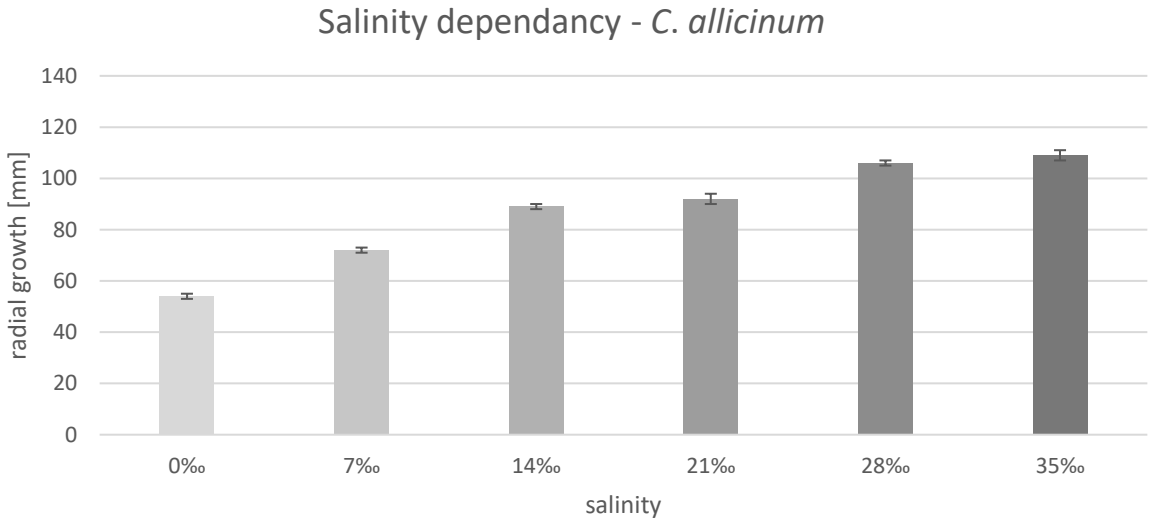

Figure 4.3 Radial growth [mm] of *C. allicinum* at different salinity levels.

For the isolate from brackish water (experiment 3), i.e., *Heydenia* cf. *alpina* levels of salinity above 7‰ were necessary to achieve an adequate growth of 124 ± 1 to 130 ± 0 mm. Below 7‰ salinity the radial growth rates of latter cultures dropped dramatically to only 67 ± 1 mm in diameter (see Figure 4.4).

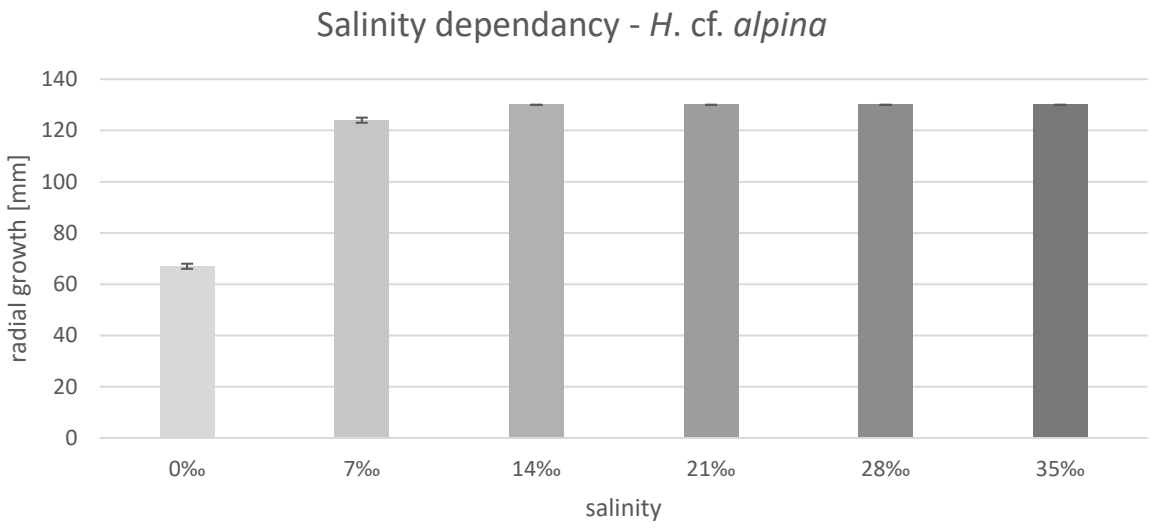

Figure 4.4 Radial growth [mm] of *H. alpina* at different salinity levels.

In both cases, growth rates were nearly halved when the growth medium was lacking appropriate concentrations of sea salts. Our results show that these fungi require high salt concentrations for optimal growth, and this suggests an adaption of the respective strains to marine conditions.

4.4 OSMAC approach for the culturing of *Emericellopsis* cf. *minima*

The production of secondary metabolites, especially the enzymes responsible for their biosynthesis, were introduced in Chapter 1 of this thesis. It was also mentioned, that the genetic information for protein expression, i.e. enzyme expression, is found in BGCs. Advances in gene sequencing, e.g. next-generation sequencing (NGS) and bioinformatic tools for genome mining, e.g. antiSMASH, evidenced the imbalance between BGCs encoding for specialised metabolites and the corresponding isolated compounds [184-187]. The reason for the lack of production of certain natural products lies in the functional state of the BGC. In order to save resources and energy, fungi produce certain secondary metabolites only, if external influences cause the expression state of respective genes to change from silent to active [188]. These influences can be of physical nature, e.g. temperature, humidity, osmotic pressure, radiation, or of chemical nature, e.g. lack of nutrients, inaccessible nutrient sources, signalling molecules, pheromones [189].

In order to investigate the production of bioactive secondary metabolites produced by *E.* cf. *minima* under different culture conditions, the OSMAC approach was conducted on cultures of the strain 809. OSMAC, short for One Strain MAny Compounds, describes a series of culture experiments performed under altered conditions [190]. This way, the strain is challenged with varying stresses that are thought to lead to differential expression of biosynthetic genes, and, in consequence to the production of different specialised metabolites.

The culture scheme contained four various culture media, i.e. MPY, BMS, TE and BPM (see Chapter 3.2.1), as well as two different microorganisms for co-culturing, i.e. *B. mega*, *E. coli*. The culture took place in 12 well plates (see Figure 4.5). BMS and MPY served as standard

cultivation media for marine-derived fungi, TE medium as a nutrient-poor and BPM as a nutrient-rich medium. All experiments were performed in triplicates, and blank medium samples were treated alike. The acetone extracts of all cultures were analysed individually, extracts of the blank medium samples were combined. All extracts were concentrated to 1 mg ml^{-1} and subjected to agar diffusion assays, in order to elucidate the effect of the culture conditions on the bioactivity against *Bacillus megaterium*.

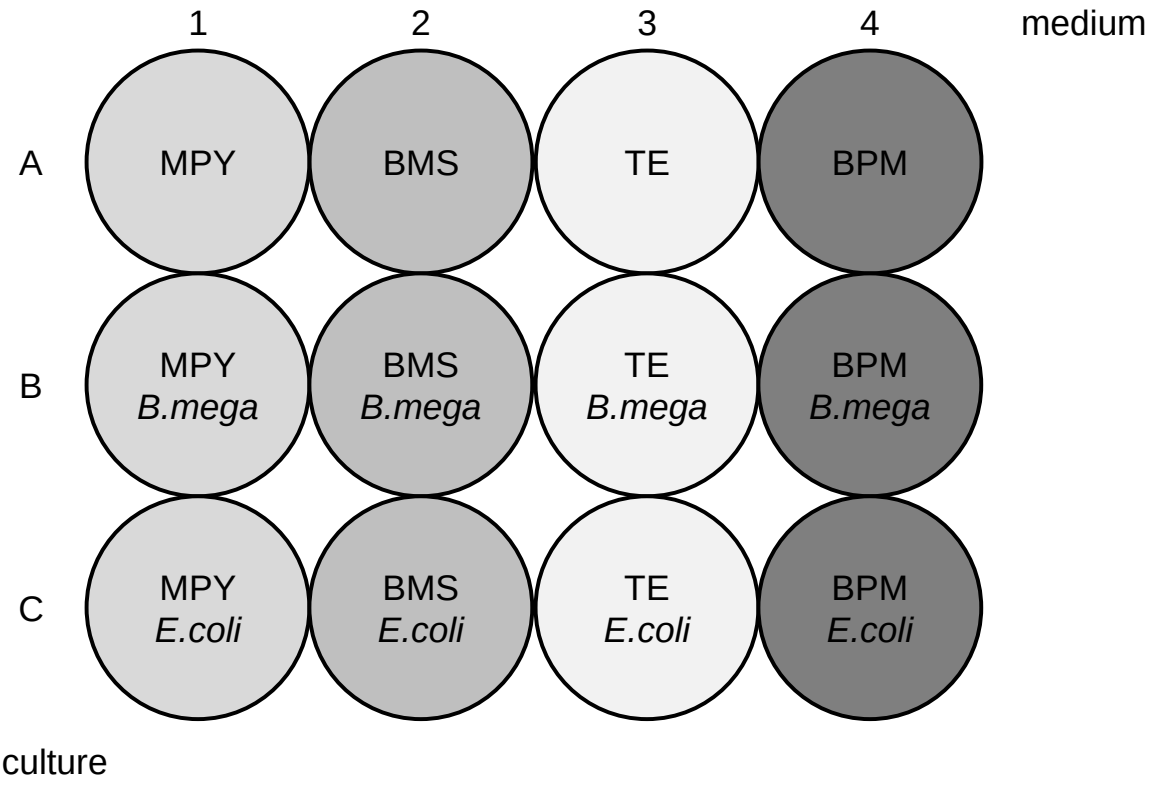

Figure 4.5 Culture scheme for OSMAC approach of *E*. cf. *minima* 809 in 12 well plates; four different media (1 – Malt-Peptone-Yeast, 2 – Biomalt Salt, 3 – Tennelin minimal medium, 4 – Pharmamedia-glycerol complex medium) and three different co-culture states (A - no co-cultivation, B – co-cultivated with *Bacillus megaterium*, C – co-cultivated with *Escherichia coli*).

The blank extracts of the four culture media (no fungal metabolites) showed no bioactivity against *B. megaterium* in respective disk diffusion assays (see Chapter 3.6.2). Additionally, no significant effect on the bioactivity could be observed regarding the co-cultivation experiments ($p < 0.01$) compared to the monocultures (see Figure 4.6). Activity of the extract was significantly increased when the strain was cultured on BPM medium. Bioactivity-guided fractionation of extracts from those BPM cultures revealed strong activity in the unpolar fraction. The high content of glycerol in the BPM medium made further separation with chromatographic tools difficult and was therefore suspended. However, the positive effect of culture medium inspired us to expand an OSMAC approach on a strain obtained by FIND (see chapter 4.5)

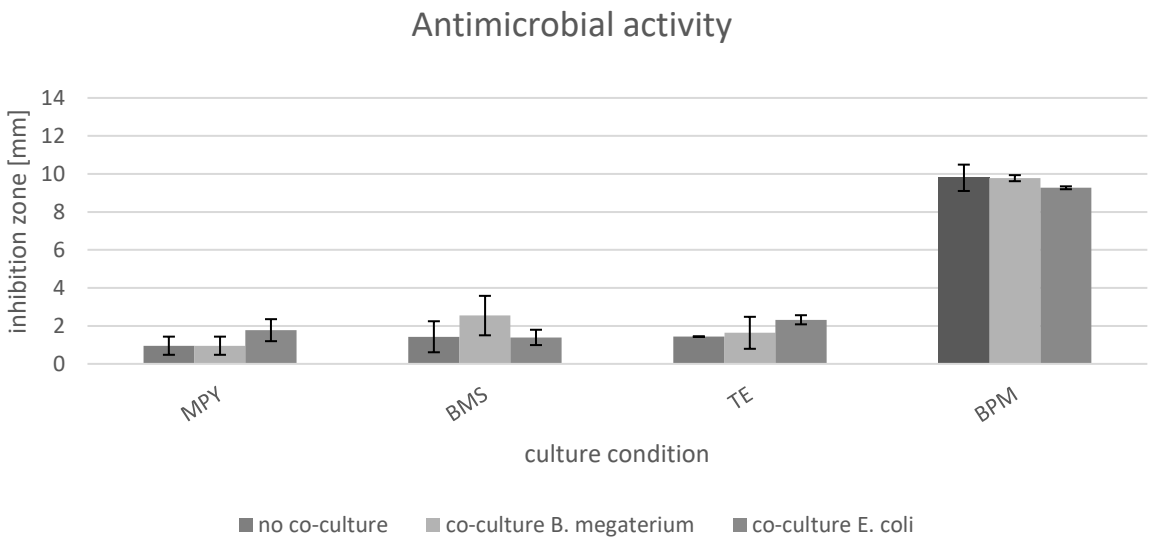

Figure 4.6 Bioactivities of extracts from the OSMAC approach of *E.* cf. *minima* against B. megaterium, sorted by culture medium, i.e. Malt-Peptone-Yeast (MPY), Biomalt Salt (BMS), Tennelin minimal medium (TE), Pharmamedia-glycerol complex medium (BPM) and co-cultivation state, i.e. no co-culture, co-cultured with B. megaterium and co-cultured with *E. coli*.

4.5 Growth quality and psychrotolerance, OSMAC approach and bioinformatic analysis of *Heydenia* cf. *alpina*

Based on the promising results of the OSMAC approach on cultures of *E*. cf. *minima* 809 (see Chapter 4.4), a second experiment was performed on cultures of the strain *H*. cf. *alpina* 824. The composition of the culture media was changed, in order to investigate the differences in bioactivity, depending on the salinity of the medium (BM/BMS), as well as the nutrient content (SNA/SDA). As Cocultivation had no significant effect in the previous experiment, this culture condition was replaced with temperature (25°C/4°C) as an alternative growth condition. Gesteinsmehl agar (GMA) medium was used to mimic environmental conditions, e.g. naked silicate rock, on which the type species of the genus, i.e. *H*. *alpina* Fresenius was found [191]. In order to analyse changes in the metabolome under the beforementioned modifications of the culture conditions, ethyl acetate extracts of all cultures, as well as medium blanks were prepared, and high-resolution tandem mass spectra were measured of all extracts. Table 4.2 gives an overview of the culture medium and the temperature of a given culture, as well as the abbreviation of the corresponding extract. In the following, the abbreviations are used to refer to the specific extracts.

Table 4.2 Overview on extracts of cultures of *Heydenia* cf. *alpina* 824, culture temperature and abbreviation of extracts

Culture medium and fungal strain	Temperature [°C]	Abbreviation
Biomalt + *Heydenia* cf. *alpina* 824	25	BM25
Biomalt + *Heydenia* cf. *alpina* 824	4	BM4
Biomalt	25	BMblank
Biomalt salt + *Heydenia* cf. *alpina* 824	25	BMS25
Biomalt salt + *Heydenia* cf. *alpina* 824	4	BMS4
Biomalt salt	25	BMSblank
Synthetic Nutrient-poor Agar + *Heydenia* cf. *alpina* 824	25	SNA25
Synthetic Nutrient-poor Agar + *Heydenia* cf. *alpina* 824	4	SNA4
Synthetic Nutrient-poor Agar	25	SNAblank
Sabouraud Dextrose Agar + *Heydenia* cf. *alpina* 824	25	SDA25
Sabouraud Dextrose Agar + *Heydenia* cf. *alpina* 824	4	SDA4
Sabouraud Dextrose Agar	25	SDAblank
Gesteinsmehl Agar + *Heydenia* cf. *alpina* 824	25	GMA25
Gesteinsmehl Agar + *Heydenia* cf. *alpina* 824	4	GMA4
Gesteinsmehl Agar	25	GMAblank

For all conducted experiments in this chapter, the beforementioned extracts were used. However, this chapter was divided into subchapters, as different aspects were investigated, i.e. the growth quality of the fungal cultures on various culture media and different temperatures (Chapter 4.5.1), differences in the antimicrobial activity of the extracts (Chapter 4.5.2), the

production of secondary metabolites by *Heydenia* cf. *alpina* 824 in general (Chapter 4.5.3) and differentiated depending on the culture conditions (Chapter 4.5.4).

4.5.1 Determination of growth quality under OSMAC conditions and psychrotolerance

The quality of fungal growth (e.g. density of mycelium, growth speed) was determined, in order to combine this information with the results from bioactivity assays and molecular networking, later on. BMS agar medium, containing artificial seawater, is a standard culture medium composition for marine-derived fungi. With BM agar medium, produced with distilled water instead of artificial seawater, the influence of the lack of salinity on the metabolome, was examined. SDA was chosen as a full medium, i.e. rich in nutrients, in contrast to SNA, which, as a minimal medium, offers only essential amounts of carbohydrates and nitrogen. This way, the effect of excess and shortage in nutrients was observed. Additionally, to determine the psychrotolerance of *H.* cf. *alpina* 824, cultures plates were also stored at 4°C.

Pieces of agar were cut from preculture plates of *H*. cf. *alpina* 824 and placed in the centre of the culture plates for the OSMAC experiment. During the incubation period, three culture plates of each medium type were observed daily for radial growth in order to create growth curves. Cultures grown on GMA agar were left out in this experiment, because three agar plugs were placed on each plate, to ensure evenly spreading of mycelium across the plates. Figure 4.7 summarises the growth curves of the cultures on BMS, BM, SDA and SNA solid medium at 25°C and 4 °C.

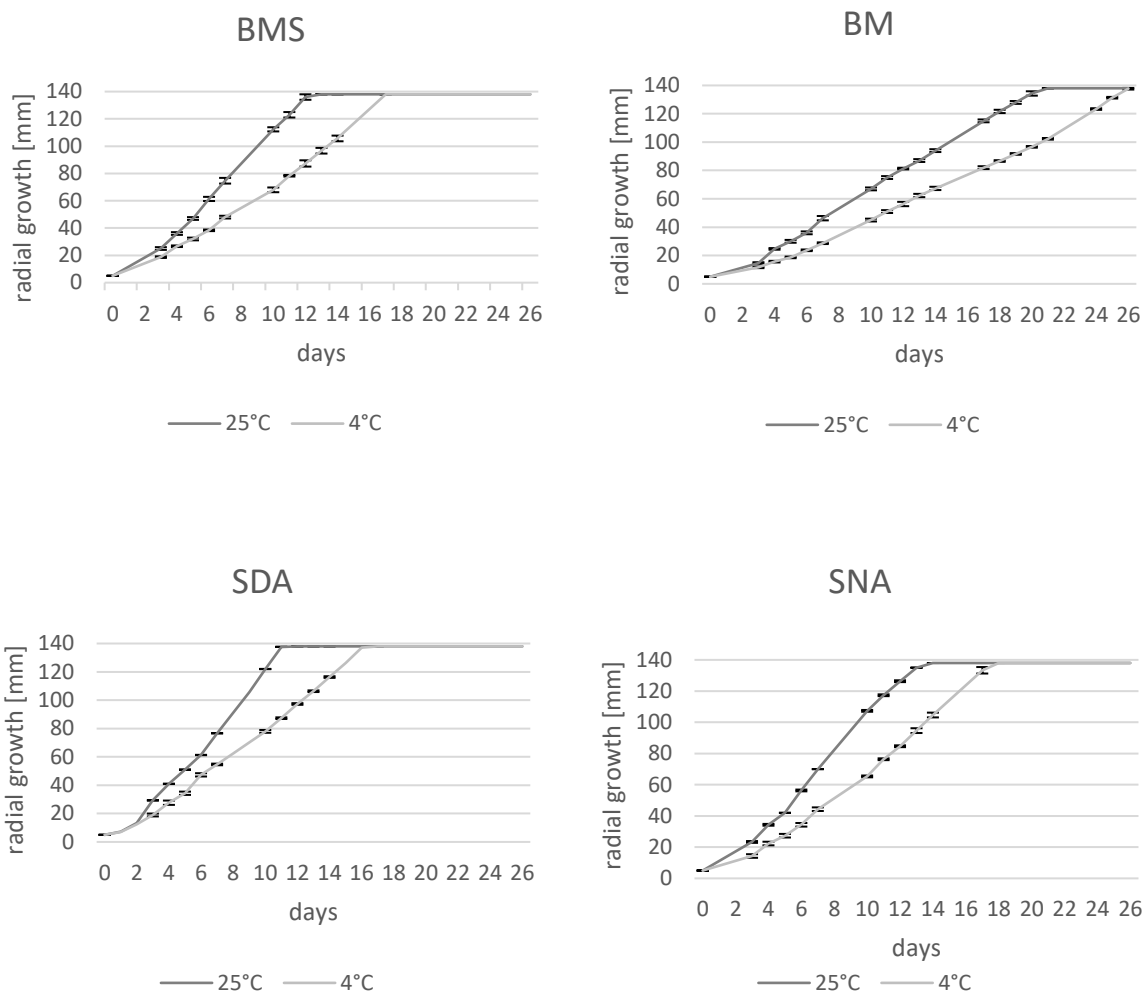

Figure 4.7 Growth curves of *H.* cf. *alpina* cultured on different media at two different temperatures. Covering of the whole plate (138mm) by mycelium was determined as the endpoint, which was achieved after 11 – 26 days.

The majority of fungi are mesophilic, meaning they show a growth optimum at temperatures between 25°C and 30°C [192]. Fungi growing at higher temperatures are either extremophiles adapted to tropic and desert regions, e.g. thermotolerant (growth up to 40°C) or thermophile (no growth below 20°C) fungi, or pathogens, that acclimated to the body temperatures of their warm-blooded hosts [193]. Mesophilic fungi, additionally, do not grow at temperatures below 15°C. Fungi growing at temperatures down to 0°C, but grow best at temperatures at around

20°C are determined psychrotolerant. Only those species with a growth optimum below 15°C are considered to be psychrophilic.

In general, growth was observed on all plates, regardless of medium composition or temperature. Overall, minor growth was detected at 4°C, compared to 25°C. Cultures spread across the plates in shortest time on the full medium SDA, and the mycelium was the densest, either. The plates were entirely covered with a tight white network of mycelium after 11 and 17 days, at 25°C and 4°C, respectively. On the standard medium BMS the maximum extension was reached after 13 and 17 days, respectively, whereas cultures on the minimal nutrient medium SNA took one day longer on average. Interestingly, mycelial growth on the latter medium was observed exclusively below the surface of the agar plate, only little ramified, heading towards the edges of the dishes in a star-shaped pattern. Due to the lack of nutrients, the cultures appeared heavily stressed. The unusual slow growth on BM medium was in accordance with the experiments on the salinity dependency (see chapter 4.3). Mycelia reached the edges of the BM plates after three weeks at 25°C and after four weeks at 4°C.

It was shown, that the strain *Heydenia* cf. *alpina* 824 is able to grow at temperatures below 15°C. In contrast, the temperature optimum, although not determined, seems to be at temperatures over 15°C. The strain *Heydenia* cf. *alpina* 824 can, therefore, be classified as psychrotolerant.

4.5.2 Bioactivity of extracts from different media

In a next series of experiments, the effect of the culture conditions on the bioactivity of this strain was investigated. After four weeks of cultivation, the plates (conditions see above) were extracted exhaustively with ethyl acetate to yield ten extracts, i.e. BM25, BM4, BMS25, BMS4, SDA25, SDA4, SNA25, SNA4, GMA25, GMA4 (See Table 4.2). Blank medium

plates, i.e. not inoculated with agar pieces from preculture plates, were treated alike, i.e. BMblank, BMSblank, SDAblank, SNAblank, GMAblank (See Table 4.2). Disk diffusion assays were performed using 50 µL of the extracts adjusted to a concentration of 10 mg mL^{-1}, resulting in 500 µg per disk. Each extract was tested in triplicates. Disks were placed on NB medium agar plates and sprayed evenly with a cell suspension containing *B. megaterium*, according to Schulz et al [176]. Plates were incubated at 37°C in an incubator for 24 hours. Inhibition zones were measured using a digital calliper and are displayed in Figure 4.8.

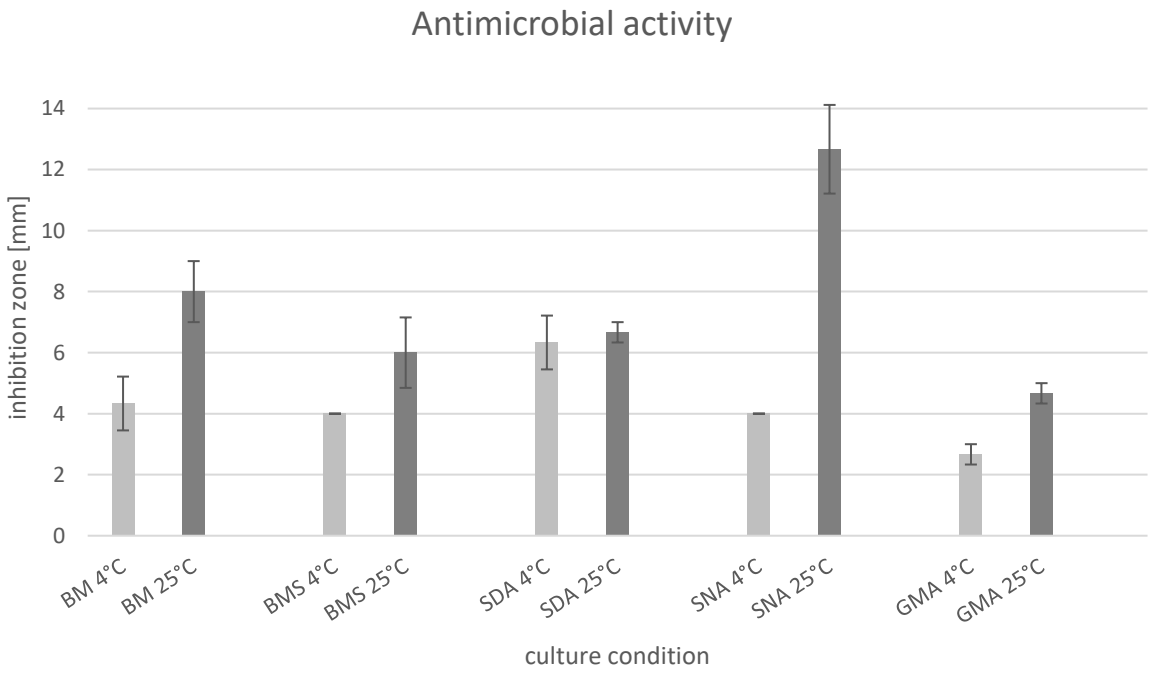

Figure 4.8 Bioactivity against *B. megaterium* of extracts of cultures of *H.* cf. *alpina* under various culture conditions: Biomalt (BM), Biomalt Salt (BMS), Sabouraud Dextrose Agar (SDA), Synthetic nutrient-poor Agar (SNA), Gesteinsmehl Agar (GMA), each at 4° Celsius and 25° Celsius, respectively. Extracts of medium blanks showed no activity.

All extracts of fungal cultures showed activity against the *B. megaterium*. Extracts of the blank media showed no activity. In general, extracts of plates cultivated at 25°C showed higher activities than those cultivated at 4°C, except for SDA extracts ($p < 0.01$). The most striking difference in bioactivity was observed in the extracts of the plates cultured on the

minimal medium SNA at 25°C, which show significantly increased inhibition zones (12 mm) compared to the one incubated at 4°C (4 mm) ($p < 0.01$). The zones are also significantly increased compared to the cultures from all other media compositions ($p < 0.01$).

In conclusion, these results show decreased antimicrobial activity of extracts from cultures stored at lower temperature (4°C) and very scarce nutrient levels (GMA), increased activity when lacking appropriate (7‰, see Chapter 4.3) salinity levels (BM) and at limited nutrient levels (SNA). No effect on the antimicrobial activity could be observed at excessive nutrient levels (SDA).

4.5.3 Visualisation and dereplication of natural products from extracts using bioinformatic tools – example *Heydenia* cf. *alpina*

In order to visualise large sets of mass spectrometric fragmentation data, molecular networks can be produced using the Global Natural Products Social (GNPS) molecular networking platform [194]. With the help of a molecular network already known compounds can be detected (dereplication), structural analogues of isolated compounds are identified and it is possible to conclude the influence of the culture conditions on the metabolomic level. For those purposes, the ethyl acetate extracts of all cultures (see Chapter 4.5.2) were solved in LCMS grade methanol, adjusted to a concentration of 1mg mL^{-1} and measured with HR-LCMS/MS to obtain high-resolution spectra. To differentiate between true fungal metabolites and media constituents, ethyl acetate extracts of the corresponding culture media were prepared and treated alike. The molecular network of data collected from the extracts of the OSMAC approach on the strain *H.* cf. *alpina*, created via GNPS, was visualised in Cytoscape, in which a total of 1156 tandem MS spectra were organised according to their similarity in fragmentation patterns [194]. Seventy-four discrete clusters were determined, in which each

consensus MS/MS spectrum is displayed as a node (circle), labelled with the precursor mass. The size of a node correlates to the number of scans of the respective spectrum. The relatedness between two or more spectra (cosine score) is expressed by edges (lines) connecting two or more nodes, respectively, indicating cosine similarity, where a cosine score of 1 represents identical spectra and a cosine score of 0 denotes no consensus in compared spectra [195]. Alternatively, the mass difference is displayed as Δ*m/z*. Spectra that were not observed multiple times or that did not build sufficient fragments were displayed as nodes with edges not connecting to other nodes (self loops), called singletons [196]. Figure 4.9 summarises all spectra collected of the extracts BM25°C, BM4°C, BMS25°C, BMS4°C, SDA25°C, SDA4°C, SNA25°C, SNA4°C, GMA25°C, GMA4°C, BMblank, BMSblank, SDAblank, SNAblank, GMAblank.

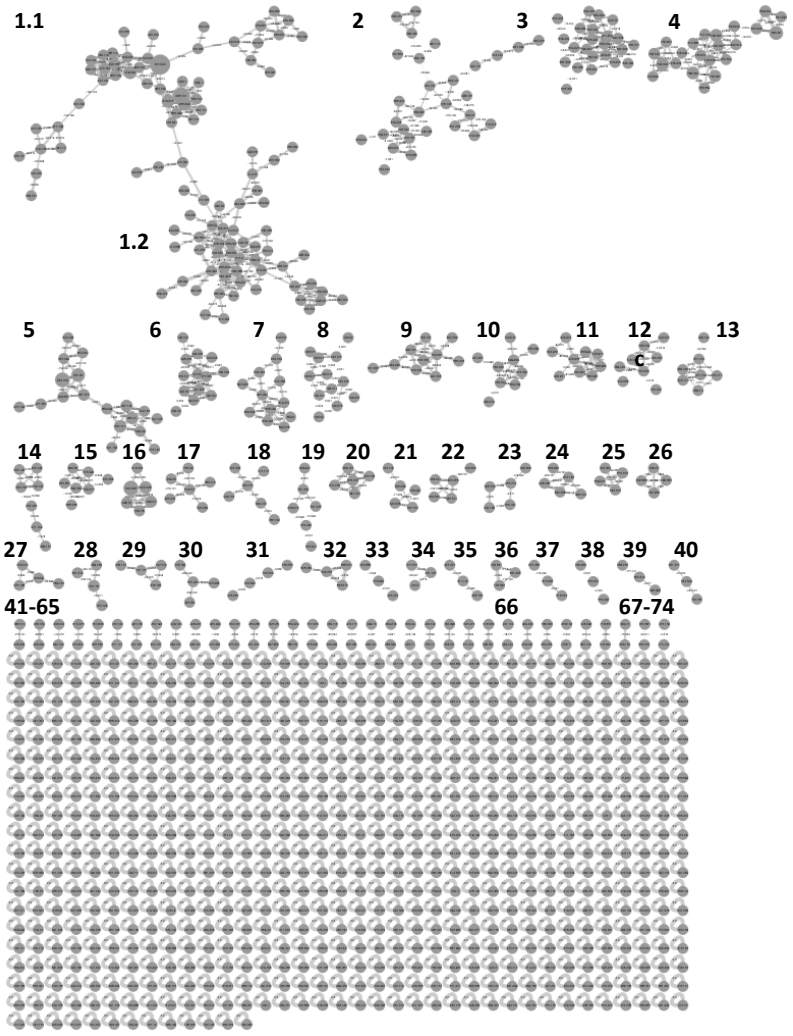

Figure 4.9 Molecular network containing all MS/MS spectra of the extracts BM25°C, BM4°C, BMS25°C, BMS4°C, SDA25°C, SDA4°C, SNA25°C, SNA4°C, GMA25°C, GMA4°C, BMblank, BMSblank, SDAblank, SNAblank, GMAblank, created with Cytoscape. Molecules sharing the same structural class appear as clusters (1.1.-74), those that show unique fragmentation patterns appear as single nodes (self loops).

The GNPS system is able to recognize fragmentation patterns of spectra from samples, here extracts of cultures of *H*. cf. *alpina*, cultured under various conditions, and to match them against all publicly available data reference spectra from data libraries (community-aquired), providing the user with useful information about the chemical structures of the analysed compounds [194]. These library hits are used for dereplication purposes, i.e identification of

known compounds, as well as to evaluate compound classes of unidentified compounds. Thus, all matches kept between network spectra and library spectra were required to have a score above 0.7 and at least 6 matched peaks. Annotation of single nodes is interesting enough, annotation of whole clusters leads to a comprehensive insight into the metabolome of the investigated organism. Therefore, the MolNetEnhancer workflow was used, which combines the output of the network with genome mining tools, e.g. MS2LDA, in silico annotation tools, e.g. DEREPLICATOR and the automated chemical classification by ClassyFire to create a full range view of the metabolome [197]. MolNetEnhancer is able to discover molecular families (MF) by adding the information on substructures achieved through MS2LDA to the GNPS molecular network [197]. MS2LDA however, recognizes frequently occurring fragmentation patterns of substructures (Mass2Motifs), enabling annotations of compounds with no reference spectra [198]. DEREPLICATOR and DEREPLICATOR+ are in silico annotation tools, comparing experimental data to library spectra [199]. Suggested library hits from both, the GNPS molecular network and the enhancement operations were validated carefully, and clusters were annotated accordingly (see Figure 4.10) [200].

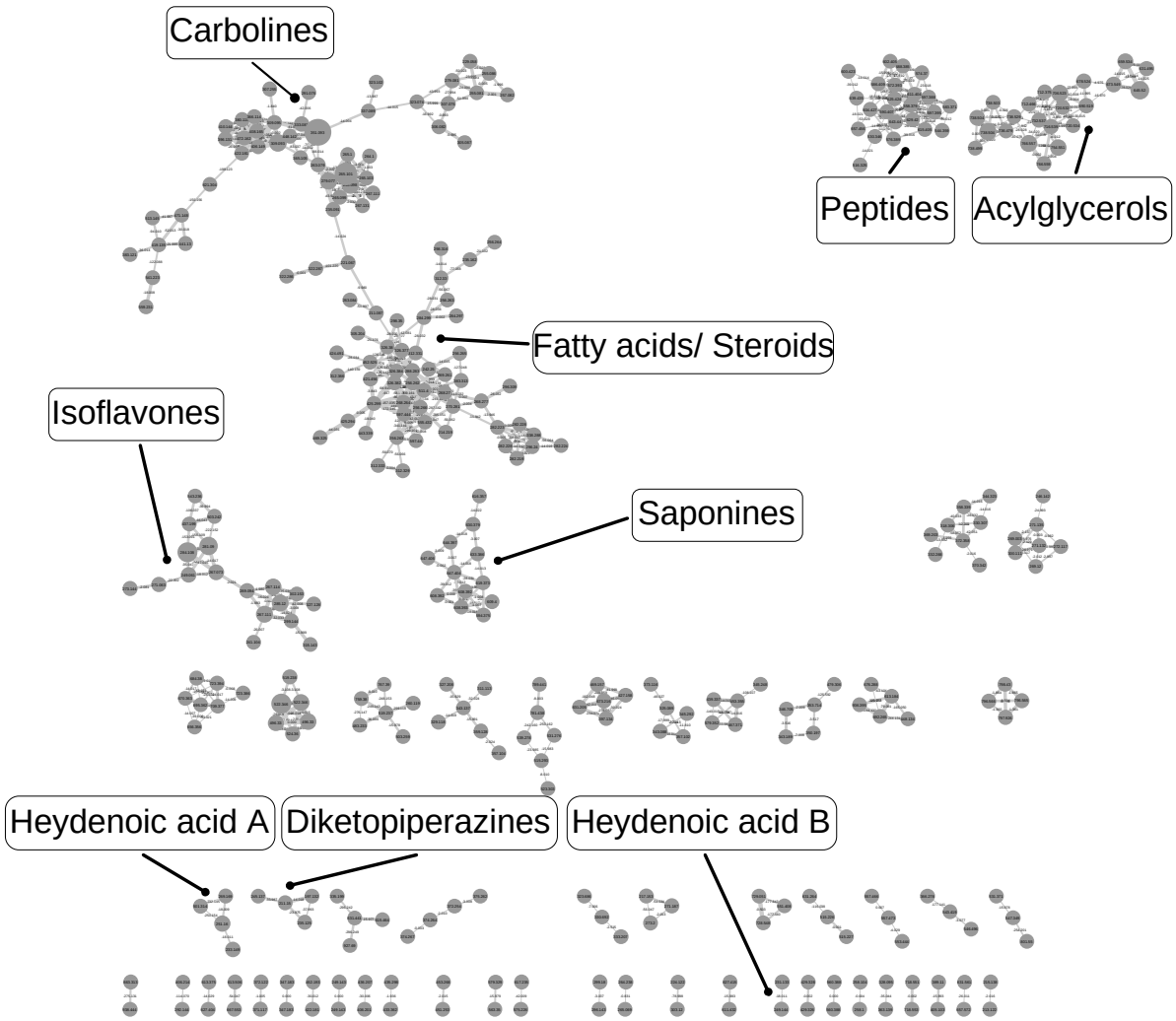

Figure 4.10 Molecular network containing all MS/MS spectra of the extracts BM25°C, BM4°C, BMS25°C, BMS4°C, SDA25°C, SDA4°C, SNA25°C, SNA4°C, GMA25°C, GMA4°C, BMblank, BMSblank, SDAblank, SNAblank, GMAblank, created with Cytoscape. Spectral clusters of compounds from the culture medium and singletons were excluded. Clusters were annotated according to in silico dereplication tools, e.g. GNPS library hits, MolNetEnhancer, as well as our own spectral collection.

The bioinformatic tools and workflows revealed a comprehensive insight into the metabolome of *H*. cf. *alpina* under several culture conditions. In the following, a detailed analysis of a selection of the individual main compound clusters was performed.

Cluster 1.1 – Carbolines

The first cluster of the molecular network, i.e. cluster 1 (see Figure 4.10), was divided into two subclusters, i.e. cluster 1.1 – carbolines (Figure 4.11) and cluster 1.2. – fatty acids/ steroid derivatives (Figure 4.13). In cluster 1.1. several spectra were aligned with those of compounds belonging to a group incorporating the β-carboline skeleton (see Figure 4.11).

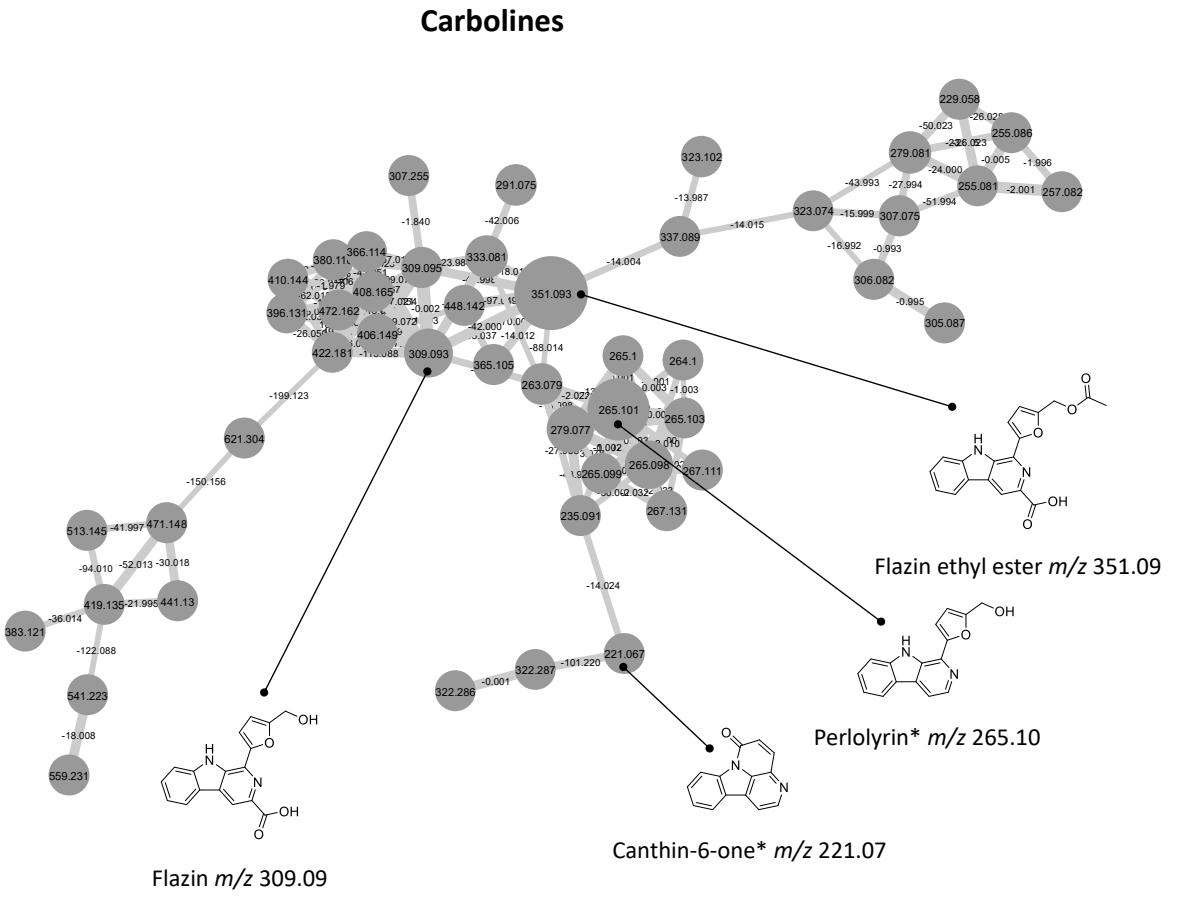

Figure 4.11 Molecular network containing all MS/MS spectra of the extracts BM25°C, BM4°C, BMS25°C, BMS4°C, SDA25°C, SDA4°C, SNA25°C, SNA4°C, GMA25°C, GMA4°C, BMblank, BMSblank, SDAblank, SNAblank, GMAblank, created with Cytoscape. Detailed view on Cluster 1.1. – Carbolines. Structures with an asterisk (*) are suggested by interpretation of the *m/z* values and their relation to dereplicated compounds in the network.

Harmalin, first isolated from the seeds of *Peganum harmala* (Zygophillaceae, Syrian Rue), gave this compound class the name harman alkaloids [201]. In general compounds of this group of natural compounds are widely distributed among plants, insects, marine organisms and mammals [202]. On the contrary, information about harman alkaloids from fungi are rather scarce and only for the entomopathogenic fungus *Conidiobolus coronatus* production of harman and norharman was reported [203]. Apart from their environmental roles as plant growth modulators, insecticidal and insect repellant agents and their antimicrobial properties, β-carbolines showed diverse effects in humans, ranging from general psychoactivity to specific modulation of enzymes present in the central nervous system [204]. In this study, the harman alkaloids harman *m/z* 183.09 $[M+H]^+$ and norharman *m/z* 169.10 $[M+H]^+$ were dereplicated in extracts of *H.* cf. *alpina*.

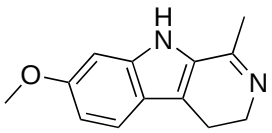

Harmalin

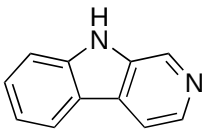

Norharman

Figure 4.12 Structure of harman alkaloids dereplicated in extracts of *H.* cf. *alpina* by GNPS molecular networking.

Also belonging to the β-carboline class of natural products, flazin was dereplicated, occurring in the extracts of several cultures. Isolated initially as a plant metabolite, it was not surprising that flazin, with the *m/z* value of 309.09 $[M+H]^+$, as well as the decarboxylation product perlolyrin *m/z*: 265.10 $[M+H]^+$, were determined in the extracts of the culture media, as these often contain legumes, e.g. soy (see Figure 4.11) [205].

Interestingly, a compound with an *m/z* value of 351.09 $[M+H]^+$ was displayed within this cluster, suggesting an acetylated furanyl substructure. After HPLC separation, aiming to isolate compounds from this cluster, a compound with this annotated mass was isolated. NMR

structure elucidation revealed indeed an acetylated flazin type molecule, which was named flazin ethyl ester (see Chapter 4.7). Flazin was isolated from Japanese soy sauce [206]. Flazin methyl ester, isolated from a *Streptomyces* strain, showed weak nematocidal and insecticidal activities against *Caenorhabditis elegans* and *Artemia salina* [207]. As flazin ethyl ester could not be detected in the extracts of the growth media, it was assumed, that it was synthesised by the fungus, or more likely, flazin from the growth media was derivatised. Nodes within this cluster that are connected to that of flazin ethyl ester through edges show very high cosine scores of up to 0.9. These nodes display derivatives of flazin ethyl ester, showing *m/z* values of 365.10 $[M+H]^+$ (methylated), 337.09 $[M+H]^+$ (deoxygenated), 333.08 $[M+H]^+$ (dehydrated), which support this hypothesis (see Figure 4.11).

The fragmentation pattern of the compound canthin-6-one, from the GNPS library, matched the one of a compound from the network with an *m/z* value of 221.07 $[M+H]^+$ (cosine: 0.83). It contains the carboline skeleton but is made up out of four rings, instead of only three, resulting in fragments differing from those of the other carbolines and its spectrum also clustered with those of steroids. Its node was thus placed between nodes of carbolines and nodes of steroids (see Figure 4.11).

Cluster 1.2 – Fatty acids/ Steroids

Secondary metabolites often share biosynthetic pathways with primary metabolites. In natural product chemistry, dereplication of primary metabolites is a major issue, as isolation and structure elucidation can be time-consuming. It is therefore beneficial to invest a look into the metabolome beforehand.

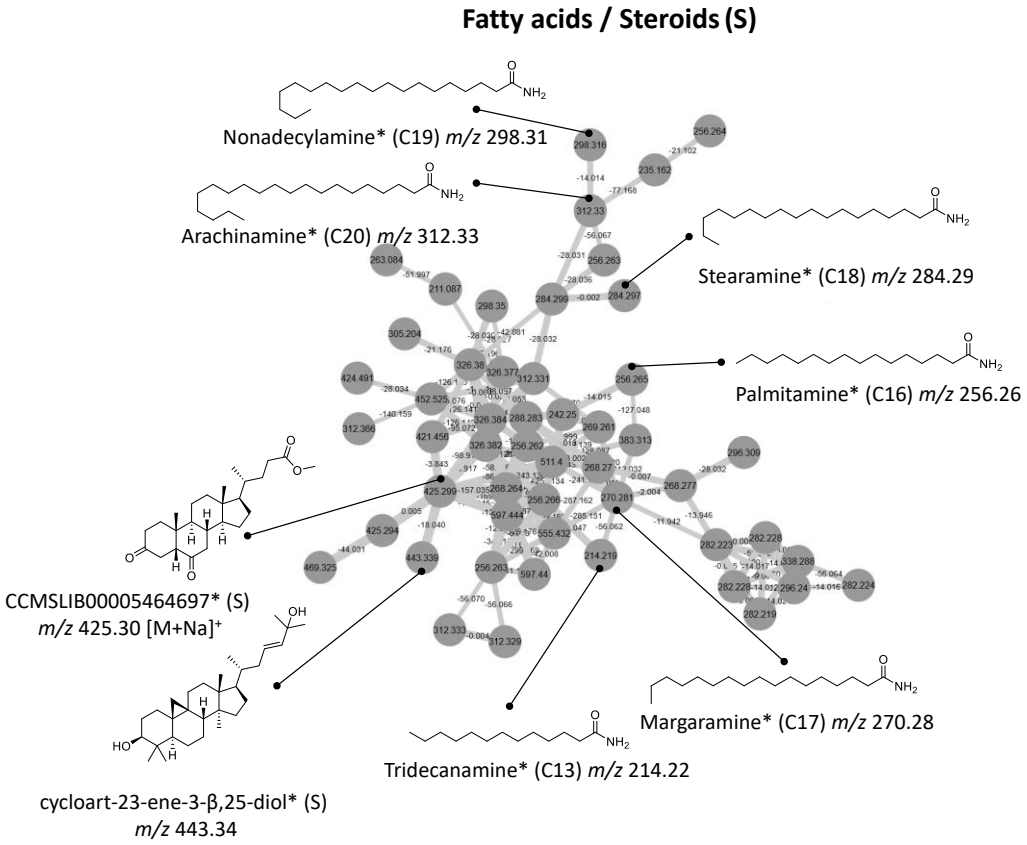

Figure 4.13 Molecular network containing all MS/MS spectra of the extracts BM25°C, BM4°C, BMS25°C, BMS4°C, SDA25°C, SDA4°C, SNA25°C, SNA4°C, GMA25°C, GMA4°C, BMblank, BMSblank, SDAblank, SNAblank, GMAblank, created with Cytoscape. Detailed view on Cluster 1.1. – Fatty acids/ Steroid (S) derivatives. Structures with an asterisk (*) are suggested by interpretation of the *m/z* values and their relation to dereplicated compounds in the network.

Library hits revealed the presence of fatty acids (ubiquitous occurring primary metabolites) and their corresponding primary amides, i.e. fatty acid amines (see Figure 4.13). The latter were reported earlier to express multifaceted biological activities from playing a crucial role in defence strategies of microorganisms to antiinflammatory processes in eukaryotic cells [208]. Extracts of the fungus *Botryodiplodia theobromae* Pat., isolated from the leaves of *Dracaena draco* L., containing fatty acid amides, e.g. palmitamine, showed broad antimicrobial activity [209]. The spectra with *m/z* values of 256.26 $[M+H]^+$ were annotated as

palmitamine (C16) and the ones with *m/z* values of 284.29 $[M+H]^+$ as stearamine (C18), according to GNPS library matches (cosines: 0.79). Further nodes with differences in *m/z* values of 14 and 28 Da (C1 and C2), connected to the beforementioned ones, verify these annotations. The node with the *m/z* value of 312.33 $[M+H]^+$ (+28 Da) can thus be annotated as arachinamine (C20) and the node with the *m/z* value of 298.31 $[M+H]^+$ (+14 Da) as nonadecylamine (C19). Interestingly, fatty acid amines with unusual chain lengths can be found in the extracts SNA25°C and SNA4°C. The node with the *m/z* value of 214.22 $[M+H]^+$ (SNA25°C and SNA4°C) can be annotated as tridecanamine (C13) and the node with the *m/z* value of 270.28 $[M+H]^+$ (SNA25°C) as margaramine (C17).

Nodes with the *m/z* values higher than 400 belong to spectra matching triterpenoids of the steroid structural class. Library hits annotated for instance cycloart-23-ene-3-β,25-diol with the *m/z* value of 443.34 $[M+H]^+$ (cosine: 0.8) or an unnamed compound with the identification label (ID) CCMSLIB00005464697 and the *m/z* value of 425.30 $[M+Na]^+$ (cosine: 0.94).

Cluster 5 – Isoflavones

The shikimate pathway is an important biosynthetic source for phenylpropanoids, which serve as precursors for flavonoid secondary metabolites [210]. Flavonoids share the chalcone bone structural motif, derived from the condensation of 4-coumaroyl-CoA with three malonyl-CoA by chalcone synthase (CHS). Flavonoids are a multifaceted group of secondary metabolites with diverse ecological and pharmacological effects [211].

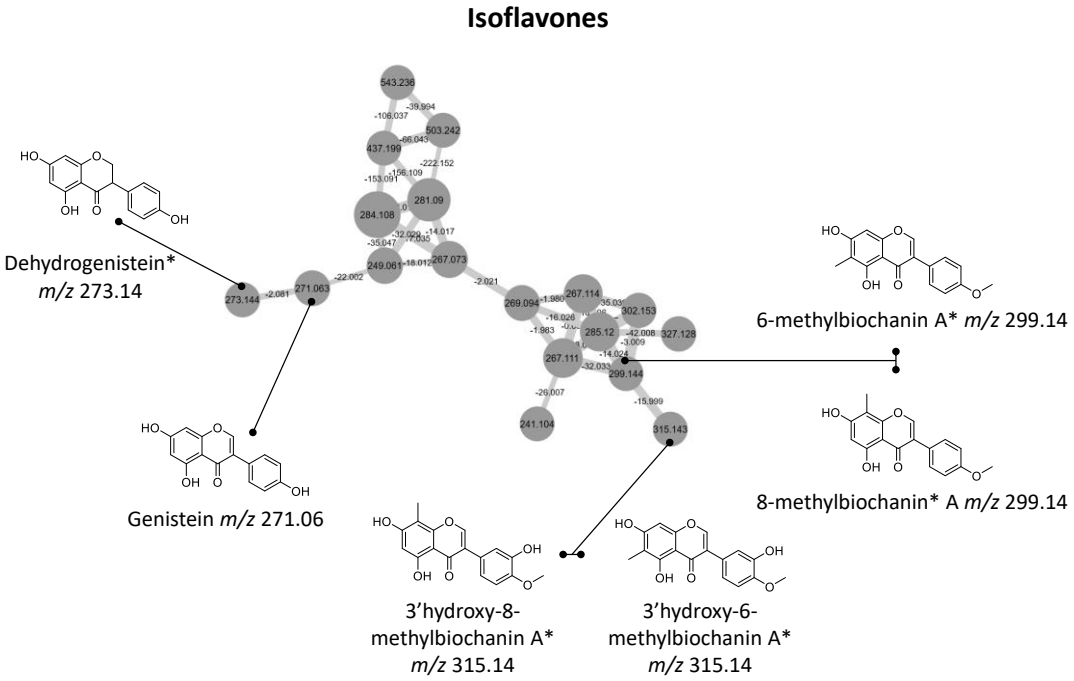

Figure 4.14 Molecular network of the extracts of 824 from the psychrotolerance experiments and the OSMAC approach, created with Cytoscape, containing MS/MS spectra of Cluster 5 – Isoflavones. Structures with an asterisk (*) are suggested by interpretation of the *m/z* values and their relation to dereplicated compounds in the network.

A crucial part in the plant hormone system play isoflavones, responsible for cell signalling, growth and reproduction [212]. Biosynthetically, isoflavones are also derived from chalcone by isomerisation of flavanones, e.g. liquiritigenin or naringenin, via isoflavone synthase (IFS), which shifts the B-Ring from C-2 to C-3 on the C-ring [213]. In fact, flavonoids were

considered exclusive plant secondary metabolites for decades, until genes for their production were found in bacteria as well [214]. In 2005, respective homologues were identified in the genome of *Aspergillus oryzae*, suggesting the production of flavonoids by fungi [215]. Several isoflavones were isolated from cultures of *A. niger* NRRL-3122, i.e. psi-tectorigenin, genistein, orobol, 8-hydroxygenistein and 3',4',5,7-tetrahydroxy-8-methoxy isoflavone. However, isoflavone rich medium ingredients, e.g. soy meal, were discussed as the origin of those structures [216]. Radiolabeling studies on chlorflavonin, a chlorinated isoflavon isolated from *A. candidus*, confirmed flavone de novo synthesis in fungi and suggested phenylalanine as the precursor with a slightly differing route via a C-6 and four C-2 units (see Figure 4.20) [217]. Additionally, the genome sequencing of *Neurospora crassa* revealed chalcone-flavanone isomerase like-genes (CHI), which catalyse the formation of flavanones, like the beforementioned liquiritigenin and naringenin, from chalcone derivatives [218]. These compounds are precursors for isoflavone biosynthesis by isoflavone synthase-like (IFS) enzymes.

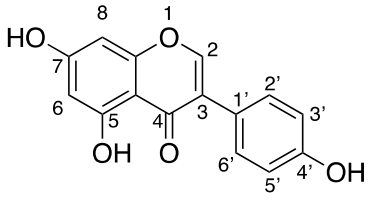

Figure 4.15 Chemical structure and numbering of isoflavones as exemplified by genistein.

In cluster 5, the spectra could be determined as resulting from the flavonoid group of natural products (see Figure 4.14). With the *m/z* value of 271.06 genistein, the aglycon of the 5-hydroxyisoflavone glycoside genistin, could be identified as a hit within the GNPS library (cosine: 0.73). A compound with the *m/z* value of 273.14, connected to the genistein node,

was annotated as dehydrogenistein, the isoflavanone derivative of genistein. Both compounds showed the usual fragmentation pattern of 5-hydroxyisoflavones with *m/z* values of 243.07 $[M+H–H_20]^+$, 215.07 $[M+H–2CO]^+$, 153.01 for the A ring ($^{1,3}A^+$) and 149.06 [M+H–B-ring–CO]$^+$, the latter two being the characteristic retro Diels-Alder fragments (see Figure 4.16) [219].

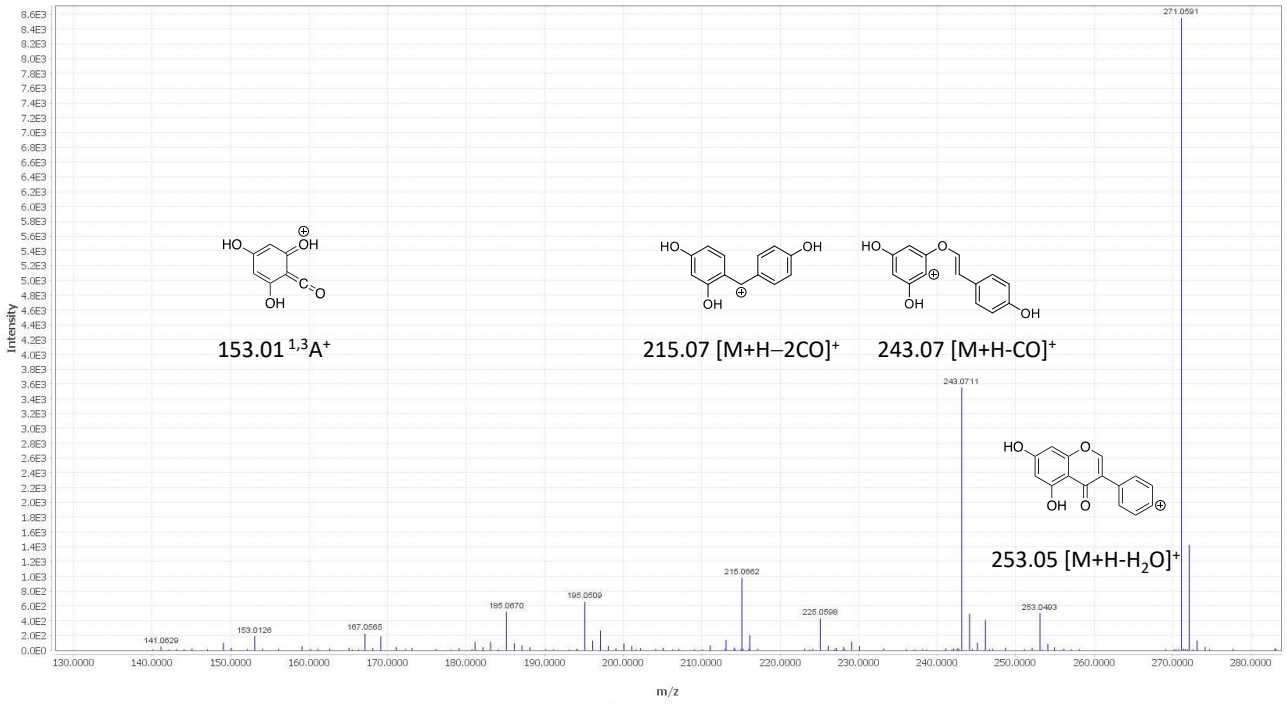

Figure 4.16 MS^2 spectrum of genistein, characteristic fragments *m/z* 153.01 $^{1,3}A^+$, *m/z* 215.07 $[M+H–2CO]^+$, *m/z* 243.07 $[M+H–CO]^+$ and *m/z* 253.05 $[M+H–H_2O]^+$ shown .

Other spectra within this cluster also showed typical fragments corresponding to 4'-O-methylated isoflavones, additionally C-methylated at the 6 or 8 position of the A-ring. This is evident when considering the *m/z* values of $^{1,3}A^+$-fragments.

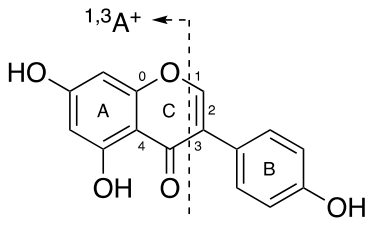

Figure 4.17 Nomenclature of relevant main MS fragment developed by Mabry and Markham [220], adapted for flavone, flavonol [221] and isoflavone aglycons [219], shown for genistein.

Figure 4.17 shows the fragmentation nomenclature of genistein for the $^{1,3}A^+$-fragment, which is formed by cleavage of the carbon-carbon bonds at position 1 and 3 of the C-ring, resulting in an *m/z* value of 153.01. The corresponding *m/z* values of $^{1,3}A^+$-fragments of beforementioned compounds (C-methylated at C-6 or C-8) are 14 Da higher, i.e. *m/z* 167.06, than those of unmethylated 5,7-dihydroxyisoflavones, e.g. genistein. Additionally, the MS/MS spectra show characteristic 4'-O-demethoxylation products with *m/z* values of 267.11 $[M+H-CH_4O]^+$ (see Figure 4.18) [219].

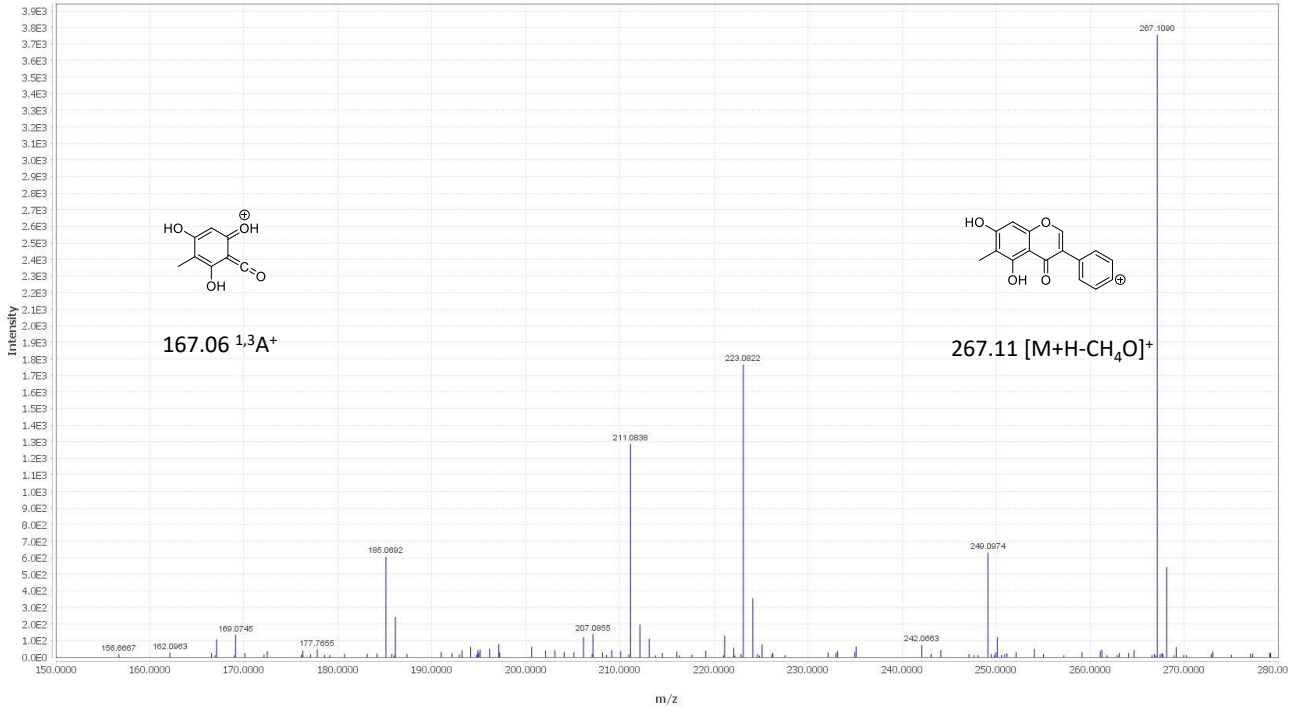

Figure 4.18 MS^2 spectrum of methylated 5,7-dihydroxyisoflavone *m/z* 299.14, characteristic fragments $^{1,3}A^+$ *m/z* 167.06, $[M+H-CH_4O]^+$ *m/z* 267.11 shown .

The compound with the *m/z* value of 299.14 $[M+H]^+$ can, therefore, be proposed as either 6-methylbiochanin A, a known compound isolated from the legume *Derris indica*, or 8-methylbiochanin A, a putative novel natural compound (see Figure 4.19) [222]. The node of the putative compound 8-methylbiochanin A is connected to a node with an m/z value 16 Da higher, i.e. 315.14 $[M+H]^+$, corresponding to a derivative with an additional oxygenation in the B-ring, as the *m/z* value $^{1,3}A^+$-fragment remains 167.06. According to biotransformation studies in several *Fusarium* strains, a hydroxylation in the 3´position of the B-ring is most likely, resulting in further putative novel derivatives of 6-methylbiochanin A or 8-methylbiochanin A, respectively, namely 3'-hydroxy-6-methylbiochanin A and 3'-hydroxy-8-methylbiochanin A 315.14 $[M+H]^+$ (compare Figure 4.14 and Figure 4.19) [223].

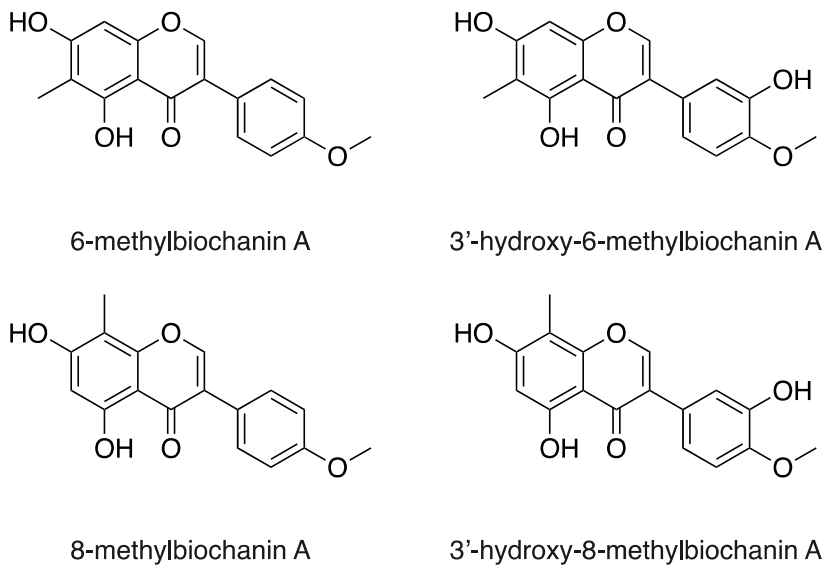

Figure 4.19 Structures of the known compound 6-methylbiochanin A, isolated from *Derris indica*, and the putative novel compounds 8-methylbiochanin A, 3'-hydroxy-6-methylbiochanin A and 3'-hydroxy-8-methylbiochanin A, detected by mass spectrometry and molecular networking.

In order to validate whether genistein was produced from *H.* cf. *alpina*, the culture medium (BM and BMS) without fungus was extracted the same way as the fungal culture and investigated on its flavonoid content. Molecular networking, in combination with the dereplication workflow MolNetEnhancer could not annotate any common flavonoids in the medium. Only the flavone glycoside camelliaside A (kaempferol-3-O-[2-O-β-D-galactose-6-O-α-L-rhamnose]-β-D-glucoside) was dereplicated with a high degree of certainty (cosine 0.81) (see Figure 4.19). Literature search on the major ingredient of biomalt, i.e. barley, revealed only traces of phytoestrogens, i.e. daidzein and genistein, glycitein or biochanin A (ng g^{-1}) [224, 225]. In contrast to the low amount of genistein in barley products, the isoflavone genistein was isolated in mg yields from the ethylacetate extracts of *H.* cf. *alpina* 824, grown on BMS medium. These results suggest at least IFS-like activity in *H.* cf. *alpina*, i.e. transformation of assimilated flavonoid sources from the medium into isoflavone compounds.

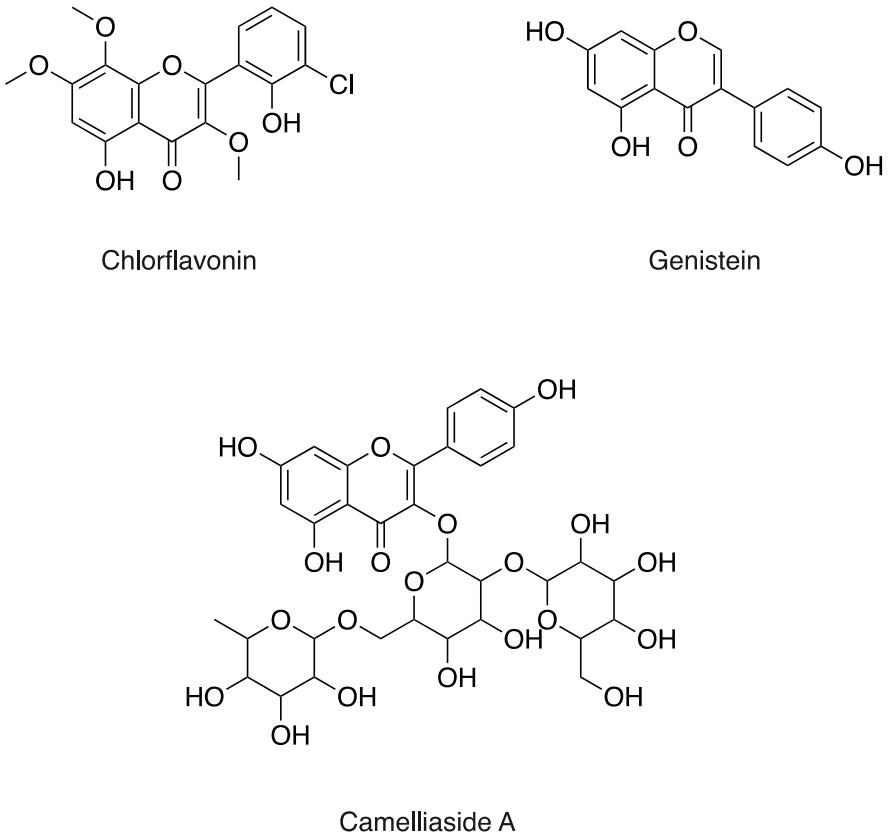

Figure 4.20 Chemical structures of the fungal flavonoid chlorflavonin, isolated from *Aspergillus candidus* [216], the isoflavone genistein, isolated from *H*. cf. *alpina* (this study) and the flavonglycoside camelliaside A, detected from the culture media BM and BMS for *H*. cf. *alpina*.

The observation of isoflavone production in filamentous fungi contributes to the understanding of flavonoid biosynthesis in microorganisms.

Cluster 28 – Heydenoic acid B

With the isolation and structure elucidation of heydenoic acid B from extracts of *H*. cf. *alpina* 824 this cluster could be annotated as resulting from heydenoic acid B with an *m/z* value of 251.16 $[M+H]^+$ (see Figure 4.21).

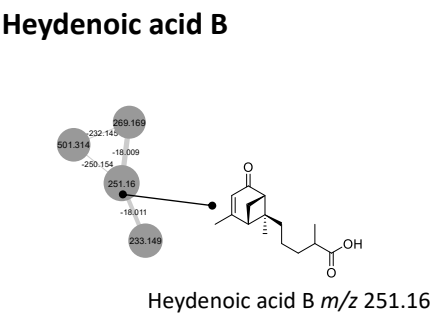

Figure 4.21 Molecular network of the extracts of 824 from the psychrotolerance experiments and the OSMAC approach, created with Cytoscape, containing MS/MS spectra of Cluster 28 – Heydenoic acid B.

Furthermore, the cluster includes a hydration product (+18 Da) with an *m/z* value of 269.17 $[M+H]^+$, the dimer of heydenoic acid B, *m/z* 501.31 $[M+H]^+$, and an unidentified compound (-18 Da) with an *m/z* value 233.15 $[M+H]^+$ (see Figure 4.21).

Cluster 66 – Heydenoic acid A

Analogous to heydenoic acid B, its derivative heydenoic acid A, *m/z* 249.14 $[M+H]^+$, clustered with an unidentified compound (-18 Da) with an *m/z* value of 231.13 $[M+H]^+$ (see Figure 4.22).

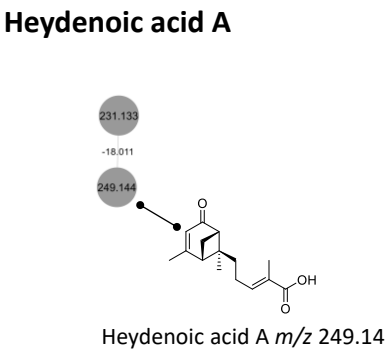

Figure 4.22 Molecular network of the extracts of 824 from the psychrotolerance experiments and the OSMAC approach, created with Cytoscape, containing MS/MS spectra of Cluster 66 – Heydenoic acid A.

Other clusters – Unidentified fungal metabolites

The remaining 43 clusters stay unidentified, i.e. have no hit in the databases, due to missing reference spectra. Compounds creating those MS spectra hold potential for being novel compounds, introducing hitherto uncharacterised structural classes and are therefore of particular interest for further studies.

4.5.4 Evaluation of the OSMAC approach on extracts of *H*. cf. *alpina*

In order to link the results from culture experiments (4.5.1) and bioactivity assays (4.5.2) to the metabolome of respective fungal cultures (4.5.3), the molecular network was mapped, i.e. a metadata file was used to provide information on culture conditions for each node. Figure 4.23 comprises the metabolome of *H.* cf. *alpina* 824 under various culture conditions. To determine which compounds are produced under each condition, nodes that exclusively appear in extracts of a given culture medium were coloured accordingly.

In the following a detailed analysis for each culture medium is presented, highlighting results unique to a respective culture condition and concluding the most striking outcomes.

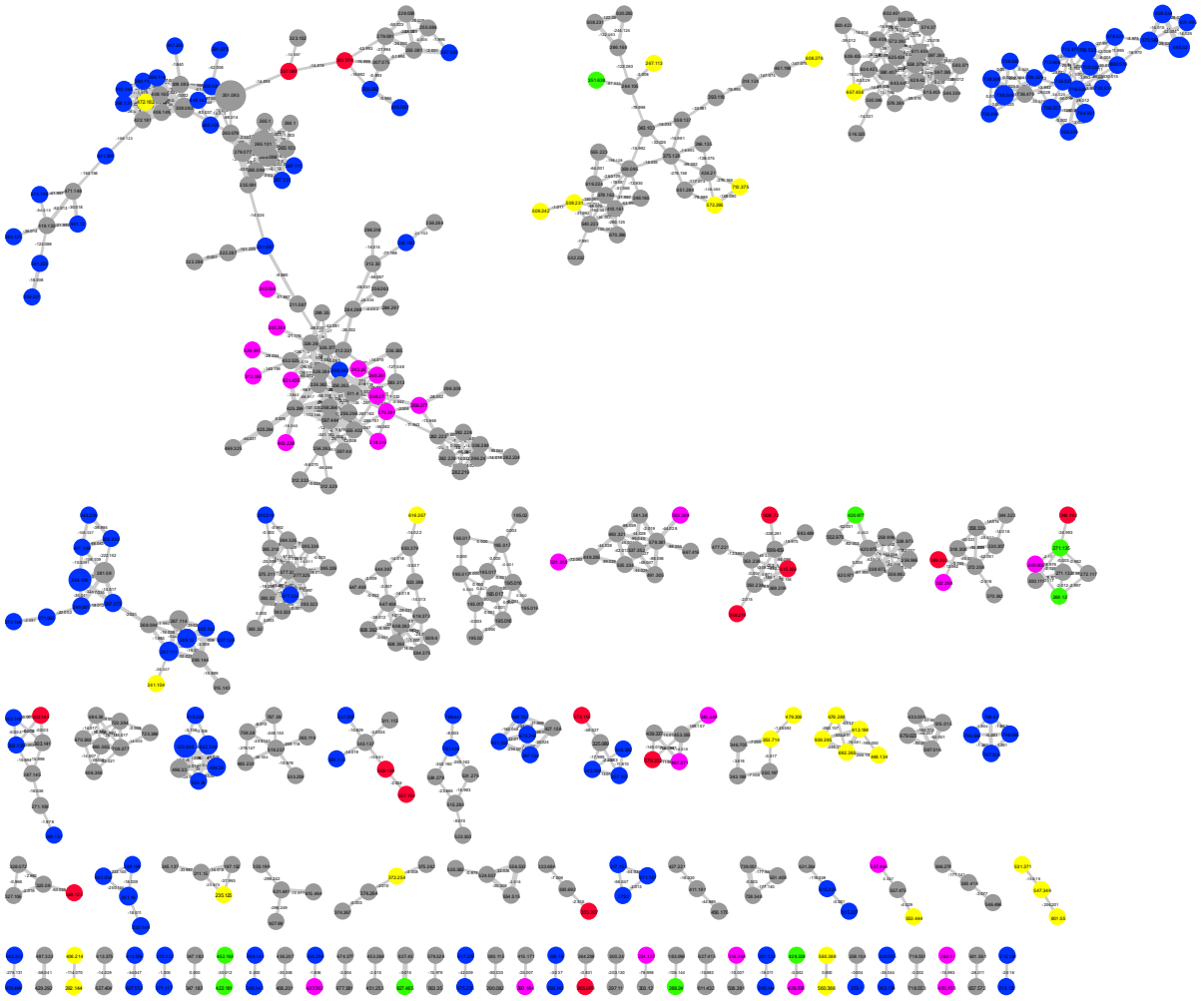

Figure 4.23 *H*. cf. *alpina* 824 cultured on five different media at 25°C and 4°C. Coloured nodes display compounds exclusively produced on the respective medium: red: BM; blue: BMS; yellow: SDA; pink: SNA; green: GMA. Grey nodes represent compounds that were found in a medium blank or were detected in extracts of two or more different culture media.

H. cf. *alpina* 824 cultivated on Biomalt medium (BM) at 25°C and 4°C

The growth of cultures on BM medium was significantly slower in comparison to the standard medium BMS at both temperatures, i.e. 25°C and 4°C (see Figure 4.7). Thus, it was concluded that an adaption of *H.* cf. *alpina* 824 to saline environments was the reason for the reduced growth in BM (see Table 8.2). The results from the bioactivity assays (see chapter 4.5.2) showed slightly increased activity of BM25 and BM4, compared to BMS25 and BMS4 (see Figure 4.8). Compounds that are exclusively produced on BM medium do not appear in annotated clusters, not leaving any information about specialised metabolite production under hyposaline conditions.

H. cf. *alpina* 824 cultivated on Biomalt Salt medium (BMS) at 25°C and 4°C

This standard growth medium provided the cultures with high amount of salts (see chapter 3.2.1), resulting in good growth rates (see chapter 4.5.1) and the extracts BMS25 and BMS4 showed moderate bioactivity against *Bacillus megaterium* with inhibition zones of 6 mm and 4 mm, respectively (see chapter 4.5.2). The production (or conversion) of carbolines and isoflavones was observed best on BMS medium, which can be concluded by accumulation of blue coloured nodes (compounds exclusively produced on BMS medium) in cluster 1.1. – carbolines and cluster 5 – Isoflavones in Figure 4.23.

H. cf. *alpina* 824 cultivated on Sabouraud Dextrose Agar (SDA) at 25°C and 4°C

The nutrient-rich culture medium SDA allowed the fastest growth among all media. With its high amount of peptone, it is responsible for multiple nodes, annotated as medium components (see Figure 4.23, yellow nodes). Nodes that exclusively appear in extracts of cultures grown on SDA (yellow coloured) nodes), often cluster with nodes from the medium

(grey coloured nodes), suggesting conversion of medium constituents by the fungus into derivatives. However, the bioactivity against *B. megaterium* for of SDA25 is comparable to the one of the standard BMS25, whereas SDA4 is slightly more active (6 mm inhibition zone) compared to BMS4 (4 mm inhibition zone) (see Figure 4.8). SDA4 is the only extract, which is not significantly less active against *B. megaterium* than its counterpart extracted from cultures stored at 25°C (see Figure 4.8).

_H_. cf. _alpina_ 824 cultivated on Synthetic Nutrient-poor Agar (SNA) at 25°C and 4°C

Cultures grown on SNA showed moderate growth rates at both temperatures. Interestingly, only subsurface mycelium in respective culture plates was observed. Intriguingly, the extract SNA25 showed the largest inhibition zones (12 mm) of all tested samples when tested against *B. megaterium* (see Figure 4.8). In Figure 4.23, the SNA-exclusive nodes are depicted in pink, exposing two clusters with prominently occurrence, i.e. cluster 1.2 – Fatty acids/ Steroids and cluster 9 - Oligopeptides.

In cluster 1.2, predominantly fatty acids and steroids are comprised. Antimicrobial activities were intensively investigated for primary fatty acid amines [226] and odd-numbered fatty acid amides [227]. The unusual odd-numbered fatty acid amines observed in the molecular network of the SNA extracts, e.g. tridecanamine *m/z* 214.22 $[M+H]^+$ and margaramine *m/z* 270.28 $[M+H]^+$, exclusively produced on SNA medium, could provide an explanation for the increased antimicrobial activity.

4.6 Structure elucidation of novel sesquiterpenoids isolated from the main culture (BMS) extract of *H.* cf. *alpina* 824

On the basis of its preferred growth on saline media, the *H.* cf. *alpina* (strain No. 824), isolated during this study, was selected for further chemical investigations. To the best of our knowledge this is the first chemical investigation of a member of the *Heydenia* genus.

From the solid, sea-salt containing cultures of *H.* cf. *alpina* the ethyl acetate soluble organic compounds were analysed. A first fractionation was achieved by vacuum liquid chromatography (VLC) on reversed-phase material yielding 4 fractions. ^{1}H NMR analysis of these indicated the presence of chemically diverse secondary metabolites in the major VLC fraction 3. Detailed HRESIMS investigation was thus performed with VLC fraction 3, which showed prominent *m/z* values for metabolites with molecular weights of 248 and 250 Da.

Subsequently repeated fractionation of VLC fraction 3 by RP-HPLC resulted in the isolation of two, structurally closely related, new secondary metabolites, **1** and **2** (Figure 4.24).

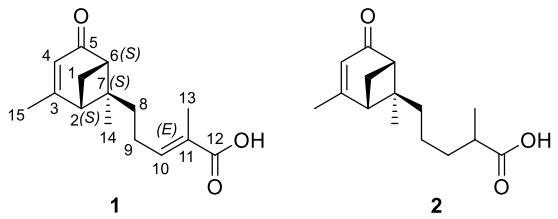

Figure 4.24 Novel bergamotene secondary metabolites isolated from *Heydenia* cf. *alpina.*

Compound **1** was obtained as a yellow oil with a molecular formula of $C_{15}H_{20}O_3$, implying 6 degrees of unsaturation (DOU), as deduced by HRESIMS (*m/z* 249.1481 $[M + H]^+$; calcd. For

$C_{15}H_{21}O_3$, 249.1485). The IR spectrum displayed an absorption band at 1670 cm^{-1} indicating the presence of an α,β-unsaturated carbonyl moiety [228].

The ^{1}H NMR spectrum (Table 4.3) exhibited characteristic singlets for three methyl groups, as well as two olefinic protons, together with the MS data pointing towards a terpenoid like structure. The ^{13}C NMR and DEPT-135 spectra of **1** (Table 4.3) displayed 15 carbon signals for three methyl, three methylene, two sp^3 methine and two sp^3 quaternary carbons. Four characteristic shifts in the ^{13}C NMR spectrum at δ_C 174.1 (C-3), 122.1 (C-4), 143.0 (C-10) and 129.5 (C-11) evidenced two carbon-carbon double bonds. Together with a carbonyl carbon at δ_C 206.6 and a carboxylic carbon at δ_C 177.8, the two remaining DOU were accounted to a bicyclic ring system.

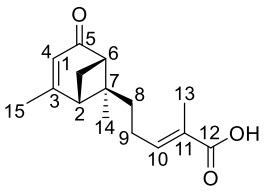

Table 4.3 ^{13}C NMR (75 MHz) and ^{1}H NMR (300 MHz) data of Heydenoic acid A (1) in MeOD.

C	δ_H	δ_C	COSY	HMBC	NOE
1	2.12, m, a	41.9, CH_2	1b	2, 3, 5, 6, 7, 14	4
	2.93, dt (10.0, 6.0), b		1a, 2, 6	2, 3, 5, 6, 7	2, 6, 8, 15
2	2.65, t (5.5, 6.0)	49.8, CH	1b, 4, 6	3, 4, 6,7, 15	1b, 14, 15
3		174.1, qC			
4	5.78, q (1.3)		2, 6, 15		14, 15
		122.1, CH			
5		206.6, qC			
6	2.73, t (5.9, 6.0)	57.2, CH	1b, 4	2, 4, 5,7	1b, 9, 14
7		58.6, qC			
8	2.07, m	38.2, CH_2	9	7, 9, 14	14
9	2.32, q (7.6)	25.0, CH_2	8, 10, 13	7, 8, 10, 11	2, 6, 13, 14
10	6.89, t (7.6)		9, 13	12, 13	8, 9
		143.0, CH			
11		129.5, qC			
12		177.8, qC			
13	1.89, s	12.5, CH_3	10	10, 11, 12	9, 14
14	1.07, s	19.2, CH_3		2, 6, 7, 8, 15	8, 15
15	2.10, d (1.3)	23.6, CH_3	4	3, 4, 5	2, 4, 14

After assigning the proton resonances to the ^{13}C resonances of directly attached carbon atoms with an HSQC experiment, analysis of the $^{1}H,^{1}H$-COSY data led to the identification of two major $^{1}H–^{1}H$ spin systems, one corresponding to the H-2–H-1$_b$–H-6 moiety (spin system A) and the second to the H_2-8–H_3-13 subunit (spin system B; Figure 4.25).

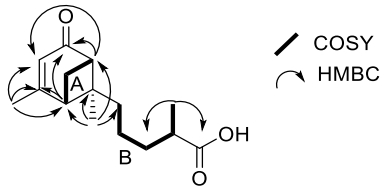

Figure 4.25 Significant $^{1}H,^{1}H$-COSY and $^{1}H,^{13}C$-HMBC correlations for compound 1.

Spin system B was extended by a carboxylic group as indicated by $^{1}H,^{13}C$-HMBC correlations from both H-10 (δ_H 6.86) and H_3-13 (δ_H 1.89) to carbon C-12 (δ_C 177.8), and identified the partial structure 2-methylpentenoic acid. HMBC correlations between the resonances of H-6 (δ_H 2.73) to both C-4 (δ_C 122.1) and C-5 (δ_C 206.6), between H_3-15 (δ_H 2.10) and C-2 (δ_C 49.8), C-3 (δ_C 174.1) and C-4 (δ_C 122.1), and between H_2-1 (δ_H 2.12; 2.93) and both C-3 (δ_C 174.1) and C-5 (δ_C 206.6) placed the methyl group CH_3-15 at carbon C-3 (δ_C 174.1), and proved the positions of the carbonyl group C-5 (δ_C 206.6) and the double bond $\Delta^{3,4}$ in the molecule, as shown in Figure 2. The second partial structure was thus a cyclohexenone ring. The proton resonances of H-2 (δ_H 2.65) and H-6 (δ_H 2.73) appear as a characteristic triplet of doublets caused by a vicinal coupling with proton H-1$_b$ (δ_H 2.93; J = 6.0 Hz), an unusually large “W” coupling to each other (J = 6.0 Hz) as well as an allylic coupling to H-4 (δ_H 5.78; J = 1.3 Hz). These couplings can only be explained with the rigid

structure of **1** supporting the presence of a bicyclo[3.1.1] ring system resembling that of verbenone [229].

HMBC correlations of H_3-14 (δ_H 1.07) to C-2 (δ_C 49.8), C-6 (δ_C 57.2), C-7 (δ_C 58.6) and C-8 (δ_C 38.2) confirmed the presence of a verbenone moiety and connected the methylpentenoic acid moiety to the quaternary carbon C-7, completing the planar structure of **1**. Compound **1** is thus a bergamotene type sesquiterpene, containing a bicyclo[3.1.1] ring system as well as a 2-methylpent-2-enoic acid moiety, accounting for all ring double bond equivalents (Figure 4.25).

The relative configuration of **1** at C-2, C-6 and C-7 was established by a NOESY spectrum (Figure 4.26). NOESY correlations between H-1_b (δ_H 2.93) and H_2-8 (δ_H 2.07) indicated that these protons were on the same side of the molecule and together with the NOESY correlation between H_3-14 and H_3-15 the relative configurations of C-2, C-6 and C-7 could thus be delineated as 2*S**, 6*S** and 7*S**, respectively.

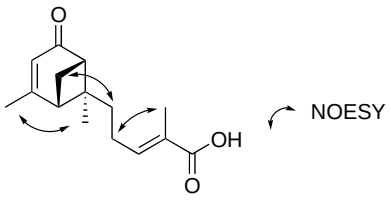

Figure 4.26 Key NOESY correlations for compound 1.

The absolute configurations of C-2, C-6 and C-7 were determined by comparison of our experimental with simulated circular dichroism (CD) spectra. The latter ones were performed by Wu et al. using (2*S*,6*S*)-verbenone and (2*R*,6*R*)-verbenone and can be applied here, because of the assumed minor effect of the side chain on the CD spectrum [230].

Experimental data for **1** showed a negative Cotton effect in the range of 320–350 nm (321 nm), which suggested according to the calculated CD spectrum of Wu et al. (321 nm) that the absolute configurations of C-2, C-6 and C-7 in **1** are 2*S*, 6*S*, and 7*S*, respectively (Figure 4.27).

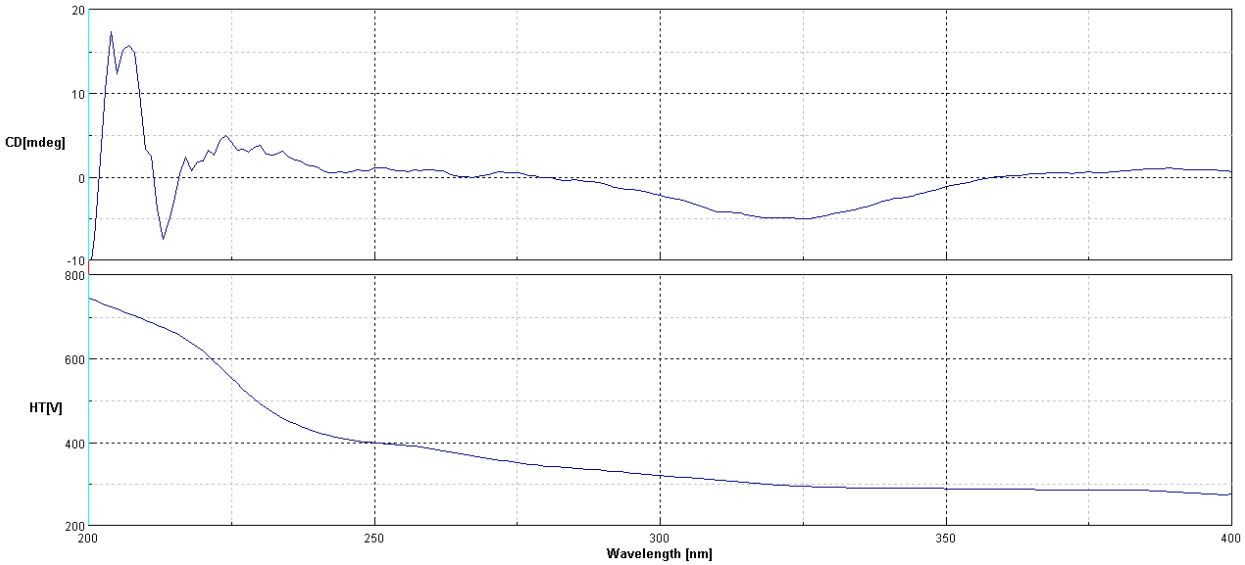

Figure 4.27 CD spectrum of Heydenoic acid A (1) in MeOH.

The configuration of the double bond $\Delta^{10,11}$ could be determined as *E* by NOESY correlations between proton signals H_2-9 (δ_H 2.32) and H_3-13 (δ_H 1.89). This was confirmed by the strong shielding in the ^{13}C NMR spectrum of carbon C-13 typically occurring in double bonds with *E* configuration [231]. Therefore, the structure was established as €-2-methyl-5-((1*S*,5*S*,6*S*)-2,6-dimethyl-4-oxobicyclo[3.1.1]hept-2-en-6-yl)pent-2-enoic acid, for which the trivial name heydenoic acid A is suggested. Notable is the occurrence of peaks containing *m/z* values attributable to isomers of the isolated metabolite.

Compound **2** has a molecular formula of $C_{15}H_{22}O_3$, (HRESIMS *m/z*: 251.1641 $[M + H]^+$; calcd. For $C_{15}H_{23}O_3$, 251.1642) implying only 5 DOU as compared to **1**.

The ^{1}H-NMR spectrum (Table 4.4) exhibited resonance signals for three methyl, four sp^3 methylene and three sp^3 methine groups, as well as one olefinic proton. The ^{13}C-NMR and DEPT-135 spectra of **2** (Table 4.4) displayed 15 carbon signals for three methyl, three methylene, two sp^3 methine and two sp^3 quaternary carbons. Two characteristic shifts in the ^{13}C-NMR spectrum at δ_C 174.2 (C-3) and 122.0 (C-4) pointed towards a carbon-carbon double bond. Together with a carbonyl at δ_C 206.9 and a carboxylic carbon at δ_C 180.8 two RDE accountable to a bicyclic [3.1.1] ring remained, and suggested the same bergamotene-class sesquiterpene as in **1**.

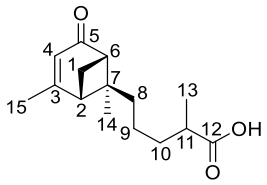

2

Table 4.4 ^{13}C NMR (75 MHz) and ^{1}H NMR (300 MHz) data of Heydenoic acid B (2) in MeOD.

C	δ_H, (J in Hz)	δ_C, mult	COSY	HMBC	NOE
1	2.10, d (9.0), a	41.9, CH_2	1b	2, 3, 5, 6, 7, 14	4
	2.89, dt (5.6) b		1a, 2, 6	2, 3, 5, 6,7	2, 6, 8, 15
2	2.59, t (5.6)	49.7, CH	1b, 4, 6	1, 3, 4, 6, 7, 8, 15	10, 15
3		174.2, qC			
4	5.77, q (1.3)	122.0, CH	2, 6, 15	2, 6, 15	15
5		206.9, qC			
6	2.67, t (5.6)	57.3, CH	1b, 2, 4	1, 2, 4, 5, 7, 8	10,
7		58.8, qC			
8	1.94, t (8.2)	39.4, CH_2	9	2, 6, 7, 9, 10, 14	1, 6, 14
9	1.37, m	23.4, CH_2	8, 10	7, 8, 10	
10	1.49, m, a	35.5, CH_2	9, 11	9, 12	14
	1.73, m, b		9, 11	9, 11, 13	
11	2.50, m	40.7, CH	10a, 10b, 13	9, 10, 12, 13	10a, 13
12		180.8, qC			
13	1.21, d (7.0)	17.8, CH_3	11	10, 11, 12	10a
14	1.01, s	19.3, CH_3		2, 6, 7, 8	4?
15	2.09, d (1.3)	23.6, CH_3	4	2, 3, 4, 5	1b

^{1}H and ^{13}C NMR data (Table 4.4) of **2** were similar to those of **1**, except for the chemical shifts of CH_2-9 (δ_H 1.37; δ_C 23.4), CH_2-10 (δ_H 1.49, 1.73; δ_C 35.5), and CH_3-13 (δ_H 1.21; δ_C 17.8). Additional proton signals for H-11 and H_2-10 (δ_H 2.50; H-11, δ_H 1.49 and δ_H 1.73;

H_2-10) proved that **2** is a derivative of **1**, in which $\Delta^{10,11}$ is saturated. COSY and HMBC data of **2** fully supported this assumption (Figure 4.28).

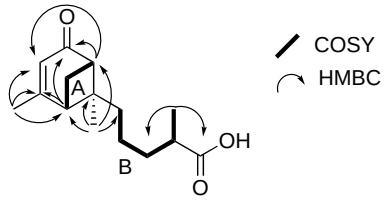

Figure 4.28 Significant ^{1}H,^{1}H-COSY and ^{1}H,^{13}C-HMBC correlations for compound 2.

NOESY correlation between H_b-1 (δ_H 2.89) and H_2-8 (δ_H 1.94) indicated the relative configurations of C-2, C-6 and C-7 to be the same as in **1** (Figure 4.29).

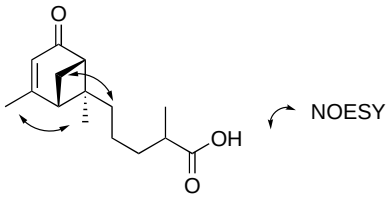

Figure 4.29 Key NOESY correlations for compound 1.

The CD spectrum of **2** also showed a negative Cotton effect as **1**, indicating the absolute configurations of C-2, C-6 and C-7 to be all *S* (Figure 4.30).

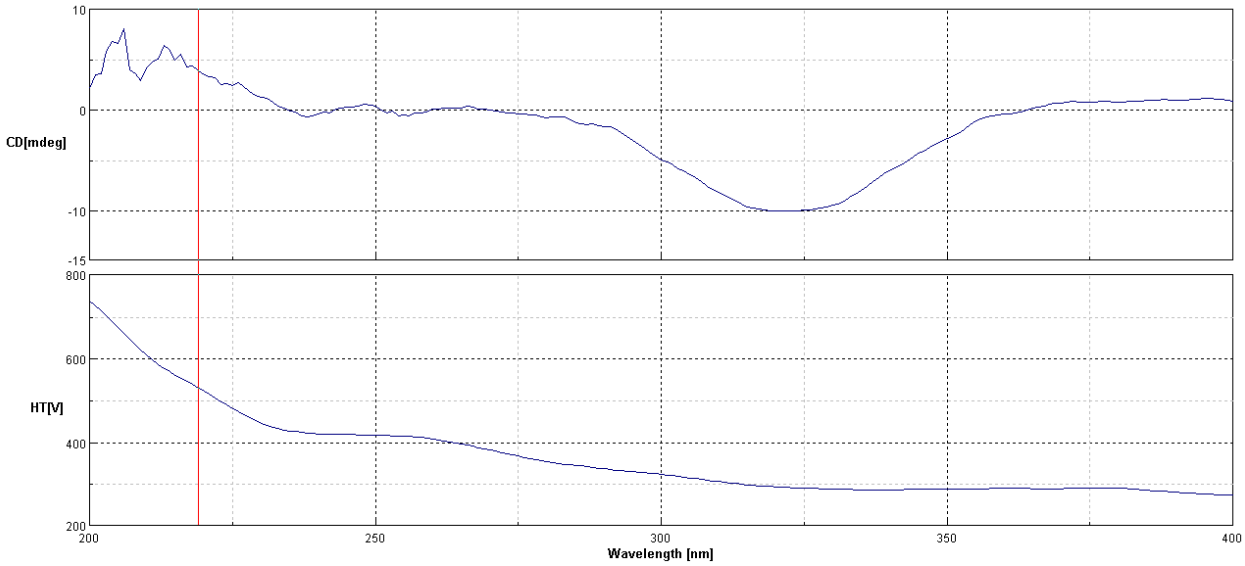

Figure 4.30 CD spectrum of Heydenoic acid B (2) in MeOH.

The configuration at C-11 could not be determined by experimental means. Thus, the structure was established as 2-methyl-5-((1*S*,5*S*,6*S*)-2,6-dimethyl-4-oxobicyclo[3.1.1]hept-2-en-6-yl)pentanoic acid, named as heydenoic acid B.

4.7 Structure elucidation of compounds isolated from the main culture (BMS) extract of *H.* cf. *alpina* 824

HPLC separation of the VLC fractions 1-3 of the main culture (BMS) extract (see Chapter 3.3.2) revealed six secondary metabolites, which are described for the first time in *Heydenia* cf. *alpina*. Two of those compounds are novel compounds. Extensive NMR spectroscopy was carried out to elucidate the chemical structure of all compounds. To the best of our knowledge, this is the first chemical characterisation of a member of the *Heydenia* genus.

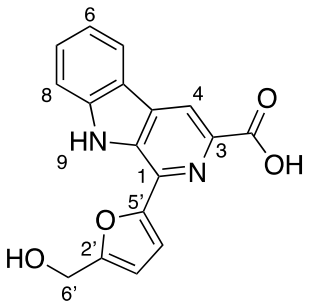

Figure 4.31 Structure of flazin (3)

Flazin (**3**)

RP-HPLC separation of fraction 3.2 of the main culture (BMS) extract of *H.* cf. *alpina* 824 yielded 4 mg of flazin (**3**) (see Figure 4.31). Comparison of NMR data of **3** and the molecular mass with the results of ß-carbolines described by Shaaban et al. proved compound 3 to be flazin [205]. We were able to affirm the results of Hufendiek et al., that flazin is a constituent of BMS agar medium by LC-ESI-MS and ^{1}H-NMR [232].

Flazin: yellow solid: ^{1}H NMR (300 MHz, MeOD): δ 8.82 (s, H-4), 8.42 (d, *J* = 8.0 Hz, H-5), 7.81 (d, *J* = 8.0 Hz, H-8), 7.65 (t, *J* = 8.0 Hz, H-7), 7.42 (d, *J* = 3.0 Hz, H-4´), 7.37 (t, *J* = 8.0 Hz, H-6), 6.67 (d, *J* = 3.4 Hz, H-3´), 4.68 (s, H_2-6´); ^{13}C NMR (75 MHz, MeOD): δ 168.4 (C-

10, qC), δ 159.1 (C-2´, qC), δ 153.1 (C-5´, qC), δ 143.3 (C-8a, qC), δ 134.3 (C-1, qC), δ 133.7 (C-9a, qC), δ 131.7 (C-3, qC), δ 130.7 (C-7, CH), δ 123.9 (C-5, CH), δ 122.8 (C- 4a, qC), δ 122.8 (C-4b, qC), δ 122.4 (C-6, CH), δ 117.6 (C-4, CH), δ 114.7 (C-8, CH), δ 112.9 (C-4´, CH), δ 111.1 (C-3´, CH), δ 57.8 (C-6´, CH_2); HR-ESI-MS *m/z* 309.0856 $[M+H]^+$ (calcd. for $C_{17}H_{13}N_2O_4^+$: 309.0870).

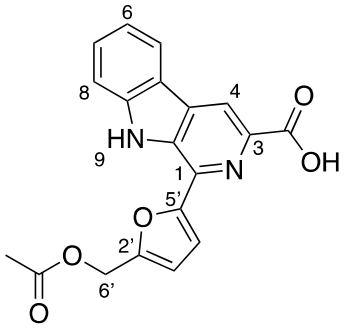

Figure 4.32 Structure of flazin ethyl ester (4)

Flazin ethyl ester (**4**)

Molecular networking revealed a derivative of flazin in the main culture (BMS) extract of *H.* cf. *alpina* 824 with the *m/z* value of 351.093 (**4**), which could be isolated by HPLC separation of fraction 3.2 (see chapter 3.3.2). The molecular mass of compound **4** differed from that of flazin by +42 Da, which corresponds to an additional acetyl (better: ethanoyl) moiety. This mass could not be detected in any of the culture media, which suggests production of this compound by the fungus, or at least acetylation of flazin. ^1H and ^{13}C NMR data of **3** were similar to those of **4**, except for the chemical shifts of CH-4' (δ_H 7.59; δ_C 112.9) and CH-3' (δ_H 6.77; δ_C 111.1). **4** showed additional proton signals for H_3C-9' (δ_H 2.18) as well as carbon signals C-8' (δ_C 170.8) and CH_3-9' (δ_C 20.5). Literature search suggested this to be a novel compound.

Flazin ethyl ester: yellow solid: ^{1}H NMR (300 MHz, MeOD): δ 8.82 (s, H-4), 8.30 (d, *J* = 8.4 Hz, H-5), 7.81 (d, *J* = 8.0 Hz, H-8), 7.65 (t, *J* = 7.6 Hz, H-7), 7.59 (d, *J* = 3.0 Hz, H-4′), 7.37 (t, *J* = 7.5 Hz, H-6), 6.77 (d, *J* = 3.4 Hz, H-3′), 4.68 (s, H_2-6′); ^{13}C NMR (75 MHz, MeOD): δ 168.4 (C-10, qC), δ 159.1 (C-2′, qC), δ 153.1 (C-5′, qC), δ 143.3 (C-8a, qC), δ 134.3 (C-1, qC), δ 133.7 (C-9a, qC), δ 131.7 (C-3, qC), δ 130.7 (C-7, CH), δ 123.9 (C-5, CH), δ 122.8 (C-4a, qC), δ 122.8 (C-4b, qC), δ 122.4 (C-6, CH), δ 117.6 (C-4, CH), δ 114.7 (C-8, CH), δ 112.9 (C-4′, CH), δ 111.1 (C-3′, CH), δ 57.8 (C-6′, CH_2); HR-ESI-MS *m/z* 351.0968 [M+H]+ (calcd. for $C_{19}H_{15}N_2O_5^+$: 351.0975).

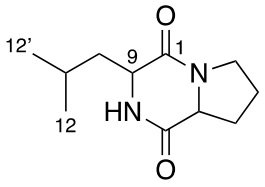

Figure 4.33 Structure of Cyclo-(L-Leu-L-Pro) (5)

Cyclo-(L-Leu-L-Pro) (**5)**

The dereplication step during the molecular networking identified a mass with the *m/z* value of 211.144 as Cyclo-(L-Leu-L-Pro) (cosine: 0.8). The compound could be isolated by HPLC separation of fraction 2.1 (2mg), and its structure was elucidated by comparison of NMR spectra with reference spectra by Li et al [233]. This compound was also detected in the medium by mass spectrometry and therefore considered a medium component.

Cyclo-(L-Leu-L-Pro): colourless solid: ^{1}H NMR (300 MHz, MeOD) δ 0.95 (d, *J* = 6.6 Hz, CH_3), 0.99 (d, *J* = 6.6 Hz, CH_3), 1.56 (m, H_2-10a), 1.75 (m, H_2-10b), 1.86 – 1.98 (m, H-11), 2.00 – 2.18 (m, H_2-4), 2.32 – 2.38 (m, H_2-5), 3.52 – 3.68 (m, H_2-3), 4.02 (dd, *J* = 9.3Hz/3.9Hz, H-9), 4.31 (t, *J* = 8.3, H-6), 6.10 (brs, NH). ^{13}C NMR (75 MHz, MeOD) δ 168.9 (s, C-1), 46.4 (t, C-3), 23.7 (t, C-4), 29.1 (t, C-5), 60.3 (d, C-6), 168.9 (s, C-7), 54.6 (d, C-9), 39.4 (t, C-10), 25.8 (d, C-11), 23.3 (q, C-12), 22.2 (q, C-12′); HR-ESI-MS *m/z* $[M+H]^+$ 211.144 (calcd. for $C_{11}H_{18}N_2O_2^+$: 211.1441).

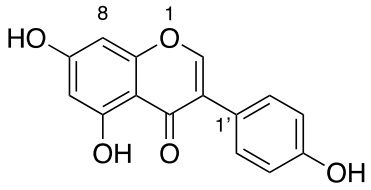

Figure 4.34 Structure of genistein

Genistein (**6**)

The isoflavone genistein could be dereplicated in the extract of the main culture (BMS) of *H.* cf. *alpina*, as well as in extract BMS25, by the GNPS system. A library hit with a cosine score of 0.73, and the annotation as isoflavone by the MolNetEnhancer suggested its presence in the polar fraction 2.1. The fact that this typical plant metabolite was found in the extracts of a fungal culture and was not found in extracts of the respective media was surprising. HPLC separation yielded 2mg of a compound, which could be identified as genistein by comparison of the NMR data with the ones of He et al. [234].

Genistein: colourless solid: ^{1}H NMR (300 MHz, MeOD) δ 8.30 (s, H-2), 7.41 (d, *J* = 8.5 Hz, H-1′), 7.39 (d, *J* = 8.5 Hz, H-4′), 6.87 (d, *J* = 8.5 Hz, H-2′), 6.87 (d, *J* = 8.5 Hz, H-3′), 6.36 (s, H-8), 6.24 (s, H-6), ^{13}C NMR (75 MHz, MeOD) δ 180.3 (C-4), 164.2 (C-7), 162.1 (C-5), 157.8 (C-4’), 157.3 (C-9), 153.7 (C-2), 129.9 (C-2’, 6’), 122.2 (C-l’), 121.3 (C-3), 114.8 (C-3’, 5’), 104.4 (C-1’), 98.9 (C-6), 93.5 (C-8). HR-ESI-MS *m/z* $[M+H]^+$ 271.060 (calcd. for $C_{15}H_{11}O_5^+$: 271.0601).

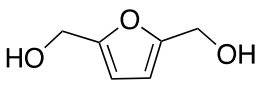

Figure 4.35 Structure of 2,5-bis(hydroxymethyl)furan

2,5-bis(hydroxymethyl)furan (**7**)

Compound **7** was isolated from the polar VLC fraction 1 (see Chapter 3.3.2) and yielded 2mg of a colourless solid. The structure was elucidated by NMR and was compared with the reference spectrum of 2,5-bis(hydroxymethyl)furan.

2,5-bis(hydroxymethyl)furan: colourless solid: ^{1}H NMR (MeOD) δ 6.0 (s, 2H), 4.53 (s, 4H), ^{13}C NMR (75 MHz, MeOD): δ 155.8 (C-2, C-5, qC), 109.1 (C-3, C-4, CH), 57.5 (C-1', C-2', CH_2).

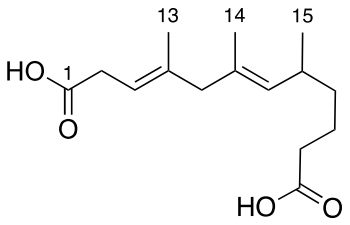

Figure 4.36 Structure of (3*E*,6*E*)-4,6,8-trimethyldodeca-3,6-diendioic acid

(3*E*,6*E*)-4,6,8-trimethyldodeca-3,6-diendioic acid (**8**)

Compound **8** was isolated from fraction 3.2 alongside the heydenoic acids. Extensive NMR structure elucidation revealed an unsaturated linear dicarboxylic acid, methylated at positions 4, 6 and 8. Literature search suggested this to be a novel compound.

(3*E*,6*E*)-4,6,8-trimethyldodeca-3,6-diendioic acid: colourless solid: ^{1}H NMR (300 MHz, MeOD) δ 5.45 (H-3), 4.81 (H-7), 3.11 (H_2-2), 2.71 (H_2-5), 2.37 (H_2-11), 2.27 (H-8), 1.81 (H_3-14), 1.60 (H_2-10), 1.58 (H_3-13), 1.45-1.33. (H_2-9), 0.98 (H_3-15) ^{13}C NMR (75 MHz, MeOD): δ 178.4 (C-12, qC), 177.9 (C-1, qC), 132.7 (C-4, qC), 131.9 (C-6, qC), 131.4 (C-7, CH), 114.5 (C-3, CH), 57.7 (C-5, CH_2), 36.1 (C-9, CH_2), 34.6 (C-11, CH_2), 34.0 (C-8, CH), 32.7 (C-2, CH_2), 26.0 (C-14, CH_3), 21.9 (C-10, CH_2), 20.4 (C-15, CH_3), 17.1 (C-13, CH_3). HR-ESI-MS *m/z* $[M+H]^+$ 269.1740 (calcd. for $C_{15}H_{11}O_5^+$: 269.1747).

4.8 Biological activity of metabolites produced by fungal strains isolated by the FIND technology

With the FIND technology, we managed to isolate rare fungi (see chapter 4.2, Table 4.1). To evaluate the potential for the biosynthesis of bioactive secondary metabolites by these fungal strains we performed screenings on antimicrobial activities against Gram-negative and Gram-positive bacteria, an ascomycete, a basidiomycete and a zygomycete, *i.e*. *Escherichia coli*, *Bacillus megaterium, Eurotium rubrum*, *Microbotryum violaceum* and *Mycotypha microspora* (see Chapter 3.6.2). Ethyl acetate extracts of *Clonostachys rosea*, *Ilyonectria europaea* grown on BM medium and of further 10 isolates (see Table 4.1) grown on BMS medium, were tested in disk diffusion assays using 50 µg of extract per disk. None of the extracts was active against the Gram-negative bacterium *E. coli.* Extracts of *Alternaria armoraciae, Auxarthron umbrinum, Chaetomium globosum, Chrysosporium* sp. 831, *Cladosporium allicinum, Clonostachys rosea, Heydenia* cf. *alpina* and *Ilyonectria europaea* inhibited the growth of *B. megaterium*, *i.e.* inhibition zones of 1, 2, 1.5, 1, 4, 5, 5 and 3 mm were reached, respectively

(Streptomycin, equally concentrated, was used as positive control with an inhibition zone of 10 mm). Additionally, the extract of *I. europaea* inhibited the growth of *M. violaceum* with an inhibition zone of 3 mm in diameter (Miconazole, half concentrated, was used as positive control with an inhibition zone of 10 mm)

The two isolated novel sesquiterpenes heydenoic acid A and B were tested for antimicrobial activities against *Staphylococcus aureus* 133, *Bacillus subtilis* 168, *Micrococcus luteus* 4698, *Arthrobacter crystallopoietes* DSM 20117, *Escherichia coli* I-11276b, and *Klebsiella pneumoniae* sp. *ozeanae* I-10910 using agar diffusion assays on Culture plates (5% sheep blood Columbia agar, BD) overlayed with growth suspension of the bacteria to be tested (see Chapter 3.6.1). None of the compounds showed antimicrobial effects at concentrations of up to 100 µM.

Heydenoic acid A and B were also tested for cytotoxicity towards HEK293 cells using the CellTiter-Blue cell viability assay (see Chapter 3.6.4). None of the compounds showed cytotoxic effects at concentrations of up to 100 µM (see Figure 4.37)

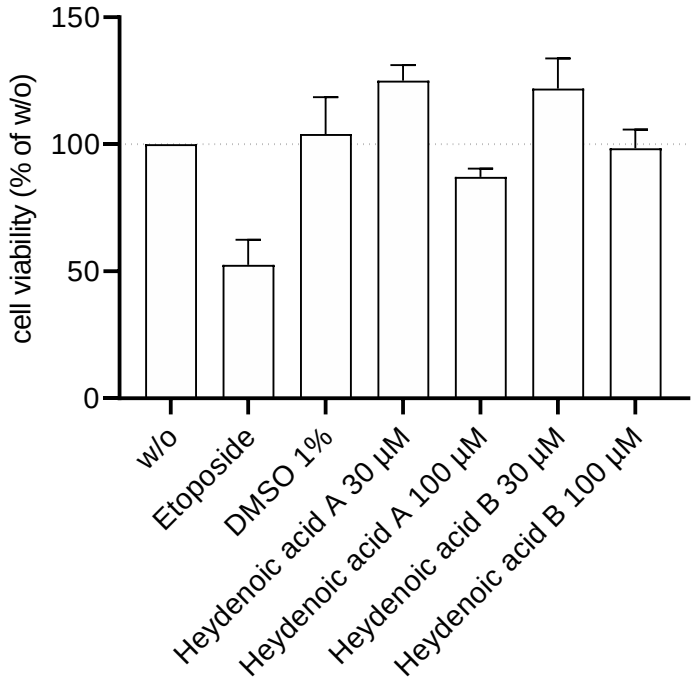

Figure 4.37 Cell viability assay on HEK293 cells. Heydenoic acid A and heydenoic acid B were tested at concentrations of 30µM and 100µM. Etoposide (50 µM) was used as a positive control.

In our continuous effort to isolate small molecules with inhibitory properties against G proteins, compounds **1** and **2** were tested for activity in a label-free dynamic mass redistribution (DMR) assay (see Chapter 3.6.3). This technique enables the detection of holistic cellular responses to extracellular stimuli in real-time without the need for fluorescently labelled proteins [235]. Cellular events, e.g. movement and rearrangement of signalling cascade components, dynamic interaction with regulatory proteins, internalization, cytoskeleton rearrangements and changes in cell shape, alter the optical density, which can be detected by a wavelength shift of light, emitted by the Corning® Epic® System (see Chapter 3.6.3) [236]. The DMR response is expressed in picometers (pm), where a positive signal deflection represents an increase in mass after ligand-induced receptor activation and vice versa. Compounds **1** and **2** (concentrated at 10^{-5} M, $10^{-4.5}$ M and 10^{-4} M) were used without

preincubation, and cell response was measured (see Figure 4.38, a and b). Furthermore, the effect of well-established agonists, i.e. prostaglandin D2 (PDG2), carbachol (Cch) and dynorphin (Dyn), for the major G protein dependent pathways, i.e. Gs, Gq and Gi, respectively, were tested after preincubation with compounds **1** (d) and **2** (e) and compared to the effect of the agonists alone (c). This way, the potential inhibitory effect of **1** and **2** on G proteins was investigated. Epidermal growth factor (EGF) was used as a GPCR independent control.

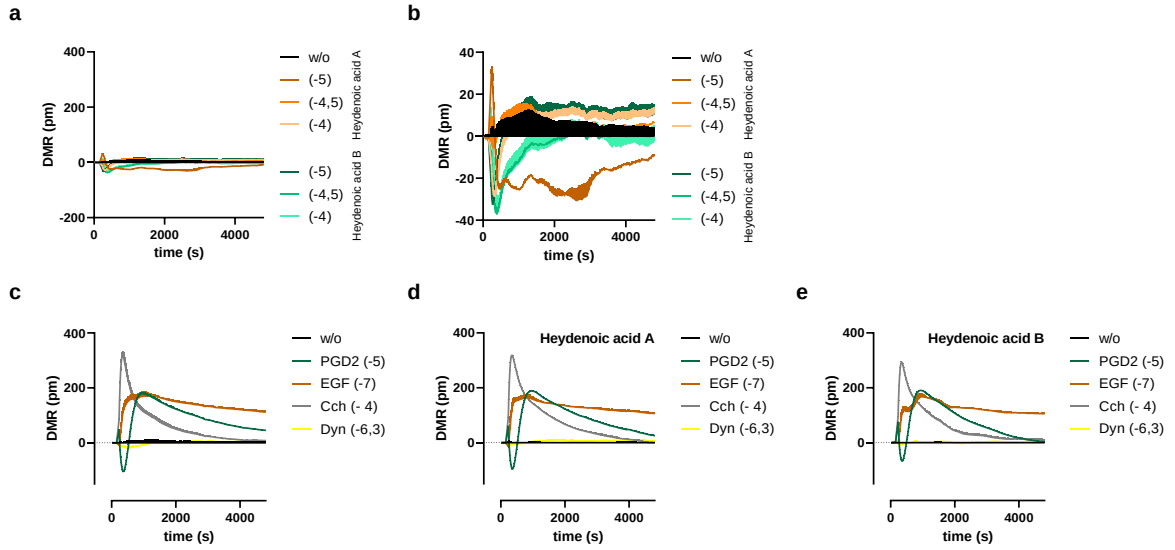

Figure 4.38 Changes in dynamic mass redistribution (DMR) of HEK293T cells, measured with the Corning® Epic® System, illustrated with Prism. Heydenoic acid A and B (10^{-5} M, $10^{-4.5}$ M and 10^{-4} M) mediated changes without preincubation (a), magnified view (b). Effect of different agonists for the major G protein dependent pathways Gs, Gq and Gi, induced by the agonists prostaglandin D2 (PDG2, 10^{-5} M), carbachol (Cch, 10^{-4} M) and dynorphin (Dyn, $10^{-6.3}$ M), respectively, on HEK293T cells without (c) and with preincubation for 90 minutes with either heydenoic acid A (d) or B (e). Epidermal growth factor (EGF, 10^{-7} M) served as a GPCR independent control.

Unfortunately, neither of the compounds provoked significant changes in mass redistribution (a and b) nor inhibited traces provoked by different controls when preincubated with the respective compound. Thus, it is most likely, that both compounds do not interfere with the G protein signalling axis and further testing on the inhibitory effects of compounds **1** and **2** was

suspended. As the control for the Gi pathway, i.e. dynorphin, showed no signal in the DMR (see Figure 4.38, c-e), no conclusions about the effect of **1** and **2** can be drawn in this regard.

4.9 Structure elucidation via SMART of compounds 1 using NMR spectra of the main culture (BMS) extract

High-resolution tandem mass spectrometry combined with molecular networking, has become a powerful tool for dereplication of known NPs and conclude structural motifs from fragmentation patterns. Nevertheless, NMR based analysis is indispensable to determine the planar and 3D structures of novel NPs. The working groups around W. H. Gerwick (Marine Biotechnology and Biomedicine, Scripps Institution of Oceanography, San Diego, California) and G. W. Cotrell (Computer Science & Engineering Department, University of California, San Diego, California) provided a new, NMR-based tool for natural products structure elucidation and dereplication. They developed the Small Molecule Accurate Recognition Technology (SMART), a system that uses a deep convolutional neural network (dCNN) that was initiallytrained on 2048 heteronuclear single quantum correlation (HSQC) spectra of NPs to predict their structure. The network learned features from a big data set and is now able to place a query HSQC near compounds with similar HSQC spectra [237].

In this study the novel iteration SMART 2.0 (query spectrum is placed within 53.076 NP database and provides the user with SMILES of the top 100 closest neighbours that can be visualised with the tensor flow embedding projector) was tested on the main culture (BMS) extract of the fungus *Heydenia* cf. *alpina*, isolated via FIND, to get an insight on its metabolite production. The SMART 2.0 system utilises datasets of HSQC experiments, i.e. tables of $^{1}H,^{13}C$-HSQC signal pairs, which can be obtained from NMR data analysis software, e.g. MestReNova. To validate SMART 2.0s precision in compound recognition of novel compounds, we used HSQC spectra of extracts of increasing purity, originated from the main culture (BMS) extract, containing compound **1**. In the following the HSQC spectrum of fraction 3.2 from the VLC fractionation (see Chapter 3.3.2) was used as dataset 1, the HSQC

spectrum of the HPLC fraction 3.2H7 from the purification procedure of compound **1** (see Chapter 4.6) was used as dataset 2, and the HSQC spectrum of the pure compound **1** was used as dataset 3 (see Chapter 4.6). The HSQC of the culture medium (BMS) was used to delete NMR signals from the datasets that originated from the culture medium.

The three datasets contained different $^{1}H,^{13}C$-HSQC signal pairs. The first dataset (1) included all NMR signals of compound **1** and other compounds in VLC fraction 3.2, which were automatically picked by the MestReNova software. The second dataset (2) contained mostly NMR signals of compound **1**, as well as some NMR signals of other compounds. Additionally, only signals labelled as *compound* by the MestReNova software were included. The third dataset (3) contained only those signals that were elaborated during structure elucidation of compound **1** (see Table 4.3). Signals found in both the HSQC spectrum of the medium (BMS) and the extract were excluded in all datasets. The results were filtered by molecular weight (250 Da), and the top 20 results were used for the analysis.

The filtered results of the SMART analysis for datasets 1 and 2 are quite similar. For both datasets, a six-membered ring, e.g. 3-methyl-2-cyclohexen-1-one motif was suggested for the majority of the predicted structures. Indeed this is found in heydenoic acid A. Overall, the pentenoic acid moiety of heydenoic acid A was recognised quite well by the SMART system and found among the top 20 results. Additionally, in most cases, this moiety was connected to the six-membered ring. The verbenone moiety could only be predicted in one case (see Figure 4.39). Figure 4.39 shows three of the suggested structures, pointing out the efficiency of the SMART technology regarding the prediction of novel natural products from mixtures. In the first structure, the backbone of sesquiterpenoids like bisabolyl or bergamotene derivatives is clearly visible. In the second structure, the α,β-unsaturated monocarboxylic acid moiety was recognised, which is also connected to a cyclic structure. The cyclic structure was interpreted

as a seven-membered ring, suggesting a compound with the carboxylic side chain being one carbon shorter than that of heydenoic acid A. The third structure correctly depicts the verbenone moiety of heydenoic acid A and shows an α,β-unsaturated monocarboxylic acid moiety, the latter being interpreted by SMART as an ester function.

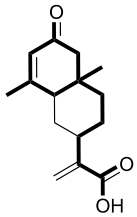

2-(4a,8-dimethyl-6-oxo-1,2,3,4,4a,5,6,8a-octahydronaphthalen-2-yl)prop-2-enoic acid

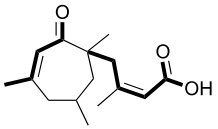

3-methyl-4-(1,4,6-trimethyl-2-oxo-cyclohept-3-en-1-yl)but-2-enoic acid

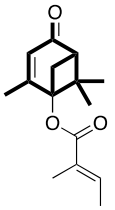

2,6,6-trimethyl-4-oxobicyclo[3.1.1]hept-2-en-1-yl 2-methylbut-2-enoate

Figure 4.39 Predicted SMART structures from datasets 1 and 2 obtained from HSQC data from extracts of the main culture of *H*. cf. *alpina* 824; Heydenoic acid A resembling moieties highlighted.

With dataset 3, the potential of determining the true nature of the pure substance was investigated. Only NMR signals that were used for structure elucidation of heydenoic acid A (see Chapter 4.6) were taken into account for this SMART experiment. Figure 4.40 shows the closest approximation to the elucidated structure of heydenoic acid A.

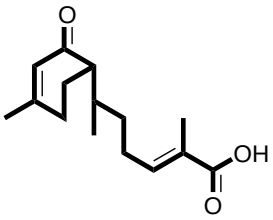

(*S*,*E*)-2-methyl-6-((*R*)-4-methyl-2-oxocyclohex-3-en-1-yl)hept-2-enoic acid

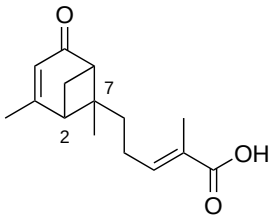

Heydenoic acid A

Figure 4.40 Left: Predicted SMART structure from dataset 3 obtained from HSQC data from extracts of the main culture of *H*. cf. *alpina* 824; Right: Heydenoic acid A for comparison; resembling moieties highlighted.

In the proposed structure, the 3-methyl-2-cyclohexen-1-one motif was recognised as well as the 2-methyl-pentenoic acid moiety. The carbon-carbon bond between C-2 and C-7 (see Figure 4.40) is missing, thus lacking the four-membered ring of the bicyclic part of heydenoic acid A. With a cosine score of 0.86 and only one C-C bond interpreted incorrectly, (*S*,*E*)-2-methyl-6-((*R*)-4-methyl-2-oxocyclohex-3-en-1-yl)hept-2-enoic acid was the closest suggested structure by the SMART 2.0 system.

The results of data sets 1 and 2 show very close predictions of structural properties directly from fungal extracts, i.e. very complex mixtures of different natural products. The results of dataset 3 illustrate the precision of SMARTs structure interpretation for pure compounds effectively.

5 Concluding remarks

In drug research, the metabolome of microorganisms provides promising and potent drug leads [238]. Recent discoveries in the field of antibiotics from underexamined or even undescribed bacteria emphasise the importance of targeting novel microorganisms [239, 86]. In both cases the authors report major difficulties in the cultivation of the respective microbes under laboratory conditions. These observations led to our effort in developing a suitable isolation procedure, which allows to challenge undiscovered habitats, as well as to enable the growth of cultures under laboratory conditions. With FIND we were able to not only access rare and underexamined microbes, but also grow them in the laboratory without difficulties.

We were able to isolate novel compounds (**1**, **2**) from one of the fungi obtained with FIND. Belonging to the bergamotene type of sesquiterpenes, compounds **1** and **2**, heydenoic acid A and heydenoic acid B, respectively, share the structural skeleton of highly potent insect and fungal pheromones, plant growth regulators and antimicrobial natural products (see chapter 1.4) [140-145]. The results from the cell viability test (see Figure 4.37) hints towards the safe use as a potential drug, which is supported by the fact that both compounds are in accordance with Lipinski's rule of five (see Table 5.1).

Table 5.1 Lipinski's rule of five for heydenoic acid A and heydenoic acid B

Rule	Heydenoic acid A	Heydenoic acid B
Molecular mass <500 Da	248 Da	250 Da
High lipophilicity logP<5	3.06	3.55
Less than 5 hydrogen bond donors	Yes	Yes
Less than 10 hydrogen bond acceptors	Yes	Yes
Molar refractivity between 40-130	44.44	44.44

In conclusion, compounds **1** and **2** bear the potential of being studied as drug candidates. Thus the investigation of their bioactivity is highly recommended in further studies.

In this respect the biosynthesis of natural compounds is required for heterologous expression or the biomimetic synthesis of structural analogues. Regarding the biosynthesis of **1** and **2**, we propose the formation of bergamotene from *E*,*E*-farnesyl-PP via an enzyme like bergamotene synthase and subsequent oxidation, e.g. via CYP-450 dependent mono-oxygenases. Figure 5.1 summarises the putative biosynthesis of heydenoic acid A.

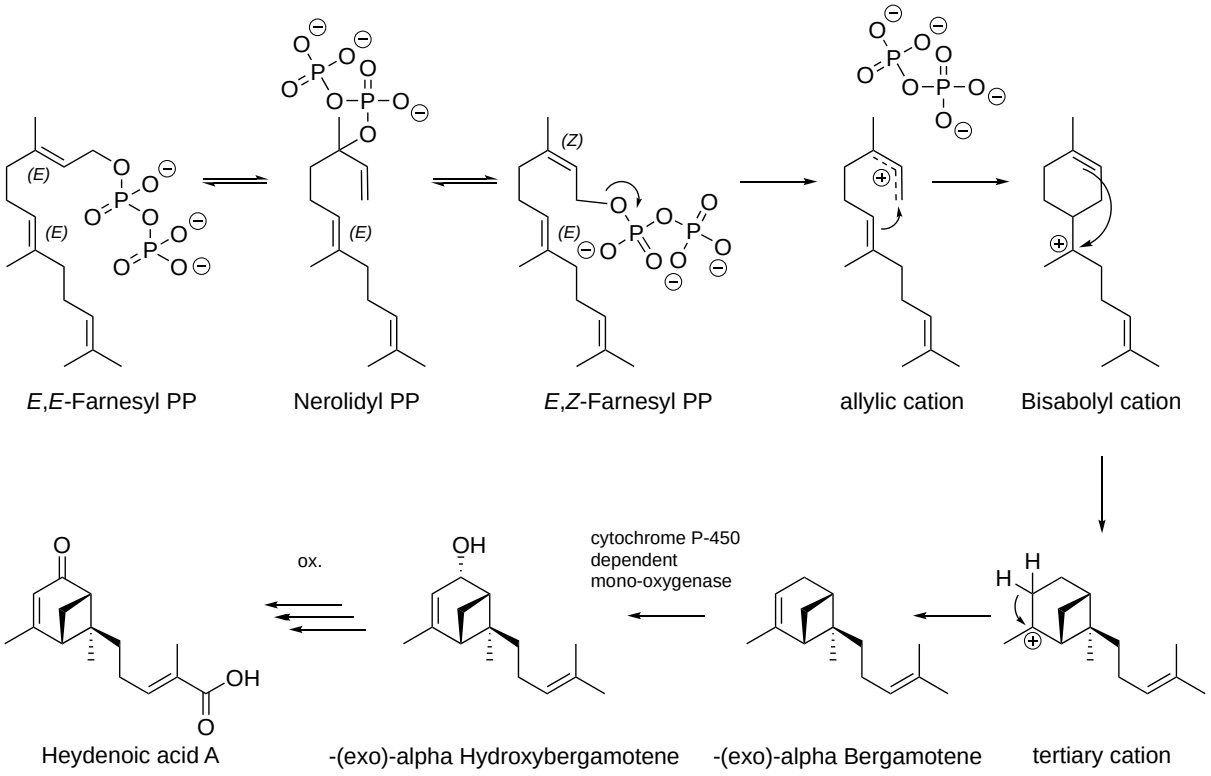

Figure 5.1 Putative biosynthesis of heydenoic acid A from *E,E*-farnesyl-PP via a bergamotene synthase-like enzyme and subsequent oxidation, e.g. by cytochrome P-450-dependent mono-oxygenase.

For the bergamotene type meroterpene fumagillin, produced by *Aspergillus fumigatus*, the precursor molecule β-*trans*-bergamotene was shown to be biosynthesised by a β-*trans*-bergamotene synthase [240]. In our proposal, *E,E*-farnesyl-PP is directly cyclised into α-*trans*-bergamotene by a α-*trans*-bergamotene synthase, an enzyme which formerly was determined in lavender (*Lavandula angustifolia*) by Landmann et al. [241]. Furthermore, Schewe et al. confirmed the introduction of a hydroxyl group at C-5 of α-pinene by $P450_{BM-3}$ using recombinant *E. coli* [242]. Comparably, hydroxylation of the α-*trans*-bergamotene precursor by cytochrome P450 enzymes in *H.* cf. *alpina* seems reasonable.

Extracts of *H.* cf. *alpina* 824 showed antimicrobial activity in the respective bioassays. The results of the OSMAC approach on cultures of *H.* cf. *alpina* 824 revealed that the activity against the Gram-positive bacterium *Bacillus megaterium* (see Figure 4.8) can be increased, if

the fungus is cultivated under optimised conditions. Molecular networking disclosed an accumulation of compounds, mainly fatty acids, fatty acid amides and steroid type triterpenes, exclusively produced on this specific culture medium (Synthetic Nutrient poor Agar medium, SNA) (see Figure 4.13). For the annotated fatty acid amides, antimicrobial activity was described in the literature [226, 227]. Also, steroid-like triterpenes were shown to have remarkable inhibitory activities against a broad spectrum of Gram-positive bacteria [243]. The first isolated antimicrobial compound with a steroid skeleton from a fungus (*Aspergillus fumigatus, mut. helvola* Yuill) was helvolic acid, whose antimicrobial range of activity was comparable to that of penicillin G [244]. After this critical discovery, a sequence of similar compounds was isolated from cultures of *Cephalosporium acremonium*, e.g. cephalosporins P1 (not to be confused with peptidoglycan synthesis inhibitor cephalosporin C), resembling helvolic acid in both chemical structure and biological activity [245]. However, it was not until the isolation and structure elucidation of fusidic acid, found in *Fusidium coccineum*, that a steroid-like antibiotic was introduced into the treatment of patients with bacterial infections [107]. Figure 5.2 depicts the structural similarities of the steroid antibiotics, mentioned above.

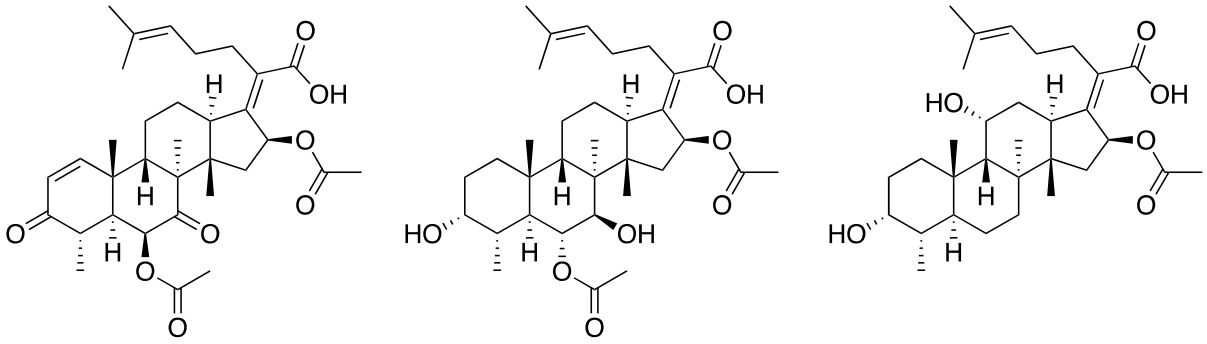

Figure 5.2 Structures of helvolic acid, cephalosporin P1 and fusidic acid, antimicrobial steroid-like triterpenes isolated from fungi.

All compounds depicted in Figure 5.2 are derived from ergosterol (molecular weight of 396 Da), thus having molecular masses between 400 and 600 Da. The molecular network, obtained using the GNPS molecular networking web system, of the metabolites produced by *H.* cf. *alpina* show masses in this range, and they all are grouped in a special cluster. This cluster is characterised by compounds sharing the typical fragmentation patterns of steroid-like triterpenes. These compounds and their respective spectra occur exclusively in extracts grown on SNA medium and are connected to nodes of dereplicated steroid-like compounds. Production of antimicrobial steroid-like compounds on SNA medium by *H*. cf. *alpina* could be a possible explanation for the increased bioactivity.

Overall, this study demonstrates the importance of targeting new source organisms for the isolation of novel natural compounds. The latter are a vital source for drug candidates and their development. With FIND we were able to access both, underexamined source organisms, as well as novel natural products.

6 Summary

Specialised metabolites from fungi belong to the most potent and valuable drugs, e.g. the penicillin antibiotics and leading immunosuppressants like mycophenolic acid. In order to find new structural types as drug leads, novel source organisms have to be targeted. However, isolation of fungi using conventional methods, i.e. dilution plating, selective isolation and baiting, barely lead to unusual or novel microbial species. Additionally, it is most challenging to obtain fungi in axenic form and to cultivate them under laboratory conditions, if only using standard methods.

It was thus the aim of this study to probe a new isolation method as most fungi on earth are still undescribed and their secondary metabolome is expected to hold promise in terms of pharmaceutically interesting products. The novel approach on the isolation of axenic fungal cultures from diverse habitats developed in this study, contributes a fast and straightforward procedure to the repertoire of classic isolation techniques. The here invented Fungal one step IsolatioN Device (FIND) comprises a multi-chambered micro agar plate, where initially only one fungal part (e.g., hyphal cell, mycelial fragment or spore) is located in each chamber. The chambers are sealed with semi-permeable membranes, and after inoculation, the device is placed back into the original natural environment of sample collection, to ensure favourable growth conditions.

With the FIND, it was possible to isolate 12 rare and underexamined axenic fungal cultures directly from their sample sources, i.e. terrestrial soil, sea sediment and seawater, without any purification or passaging steps. The taxonomy of nine of these strains could be determined to species level by DNA sequencing, i.e. *Alternaria armoraciae, Auxarthron umbrinum, Chaetomium globosum, Cladosporium allicinum, Clonostachys rosea, Heydenia* cf. *alpina,*

Ilyonectria europaea, *Metarhizium carneum* and *Scopulariopsis brevicaulis*. Except for *S. brevicaulis*, none of these fungi is considered to be common. For three fungal cultures, i.e. *Cadophora* sp. 829, *Chrysosporium* sp. 831, *Leucothecium* sp. 828, no species could be assigned. We could show however, that it is most likely, that the strain *Cadophora* sp. 829 is a hitherto undescribed species, as the DNA sequences of the internal transcribed spacer region (ITS) of this strain does not match any of the reference sequences deposited in MycoBank. The isolation and cultivation of unusual and undescribed fungal species is a crucial step for successful natural product discovery. Our results provide evidence, that with FIND it is possible to obtain axenic fungal cultures in a single step and at the same time restrain fast-growing fungi in favour of rare and underexamined species.

One of the isolated fungi, i.e. *Heydenia* cf. *alpina* (strain 824) was never before investigated chemically and cultures of our strain yielded three novel compounds, namely heydenoic acid A (**1**), heydenoic acid B (**2**) and (3*E*,6*E*)-4,6,8-trimethyldodeca-3,6-diendioic acid (**8**). The first two compounds belong to the sesquiterpene family of bergamotenes. Structure elucidation was performed using extensive 1D and 2D NMR spectroscopy. The absolute configuration of the [3.1.1]bicyclo ring system in **1** and **2** was determined by circular dichroism (CD) spectroscopy, making use of their resemblance to verbenone. The negative Cotton effects of compounds **1** and **2** were identical to those of (2*S*,6*S*)-verbenone, suggesting the stereocenters in **1** and **2** to be all *S*. In summary, the isolation of novel compounds from a fungal culture, obtained with the FIND technology, supports our strategy in the respect, that underexamined fungal species are a vital source for undescribed specialised metabolites.

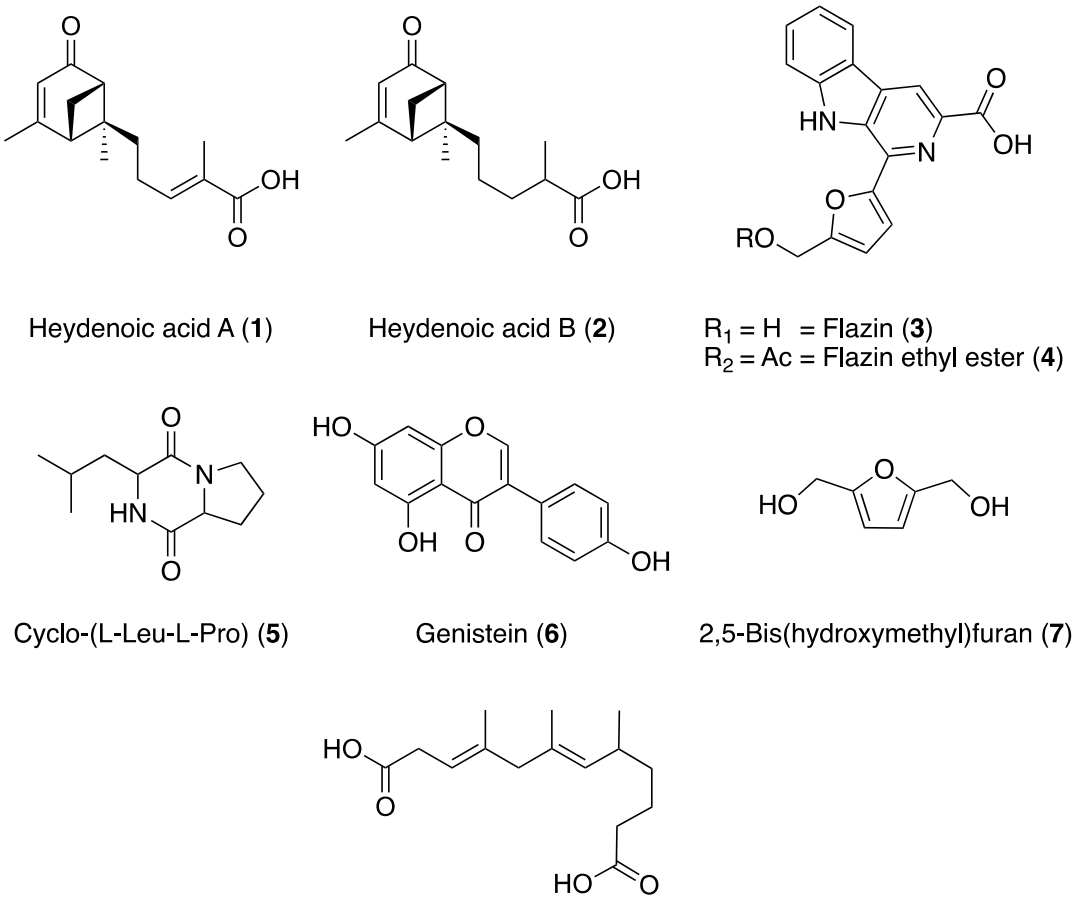

Structures of compounds isolated from a biomalt salt culture extract of *Heydenia* cf. *alpina* 824.

In order to evaluate the physiology and metabolome of *H.* cf. *alpina* 824 more deeply, cultivation conditions were altered and novel bioinformatic tools were used. The strain was isolated from a seawater sample, collected at the Schlei region in northern Germany and indeed our results from experiments examining the salinity dependency of growth revealed an adaption to marine habitats, as cultures of this fungus grew significantly slower on culture plates lacking appropriate amounts of sea salts.

In order to further investigate the metabolome of *H.* cf. *alpina* 824 Global Natural Product Social (GNPS) molecular networking, MolNetEnhancer motif annotation and Small Molecule Accurate Recognition Technology (SMART 2.0) mixture analysis were applied. By matching High-Resolution Electrospray Ionization Tandem Mass Spectrometry data (HR-ESI-MS/MS) of extracts from cultures of *H.* cf. *alpina* 824, cultivated on different media, with the GNPS public spectral library, it was possible to identify four known compounds, from this species for the first time, i.e. the β-carboline flazin (**3**), the diketopiperazine cyclo-(L-Pro-L-Leu) (**5**), the isoflavone genistein (**6**) and the furanoid 2,5-bis(hydroxymethyl)furan (**7**). Further, we were able to isolate a further novel compound (**4**), with the help of the GNPS molecular networking in combination with the motif annotation workflow MolNetEnhancer. In the β-carboline cluster, compound **3** was connected to a compound differing in its molecular weight by the mass of an acetyl group (+42 Dalton). NMR guided fractionation of the main culture (BMS) extract by RP HPLC led to the isolation of flazin ethyl ester (**4**), an undescribed derivative of (**3**). In the isoflavone cluster, we were able to dereplicate genistein (**6**) and to isolate it from the same extract. Additionally, we could propose several methylated derivatives of genistein by analysis of their MS/MS fragments, i.e. 6-methylbiochanin A and the putative novel compounds 8-methylbiochanin A, 3'-hydroxy-6-methylbiochanin A and 3'-hydroxy-8-methylbiochanin A.

In conclusion, FIND, developed in this study, established a novel procedure for the isolation of axenic fungal cultures from marine and terrestrial samples in a single step. Using this technology, unusual and hitherto undescribed fungal species can be obtained. One of the fungal cultures obtained with FIND, *H.* cf. *alpina* 824, was shown to be a producer of novel compounds. State-of-the-art bioinformatic tools allowed an in-depth analysis on the metabolome of *H.* cf. *alpina* 824.

7 References

1. Hyde, K. D., Xu, J., Rapior, S., Jeewon, R., Lumyong, S., Niego A. G. T., Abeywickrama, P. D., Aluthmuhandiram, J. V. S., Brahamanage, R. S., Brooks, S., Chaiyasen, A., Chethana, K. W. T., Chomnunti, P., Chepkirui, C., Chuankid, B., de Silva, N. I., Doilom, M., Faulds, C., Gentekaki, E., Gopalan, V., Kakumyan, P., Harishchandra, D., Hemachandran, H., Hongsanan, S., Karunarathna, A., Karunarathna, S. C., Khan, S., Kumla, J., Jayawardena, R. S., LiuNingguo Liu, J.-K., Luangharn, T., Macabeo, A. P. G., Marasinghe, D. S., Meeks, D., Mortimer, P. E., Mueller, P., Nadir, S., Nataraja, K. N., Nontachaiyapoom, S., O'Brien, M., Penkhrue, W., Phukhamsakda, C., Shaanker, U., Rathnayaka, R. A. R., Sadaba, R. B., Sandargo, B., Samarakoon, B. C., Tennakoon, D. S., Siva, R., Sriprom, W., Suryanarayanan, T. S., Sujarit, K., Suwannarach, N., Suwunwong, T., Thongbai, B., Thongklang, N., Wei, D., Wijesinghe, N. S., Winiski, J., Yan, J., Yasanthika, E., Stadler, M., The amazing potential of fungi: 50 ways we can exploit fungi industrially, *Fungal Divers*, **2019**, *97*, 1-136

2. Koehn, F. E., Biosynthetic medicinal chemistry of natural product drugs, *Med Chem Commun*, **2012**, *3*, 854–865, 10.1039/c2md00316c

3. Bills, G. F., Gloer, J. B., Biologically Active Secondary Metabolites from the Fungi, *Microbiol Spectr*, **2016**, *4*, 10.1128/microbiolspec.FUNK-0009-2016.

4. Dias, D. A., Urban, S., Roessner, U., A historical overview of natural products in drug discovery, *Metabolites*, **2012**, *2*, 303–336, 10.3390/metabo2020303

5. Denham, S. T., Wambaugh, M. A., Brown, J. C. S., How Environmental Fungi Cause a Range of Clinical Outcomes in Susceptible Hosts, *J Mol Biol*, **2019**, *431*, 2982-3009. 10.1016/j.jmb.2019.05.003

6. Leyronas, C., Duffaud, M., Nicot, P. C., Compared efficiency of the isolation methods for *Botrytis cinerea*, *Mycology*, **2012**, *3*, 221-225, 10.1080/21501203.2012.727484

7. Lebowitz, R. A., Waltzman, M. N., Jacobs, J.B., Pearlman, A., Tierno, P.M., Isolation of fungi by standard laboratory methods in patients with chronic rhinosinusitis, *Laryngoscope* **2002**, *112*, 2189-2191, 10.1097/00005537-200212000-00012

8. Souza, A. R., Baldoni, D. B., Lima, J., Porto, V., Marcuz, C., Machado, C., Ferraz, R. C., Kuhn, R.C., Jacques, R. J., Guedes, J. V., Mazutti, M. A., Selection, isolation, and identification of fungi for bioherbicide production. *Brazilian journal of microbiology*, **2017**, *48*, 101–108. 10.1016/j.bjm.2016.09.004

9. Hawksworth, D. L., Naming fungi involved in spoilage of food, drink, and water, *Curr Opin Food Sci*, **2015**, *5*, 23-28, doi.org/10.1016/j.cofs.2015.07.004

10. Richardson, M., Bowyer, P., Sabino, R., The human lung and Aspergillus: You are what you breathe in? *Medical mycology*, **2019**, 57, 145–154. 10.1093/mmy/myy149

11. Chilaka, C. A., De Boevre, M., Atanda, O. O., De Saeger, S., The Status of Fusarium Mycotoxins in Sub-Saharan Africa: A Review of Emerging Trends and Post-Harvest Mitigation Strategies towards Food Control. *Toxins*, **2017**, *9*, 19, 10.3390/toxins9010019

12. Frisvad, J., Smedsgaard, J., Larsen, T. O., Samson, R., Mycotoxins and other extrolites produced by species in Penicillium subgenus Penicillium. *Studies in Mycology*. **2004**, 201-241.

13. Gaynes R., The Discovery of Penicillin—New Insights After More Than 75 Years of Clinical Use. *Emerging Infectious Diseases*, **2017**, *23*, 849–85, 10.3201/eid2305.161556

14. Aminov R. I., A brief history of the antibiotic era: lessons learned and challenges for the future. *Frontiers in microbiology*, **2010**, *1*, 134, 10.3389/fmicb.2010.00134

15. Hoeksma, J., Misset, T., Wever, C., A new perspective on fungal metabolites: identification of bioactive compounds from fungi using zebrafish embryogenesis as read-out. *Sci Rep*, **2019**, *9*, 17546, 10.1038/s41598-019-54127-9

16. Prakash, O., Shouche, Y., Jangid, K., Microbial cultivation and the role of microbial resource centers in the omics era, *Appl Microbiol Biotechnol*, **2013**, *97*, 51-62, 10.1007/s00253-012-4533-y

17. Narisco, J. A., Parish, M. , Direct plating: A method for detecting fungal contamination in paperboard cartons, *Journal of Food Safety*, **2001**, *21*, 141-150, 10.1111/j.1745-4565.2001.tb00314.x

18. Rajala, T., Tuomivirta, T., Pennanen, T., Mäkipää, R., Habitat models of wood-inhabiting fungi along a decay gradient of Norway spruce logs, *Fungal Ecology*, **2015**, *18*, 48-55, 10.1016/j.funeco.2015.08.007.

19. Porras-Alfaro, A., Bayman, P., Hidden Fungi, Emergent Properties: Endophytes and Microbiomes, Annual Review of Phytopathology, **2011**, *49*, 291-315, 10.1146/annurev-phyto-080508-081831

20. Feng, T., Shui, M., Song, S., Zhuang, H., Sun, M., Yao, L., Characterization of the Key Aroma Compounds in Three Truffle Varieties from China by Flavoromics Approach, *Molecules*, **2019**, *24*, 3305, 10.3390/molecules24183305

21. McKeen, C. D., Thorpe, H.J., An adaptation of a moist-chamber method for isolating and identifying Verticillium spp., *Can J Microbiol*, **1971**, 17, 1139-1141. 10.1139/m71-179

22. Keyworth, W.G., A Petri-Dish Moist Chamber, *Trans Brit Myc Soc*, **1951**, *34*, 291-292, https://doi.org/10.1016/S0007-1536(51)80054-8

23. Czaban, J., Wroblewska B., A simple, direct plating method, alternative to dilution plating, for estimation of the abundance of Penicillium verrucosum on incubated cereal grain, *Pol J Microbiol*, **2006**, *55*, 237-241

24. Rabie, C. J., Lübben, A., Marais, G. J., Jansen van Vuuren, H., Enumeration of fungi in barley, *Int J Food Microbiol*, **1997**, *35*, 117-127

25. Hartman D., Perfecting your spread plate technique. *J Microbiol Biol Educ*, **2011**, *12*, 204–205, 10.1128/jmbe.v12i2.324

26. Sanders E. R., Aseptic laboratory techniques: plating methods. *J Vis Exp*, **2012**, *63*, e3064, 10.3791/3064

27. Nagano, Y., Millar, B. C., Goldsmith, C. E., Walker, J. M., Elborn, J. S., Rendall, J., Moore, J. E., Development of selective media for the isolation of yeasts and filamentous fungi from the sputum of adult patients with cystic fibrosis (CF), *J Cyst Fibros*, **2008**, *7*, 566-72, 10.1016/j.jcf.2008.06.007

28. Mentese, S., Otkun, M. T., Palaz, E. *Aerobiologia*, **2017**, *33*, 211–219, 10.1007/s10453-016-9462-2

29. Morring, K. L., Sorenson, W. G., Attfield, M. D., Sampling for airborne fungi: a statistical comparison of media, *Am Ind Hyg Assoc J*, **1983**, *44*, 662-664. 10.1080/15298668391405526

30. Baggerman, W. I., A Modified Rose Bengal Medium for the Enumeration of Yeasts and Moulds from Foods, *European J Appl Microbiol Biotechnol*, **1981**, *12*, 242-247

31. Greenfield, M., Pareja, R., Ortiz, V., Gómez-Jiménez, M. I., Vega, F. E., Parsa, S., A novel method to scale up fungal endophyte isolations, *Biocontrol Sci Techn*, **2015**, *25*, 1208-1212, 10.1080/09583157.2015.1033382

32. Kern, K. A., Pergo, E. M., Kagami, F. L., Arraes, L. S., Sert, M. A., Ishii-Iwamoto, E. L., The phytotoxic effect of exogenous ethanol on Euphorbia heterophylla L., *Plant Physiol Biochem*, **2009**, *47*, 1095-101. 10.1016/j.plaphy.2009.07.002

33. van der Burg, W. J., Effect of hydrogen peroxide spraying on Hydrocotyle ranunculoides L.f. survival, *Plant Research International,* **2010**, not published

34. Thomas, P., Sekhar, A. C., Upreti, R., Mujawar, M. M., Pasha, S. S., Optimization of single plate-serial dilution spotting (SP-SDS) with sample anchoring as an assured method for bacterial and yeast cfu enumeration and single colony isolation from diverse samples. *Biotechnology reports*, **2015**, *8*, 45–55, 10.1016/j.btre.2015.08.003

35. Zhang, Z., Qu, Y., Li, S., Feng, K., Wang, S., Cai, W., Liang, Y., Li, H., Xu, M., Yin, H., Deng, Y., Soil bacterial quantification approaches coupling with relative abundances reflecting the changes of taxa, *Sci.* Rep, **2017**, *7*, No. 4837, 10.1038/s41598-017-05260-w

36. Lawlor, K., Knight, B. P., Barbosa-Jefferson, V. L., Lane, P. W., Lilley, A. K., Paton, G., I., McGrath, S. P., O'Flaherty, S. M., Hirsch, P. R., Comparison of methods to investigate microbial populations in soils under different agricultural management, *FEMS Microbiology Ecology*, **2000**, *33*, 129–137, 10.1111/j.1574-6941.2000.tb00735.x

37. Overy, D. P., Rämä, T., Oosterhuis, R., Walker, A. K., & Pang, K. L. (2019). The Neglected Marine Fungi, *Sensu stricto*, and Their Isolation for Natural Products' Discovery. *Marine drugs*, *17*(1), 42. doi:10.3390/md17010042

38. Pitt, J. I., Hocking A. D., Fungi and Food Spoilage, Chapter 4 Methods for Isolation, Enumeration and Identification, ©Springer Science + Business Media, LLC Dordrecht Heidelberg London New York, **2009**

39. Pepper, I. L., Gerba, C. P., & Gentry, T. J., Environmental Microbiology: *Third Edition*. ©Elsevier, Inc., Amsterdam Boston Heidelberg London New York Oxford Paris San Diego San Francisco Singapore Sydney Tokyo

40. Noman, E, Al-Gheethi, A. A., Rahman, N. K., Talip, B., Mohamed, R, Kadir, N. H., Kadir, O. A., *IOP Conf Ser: Earth Environ Sci*, **2018**, *140*, 012055, 10.1088/1755-1315/140/1/012055

41. Calhim, S., Halme, P., Petersen, J. H., Læssøe, T., Bässler, C., Heilmann-Clausen, J., Fungal spore diversity reflects substrate-specific deposition challenges. *Sci Rep*, **2018**, *8*, 5356 10.1038/s41598-018-23292-8

42. Choi, Y. W., Hyde, K. D., Ho, W. H., Single spore isolation of fungi, *Fungal Divers*, **1999**, *3*, 29-38,

43. Zhang, K., Yuan-Ying, S., Cai, L., An Optimized Protocol of Single Spore Isolation for Fungi, *Cryptogamie Mycologie*, **2013**, *34*, 349-356

44. Stolze-Rybczynski, J. L., Cui, Y., Stevens, M. H., Davis, D. J., Fischer, M. W., Money, N. P. Adaptation of the spore discharge mechanism in the basidiomycota. *PloS one*, **2009**, *4*, e4163, 10.1371/journal.pone.0004163

45. Kofler, L., A Method to Use Lichen Spores in Quantitative Studies on Germination. *Bryologist*, **1970**, *73*, 602-606, 10.2307/3241499

46. Hong, G., Miller, H. B., Allgood, S., Lee, R., Lechtzin, N., Zhang, S. X., Use of Selective Fungal Culture Media Increases Rates of Detection of Fungi in the Respiratory Tract of Cystic Fibrosis Patients. *J Clin Microbiol*, **2017**, *55*, 1122–1130. 10.1128/JCM.02182-16

47. Pham, T., Giraud, S., Schuliar, G., Rougeron, A., Bouchara, J. P., Scedo-Select III: a new semi-selective culture medium for detection of the Scedosporium apiospermum species complex, *Med Mycol*, **2015**, *53*, 512-519, 10.1093/mmy/myv015

48. Gielen, S., Aerts, R., Seels, B., Development of a selective medium for the determination of the spore concentrations of Botrytis cinerea in the air, *Commun Agric Appl Biol Sci*, **2003**, *68*, 685-93

49. Lin, C. K., Germination of the Conidia of Sclerotinia Fructicola, with Special Reference to the Toxicity of Copper. *Cornell Univ Agr Exp Sta*, Mem. 233: 1-30. 1940.

50. Lin, C. K., Nutrient Requirements In The Germination Of The Conidia Of Glomerella Cingulata, *Am J Bot*, **1945**, *32*, 296–298.

51. Miotto, M., Olimpieri, P. P., Di Rienzo, L., Ambrosetti, F., Corsi, P., Lepore, R., Tartaglia, G. G., Milanetti, E., Insights on protein thermal stability: a graph representation of molecular interactions. *Bioinformatics*, **2019**, *35*, 2569-2577, 10.1093/bioinformatics/bty1011

52. Hassan, N., Rafiq, M., Hayat, M., Nadeem, S., Shah, A. A., Hasan, F., *Appl Ecol Env Res*, **2017**, *15*, 1157-1171, 10.15666/aeer/1503_11571171

53. Bhabhra, R., Miley, M. D., Mylonakis, E., Disruption of the Aspergillus fumigatus gene encoding nucleolar protein CgrA impairs thermotolerant growth and reduces virulence, *Infect Immun*, **2004**, *72*, 4731–4740, 10.1128/IAI.72.8.4731-4740.2004

54. Guimarães, A. J., de Cerqueira, M. D., Nosanchuk, J. D. Surface architecture of histoplasma capsulatum, *Front Microbiol*, **2011**, *2*, 225, 10.3389/fmicb.2011.00225

55. Nicholls S, Leach MD, Priest CL, Brown AJ. Role of the heat shock transcription factor, Hsf1, in a major fungal pathogen that is obligately associated with warm-blooded animals. Mol Microbiol. 2009;74(4):844–861. doi:10.1111/j.1365-2958.2009.06883.x

56. Gottlieb, D. (1950). The Physiology of Spore Germination in Fungi. Botanical Review, 16(5), 229-257. Retrieved from www.jstor.org/stable/4353434

57. Rousk J, Brookes PC, Bååth E. Contrasting soil pH effects on fungal and bacterial growth suggest functional redundancy in carbon mineralization. Appl Environ Microbiol. 2009;75(6):1589–1596. doi:10.1128/AEM.02775-08

58. Gross, S. & Robbins, E.I. *Hydrobiologia* (2000) *433*: 91. https://doi.org/10.1023/A:1004014603333; Kladwang, W., Bhumirattana, A., Hywel-Jones, N. *Fungal Diversity* 2003 *13*: 69-83.

59. Loefer, John B., et al. "Inhibition and Enhancement of the Growth of Fungi with Streptomycin." Bulletin of the Torrey Botanical Club, vol. 79, no. 3, 1952, pp. 242–250. JSTOR, www.jstor.org/stable/2482304.

60. Rooke, DM., Shattock, RC., Journal of General Microbiology, 1983, 129, 3401-3410

61. Veen, K.H., Ferron P, J. Invertebr. 1966, *8*, 268-269; Whiffen, AO., J. Bacterial., 1948, *56*, 283.

62. Plemenitaš A, Lenassi M, Konte T, Kejžar A, Zajc J, Gostinčar C and Gunde-Cimerman N (2014) Adaptation to high salt concentrations in halotolerant/halophilic fungi: a molecular perspective. Front. Microbiol. 5:199. doi: 10.3389/fmicb.2014.00199

63. Mohammadian Fazli M, Soleimani N, Mehrasbi M, Darabian S, Mohammadi J, Ramazani A. Highly cadmium tolerant fungi: their tolerance and removal potential. J Environ Health Sci Eng. 2015;13:19. Published 2015 Mar 14. doi:10.1186/s40201-015-0176-0

64. Bajpai, V., Govindaswamy, A., Sagar, S., Kumar, S., Garg, P., Xess, I., Malhotra, R., and Mathur, P. Microbial Drug Resistance. 2019, http://doi.org/10.1089/mdr.2019.0021

65. Ballhausen, M. B., van Veen, J. A., Hundscheid, M. P., & de Boer, W, Methods for Baiting and Enriching Fungus-Feeding (Mycophagous) Rhizosphere Bacteria. *Front Microbiol*, 2015, *6*, 1416, 10.3389/fmicb.2015.01416

66. Simpanya, M. F., Baxter, M., Isolation of fungi from soil using the keratin-baiting technique, *Mycopathologia*, **1996**, *136*, 85-89, 10.1007/BF00437500

67. Orr, G. F., Keratinophilic fungi isolated from soils by a modified hair bait technique, *Sabouraudia*, **1969**, *7*, 129-134, 10.1080/00362177085190231

68. Overy, D. P., Bayman, P., Kerr, R. G., Bills, G. F., An assessment of natural product discovery from marine (sensu strictu) and marine-derived fungi. *Mycology*. **2014**, *5*, 145–167, 10.1080/21501203.2014.931308.

69. Ulfig, K., Płaza, G., Terakowski, M., Staszewski, T., A study of keratinolytic fungi in mountain sediments. I. Hair-baiting data, *Rocz Panstw Zakl Hig*, **1998**, *49*, 469-479,

70. Sundaram, B. M., Fungal flora of rice field soils, *Proc Indian Acad Sci*, **1976**, *85*, 90-99

71. Avanzato, M.V. and C.S. Rothrock. 2010. Use of Selective Media and Baiting to Detect and Quantify the Soilborne Plant Pathogen Thielaviopsis basicola on Pansy. The Plant Health Instructor. DOI: 10.1094/PHI-I-2010-0610-01

72. Klingen, I., Eilenberg, J., Meadow, R., Effects of farming system, field margins and bait insect on the occurrence of insect pathogenic fungi in soils. 2002, *91*, 191-198

73. Denton, J. F., DiSalvo, A. F., Isolation of Blastomyces Dermatitidis from Natural Sites at Augusta, Georgia, *Am J Trop Med Hyg*, **1964**, *13* , 716-722, 10.4269/ajtmh.1964.13.716

74. Pfaller MA, Diekema DJ. Unusual fungal and pseudofungal infections of humans. J Clin Microbiol. 2005;43(4):1495–1504. doi:10.1128/JCM.43.4.1495-1504.2005

75. Mendoza L, Hernandez F, Ajello L. Life cycle of the human and animal oomycete pathogen Pythium insidiosum [published correction appears in J Clin Microbiol 1994 Jan;32(1):276]. J Clin Microbiol. 1993;31(11):2967–2973.

76. Mahariya, S., Sharma, M., Fungal Succession on Keratinous Hair and Nail Baits of Human Origin, *Mycopathologia*, **2018**, *183*, 631-635, 10.1007/s11046-016-0055-y

77. Winterberg, H., Zur Methodik der Bakterienzählung, *Zeitschr. f. Hygiene*, **1898**, *29*, 75-93, 10.1007/BF02217377

78. Razumov, A. S., The direct method of calculation of bacteria in water: a comparison to the Koch method, Mikrobiologija, **1932**, *1*, 131-46

79. Staley, J. T., Konopka, A., Measurement of in situ activities of nonphotosynthetic microorganisms in aquatic and terrestrial habitats, *Ann. Rev. Microbiol*. **1985**, *39*, 321–346.

80. Srinivasan, A., Lopez-Ribot, J. L., Ramasubramanian, A. K., Microscale microbial culture, *Future microbiology*, 2015, *10*, 143–146, 10.2217/fmb.14.129

81. Wade, W., Unculturable bacteria--the uncharacterized organisms that cause oral infections, *Journal of the Royal Society of Medicine*, **2002**, *95*, 81–83, 10.1258/jrsm.95.2.81

82. Stewart E. J., Growing unculturable bacteria, *J Bacteriol*, **2012**, *194*, 4151–4160, 10.1128/JB.00345-12

83. Unterseher, M., Schnittler, M., Dilution-to-extinction cultivation of leaf-inhabiting endophytic fungi in beech (Fagus sylvatica L.)--different cultivation techniques influence fungal biodiversity assessment, Mycol Res, **2009**, *113*, 645-654 10.1016/j.mycres.2009.02.002

84. Bollmann, A., Lewis, K., Epstein, S. S., Incubation of environmental samples in a diffusion chamber increases the diversity of recovered isolates. *Appl Environ Microbiol*, 2007, *73*, 6386–6390, 10.1128/AEM.01309-07

85. Nichols, D.; Cahoon, N.; Trakhtenberg, E. M.; Pham, L.; Mehta, A.; Belanger, A.; Kanigan, T.; Lewis, K.; Epstein, S. S. J., Use of ichip for high-throughput in situ cultivation of "uncultivable" microbial species, *Appl Environ Microbiol*, **2010**, *76*, 2445–2450, 10.1128/AEM.01754-09

86. Ling, L. L., Schneider, T., Peoples, A. J., Spoering, A. L., Engels, I., Conlon, B. P., Mueller, A., Schäberle, T. F., Hughes, D. E., Epstein, S., Jones, M., Lazarides, L., Steadman, V. A., Cohen, D. R., Felix, C. R., Fetterman, K. A., Millett, W. P., Nitti, A. G., Zullo, A. M., Chen, C., Lewis, K., A new antibiotic kills pathogens without detectable resistance, *Nature*, **2015**, *517*, 455-459, 10.1038/nature14098

87. Liu, Y., Chan-Park, M. B., & Mu, Y. Binding Modes of Teixobactin to Lipid II: Molecular Dynamics Study, *Scientific reports*, **2017**, *7*, 17197. 10.1038/s41598-017-17606-5

88. Hannigan, G. D., Prihoda, D., Palicka, A., Soukup, J., Klempir, O., Rampula, L., Durcak, J., Wurst, M., Kotowski, J., Chang, D., Wang, R., Piizzi, G., Temesi, G., Hazuda, D. J., Woelk, C. H., Bitton, D. A., A deep learning genome-mining strategy for biosynthetic gene cluster prediction. *Nucleic Acids Res*, **2019**, *47*, e110. 10.1093/nar/gkz654

89. Keller, N. P., Fungal secondary metabolism: regulation, function and drug discovery. *Nat Rev Microbiol*, **2019**, *17*, 167–180 doi:10.1038/s41579-018-0121-1

90. Bloudoff, K., Schmeing, T.M., Structural and functional aspects of the nonribosomal peptide synthetase condensation domain superfamily: discovery, dissection and diversity, *Biochim Biophys Acta*, **2017**, *1865*, 1587-1604

91. Brakhage, A.A., Regulation of fungal secondary metabolism, *Nat Rev Microbiol*, **2013**, *11*, 21–32, 10.1038/nrmicro2916

92. Boruta, T., Uncovering the repertoire of fungal secondary metabolites: From Fleming's laboratory to the International Space Station, *Bioengineered*, **2018**, *9*, 12-16, DOI: 10.1080/21655979.2017.1341022

93. Langfelder, K., Streibel, M., Jahn, B., Haase, G., Brakhage, A. A., Biosynthesis of fungal melanins and their importance for human pathogenic fungi, Fungal Genet Biol, **2003**, *38*, 143-158

94. Walsh, E., Duan, W., Mehdi, M., Naphri, K., Khiste, S. Scalera, A., Zhang, N., *Cadophora meredithiae* and *C. interclivum*, new species from roots of sedge and spruce in a western Canada subalpine forest, *Mycologia.* **2018**, *110*, 201-214.

95. Dias, D. A.; Urban, S.; Roessner, U. *Metabolites* **2012,** *2,* 303–336. 10.3390/metabo2020303

96. Chooi, Y. H., Cacho, R., & Tang, Y., Identification of the viridicatumtoxin and griseofulvin gene clusters from Penicillium aethiopicum. *Chemistry & biology*, **2010**, *17*, 483–494. doi:10.1016/j.chembiol.2010.03.015

97. Endo A., A historical perspective on the discovery of statins. *Proceedings of the Japan Academy. Series B, Physical and biological sciences*, **2010**, *86*, 484–493. doi:10.2183/pjab.86.484

98. Zhang, Q., Catti, L., Syntrivanis, L. D., Tiefenbacher, K., En route to terpene natural products utilizing supramolecular cyclase mimetics, *Nat Prod Rep*, **2019**, *36*, 1619-1627, 10.1039/c9np00003h

99. Buckingham J., Cooper C. M., Purchase R., Natural Products Desk Reference; CRC Press, Taylor & Francis Group: Boca Raton, **2016**; p 235

100. Kawasaki, T., Hayashi, Y., Kuzuyama, T., Furihata, K., Itoh, N., Seto, H., Dairi, T., Journal of Bacteriology, 2006, 188, 1236-1244, 10.1128/JB.188.4.1236-1244.2006

101. Zhao, J., Li, Q., Sun, T., Zhu, X., Xu, H., Tang, J., Zhang, X., Ma, Y., Engineering central metabolic modules of Escherichia coli for improving β-carotene production, *Metab Eng*, **2013**, *17*, 42-50, 10.1016/j.ymben.2013.02.002

102. Vattekkatte, A., Garms, S., Brandt, W., Boland, W., *Org. Biomol Chem*, **2018**, *16*, 348-362, 10.1039/c7ob02040f

103. Gao, Y., Honzatko, R. B., & Peters, R. J., Terpenoid synthase structures: a so far incomplete view of complex catalysis. *Nat prod rep*, **2012**, *29*, 1153–1175, 10.1039/c2np20059g

104. Tian, B., Poulter, C. D., & Jacobson, M. P. Defining the Product Chemical Space of Monoterpenoid Synthases. *PLoS computational biology*, **2019**, *12*, e1005053, 10.1371/journal.pcbi.1005053

105. Quin, M. B., Flynn, C. M., & Schmidt-Dannert, C., Traversing the fungal terpenome. *Natural product reports*, **2014**, *31*, 1449–1473, 10.1039/c4np00075g

106. Niu, S., Xie, C.-L., Zhong, T., Xu, W., Luo, Z.-H., Shao, Z., Yang, X.-W., Sesquiterpenes from a deep-sea-derived fungus Graphostroma sp. MCCC 3A00421**,** *Tetrahedron*, **2017**, *73*, 7267-7273, 10.1016/j.tet.2017.11.013

107. Godtfredsen, W. O., Jahnsen, S., Lorck, H., Roholt, K., Tybring, L., Fusidic acid: a new antibiotic, *Nature*, **1962**, *193*, 987, 10.1038/193987a0

108. Zhao, M., Gödecke, T., Gunn, J., Duan, J. A., Che, C. T., Protostane and fusidane triterpenes: a mini-review, *Molecules*), **2013**, *18*, 4054–4080, 10.3390/molecules18044054

109. Wilkinson, J. D., Fusidic acid in dermatology, *Br J Dermatol*, **1998,** *139*, 37-40, 10.1046/j.1365-2133.1998.1390s3037.x

110. Schöfer, H., Simonsen, L., Fusidic acid in dermatology: an updated review, *Eur J Dermatol*, **2010**, *20*, 6-15, 10.1684/ejd.2010.0833

111. Borg, A., Pavlov, M., Ehrenberg, M., Mechanism of fusidic acid inhibition of RRF- and EF-G-dependent splitting of the bacterial post-termination ribosome. *Nucleic acids res*, **2016**, *44*, 3264–3275, 10.1093/nar/gkw178

112. Godtfredsen, W. O., Lorck, H., van Tamelen, E. E., Willett, J. D., Clayton, R. B., Biosynthesis of fusidic acid from squalene 2,3-oxide, *J Am Chem Soc*, **1968,** *90*, 208-209, 10.1021/ja01003a036

113. Christianson D. W., Structural and Chemical Biology of Terpenoid Cyclases. *Chemical reviews*, **2017**, *117*, 11570–11648, 10.1021/acs.chemrev.7b00287

114. Henninot, A., Collins, J. C:, Nuss, J. M., *Journal of Medicinal Chemistry*, **2018**, *61*, 1382-1414, 10.1021/acs.jmedchem.7b00318

115. Lobanovska, M., & Pilla, G., Penicillin's Discovery and Antibiotic Resistance: Lessons for the Future? *The Yale journal of biology and medicine*, **2017**, *90*, 135–145.

116. Walton, J. D., Hallen-Adams, H. E., & Luo, H., Ribosomal biosynthesis of the cyclic peptide toxins of Amanita mushrooms. *Biopolymers*, **2010**, *94*, 659–664. doi:10.1002/bip.21416

117. Soukup, A. A., Keller, N. P., & Wiemann, P., Enhancing Nonribosomal Peptide Biosynthesis in Filamentous Fungi. *Methods in molecular biology (Clifton, N.J.)*, **2016**, *1401*, 149–160. doi:10.1007/978-1-4939-3375-4_10

118. Sayari, M., van der Nest, M. A., Steenkamp, E. T., Soal, N. C., Wilken, P. M., & Wingfield, B. D., Distribution and Evolution of Nonribosomal Peptide Synthetase Gene Clusters in the *Ceratocystidaceae*. *Genes*, **2019**,*10*, 328. doi:10.3390/genes10050328

119. Hamamoto, K., Kida, Y., Zhang, Y., Shimizu, T., Kuwano, K., Antimicrobial activity and stability to proteolysis of small linear cationic peptides with D-amino acid substitutions. *Microbiol Immunol*. **2002**, 46, 741-749.

120. Hur, G. H., Vickery, C. R., Burkart, M. D., Explorations of catalytic domains in non-ribosomal peptide synthetase enzymology. *Natural product reports*, **2012**, *29*, 1074–1098. doi:10.1039/c2np20025b

121. Bockus A. T., McEwen C. M., Lokey R. S., "Form and Function in Cyclic Peptide Natural Products: A Pharmacokinetic Perspective", *Current Topics in Medicinal Chemistry*, **2013**, *13*, 821-836, https://doi.org/10.2174/1568026611313070005

122. Wang, X., Gong, X., Li, P., Lai, D., & Zhou, L. (2018). Structural Diversity and Biological Activities of Cyclic Depsipeptides from Fungi. Molecules, **2008**, *23*, 169. doi:10.3390/molecules23010169

123. Rhodes, C. A., Pei, D. Bicyclic Peptides as Next-Generation Therapeutics. Chemistry, **2017**, *23*, 12690–12703, 10.1002/chem.201702117

124. Keller N. P., Fungal secondary metabolism: regulation, function and drug discovery. Nature reviews. Microbiology, **2019**, *17*, 167–180, 10.1038/s41579-018-0121-1

125. Dunkel, M., Fullbeck, M., Neumann, S., & Preissner, R., SuperNatural: a searchable database of available natural compounds. *Nucleic acids research*, **2006**, *34*, D678–D683, 10.1093/nar/gkj132

126. Liu, K., Azamimi Abdullah, A., Huang, M., Nishioka, T., Altaf-Ul-Amin, M., Kanaya, S., Novel Approach to Classify Plants Based on Metabolite-Content Similarity, *BioMed Research International*, **2017**, Article ID 5296729, doi:10.1155/2017/5296729.

127. Gunatilaka, L. A. A, Natural Products from Plant-associated Microorganisms: Distribution, Structural Diversity, Bioactivity, and Implications of Their Occurrence *J Nat Prod*. **2006**, *69*: 509–526, 10.1021/np058128n

128. Gallagher K. A., Fennical, W., Jennsen, P. R., Hybrid isoprenoid secondary metabolite production in terrestrial and marine actinomycetes, *Current Opinion in Biotechnology*, **2010** *21*, 794-800

129. Matsuda, Y., Abe, I., Biosynthesis of fungal meroterpenoids, *Nat. Prod. Rep.*, **2016**, *33*, 26-53

130. Schultz, A. W., Oh, D. C., Carney, J. R., Williamson, R. T., Udwary D. W., Jensen, P. R., Gould J. R., Fenical, W. Moore, B. S., Biosynthesis and structures of cyclomarins and cyclomarazines, prenylated cyclic peptides of marine actinobacterial origin, *J Am Chem Soc* **2008**, 130, 4507-4516

131. Liu, J., Yang, Z. J., Meng, Z. H., The isolation, purification and identification of fumitremorgin B produced by *Aspergillus fumigatus*, *Biomed Environ Sci*. **1996**, *9*, 1-11

132. Navarra, M., Mannucci, C., Delbò, M., Calapai, G., *Citrus bergamia* essential oil: from basic research to clinical application. *Frontiers in pharmacology*, **2015**, *6*, 36, 10.3389/fphar.2015.00036

133. Chandra, A., Misra, L. N., Thakur, R. S., Tanavulgarol, an oxygenated sesquiterpene with an uncommon skeleton from *Tanacetum vulgare*, *Phytochemistry*, **1987**, *26*, 3077-3078, 10.1016/S0031-9422(00)84600-2

134. Guo, Z., Ren, F., Che, Y., Liu, G., Liu, L., New Bergamotane Sesquiterpenoids from the Plant Endophytic Fungus *Paraconiothyrium brasiliense*. *Molecules*, **2015**, 20, 14611–14620. 10.3390/molecules200814611

135. Deng, Q., Li, G., Sun, M., Yang, X., Xu, J., A new antimicrobial sesquiterpene isolated from endophytic fungus *Cytospora* sp. from the Chinese mangrove plant *Ceriops tagal*, *Natural Product Research*, **2018**, 10.1080/14786419.2018.1512993

136. Douglass, S.K., Juvik, J.A., Pyun, HJ., *J Chem Ecol*, Structure-activity relationships for analogs of (+)-(E)-endo-B-bergamoten-12-oic acid, an oviposition stimulant of *Helicoverpa zea* (Boddie), **1993**, *19*, 11-27, 10.1007/BF00987467

137. Zhang, L.-H., Feng, B.-M., Chen, G., Li, S.-G., Sun, Y., Wu, H.-H., Bai, J., Hua, H.-M., Wang, H.-F., Pei, Y.-H., Sporulaminals A and B: a pair of unusual epimeric spiroaminal derivatives from a marine-derived fungus *Paraconiothyrium sporulosum* YK-03, *RSC Adv*., **2016**, *6*, 42361-42366

138. Wu, Z.-Y.; Wu, Y.; Chen, G.-D.; Hu, D.; Li, X.-X.; Sun, X.; Guo, L.-D.; Li, Y.; Yao, X.-S.; Gao, H., Xylariterpenoids A–D, four new sesquiterpenoids from the Xylariaceae fungus, *RSC Adv*, **2014,** *4*, 54144–54148, 10.1039/c4ra10365c

139. Roussis, V., Vagias, C., Tsitsimpikou, C., Diamantopoulou, N., Chemical variability of the volatile metabolites from the Caribbean corals of the genus Gorgonia, *Z Naturforsch C J Biosci*, **2000**, *55*, 431-41, 10.1515/znc-2000-5-620

140. Coates, R.M., Denissen, J. F., Juvik, J. A., Babka, B.A., Identification of α-Santalenoic and endo-β-Bergamotenoic Acids as Moth Oviposition Stimulants from Wild Tomato Leaves *J. Org. Chem.* **1988**, 53, 2186-2192

141. Kimura, Y., Nakajima, H., Hamasaki, T., Sugawara, F., Parkanyi, L., Clardy, J., Pinthunamide, a new tricyclic sesquiterpene amide produced by a fungus, *Ampullifernia* sp., *Tetrahedron Lett.* **1989**, *30*, 1267-1270, 10.1016/S0040-4039(00)72732-8

142. Kimura, Y., Nakajima, H., Hamasaki, T., Matsumoto, T., Matsuda, Y., Tsuneda, A., Ampullicin and isoampullicin, new metabolites from an ampulliferina-like fungus sp. No. 27, *Agric. Biol. Chem.* **1990**, *54*, 813-814, 10.1080/00021369.1990.10869993

143. Pirrung M. C., Morehead, A. T. Jr., Young, B. G., Bicyclic and Tricyclic Sesquiterpenes, The Total Synthesis of Natural Products, Volume 11, ©John Wiley & Sons, Inc New York Chichester Weinheim Brisbane Singapore Toronto, **2000**

144. Perry N. B., Burgess, E. J., Foster, L. M., Gerard, P. J., Toyota, M., Asakawa, Y., Insect antifeedant sesquiterpene acetals from the liverwort *Lepidolaena clavigera*. 2. structures, artifacts, and activity, *J. Nat. Prod.* **2008**, *71*, 258-261, 10.1021/np070644l

145. Yin, J. L., & Wong, W. S., Production of santalenes and bergamotene in Nicotiana tabacum plants. *PloS one*, **2019**, *14*(1), e0203249, 10.1371/journal.pone.0203249

146. Köllner, T. G., Schnee, C., Gershenzon, J., Degenhardt, J., The variability of sesquiterpenes emitted from two *Zea mays* cultivars is controlled by allelic variation of two terpene synthase genes encoding stereoselective multiple product enzymes. *Plant cell*, **2004** 16, 1115–1131, 10.1105/tpc.019877

147. Cĵnsoli, F. L., Williams, H. J., Vinson, S. B., Matthews, R. W., Cooperband, M. F., Trans-bergamotenes-male pheromone of the ectoparasitoid *Melittobia digitata*, *J Chem Ecol*, **2002** *28*, 1675-1689, 10.1023/a:1019940932605

148. Snyder, J. C., Guo, Z., Thacker, R., Goodman, J. P., Pyrek, J.S., 2,3-Dihydrofarnesoic acid, a unique terpene from trichomes of *Lycopersicon hirsutum*, repels spider mites, *J Chem Ecol*, **1993**, 19, 2981–2997, 10.1007/BF00980597

149. Perry N. B., Burgess, E. J., Foster, L. M., Gerard, P. J., Insect antifeedant sesquiterpene acetals from the liverwort *Lepidolaena clavigera*, *Tetrahedron Lett*, **2003**, *44*, 1651-1653, 10.1016/S0040-4039(03)00040-6

150. Keskitalo, M., Pehu, E., Simon, J. E., Variation in volatile compounds from tansy (*Tanacetum vulgare* L.) related to genetic and morphological differences of genotypes, *Biochem Syst Ecol*, **2001**, *29*, 267-285, 10.1016/s0305-1978(00)00056-9

151. Pettersson, E. M., Volatile attractants for three Pteromalid parasitoids attacking concealed spruce bark beetles, *Chemoecology*, **2001**, *11*, 89-95, 10.1007/PL00001837

152. Abbott, S.P., Insects and other arthropods as agents of vector-dispersal in fungi. *unpublished* **2002** Online version: http://www.thermapure.com/pdf/AbbottInsectdispersal.pdf (accessed Jan 17, 2020)

153. Spaulding, P., The Relations of Insects to Fungi, *The Plant World*, **1903**, *6*, 182-184.

154. Boone, C. K., Six, D. L., Zheng, Y., Raffa, K. F., Parasitoids and dipteran predators exploit volatiles from microbial symbionts to locate bark beetles, *Environ Entomol*, **2008**, 37, 150-161 10.1603/0046-225x(2008)37[150:padpev]2.0.co;2

155. Machlis, L., Nutting, W. H., Williams, M. W., Rapoport H., Production, isolation, and characterization of sirenin, *Biochemistry*, **1966**, *5*, 2147-52, 10.1021/bi00871a001

156. Gooday, G. W., Carlile, M. J., The discovery of fungal sex hormones: III. Trisporic acid and its precursors. *Mycologist*, **1997**, *11*, 126–130, 10.1016/s0269-915x(97)80017-1

157. Gross, D., Parthier, B., Novel natural substances acting in plant growth regulation., *J Plant Growth Regul*, **1994**, *13*, 93-114, 10.1007/BF00210953

158. Wright, A. E., Schäfer, M., Midland, S., Munnecke, D. E., Sims, J. J., Lateral root inducing compounds from the bacterium *Erwinia quercina*: Isolation, structure and synthesis, Tetrahedron Lett, **1989**, 30, 5699-5702, 10.1016/S0040-4039(00)76174-0

159. Kato-Noguchi, H., Occurrence of a growth inhibitor, 3-hydroxy-β-ionone, in seven cultivars of Phaseolus vulgaris and its role in light-induced growth inhibition, *Phytochemistry*, **1994**, 36, 273-275, 10.1016/S0031-9422(00)97060-2

160. Massias, M., Rebuffat, S., Molho, L., Chiaroni, A., Riche, C., Bodo, B., Expansolides A and B: Tetracyclic Sesquiterpene Lactones from *Penicillium expansum*, *J Am Chem Soc*, **1990**, *112*, 8112-8115, 10.1021/ja00178a039

161. Macías, F. A., Varela R. M., Simonet, A. M., Cutler, H. G., Cutler, S. J., Hill, R., Absolute configuration of bioactive expansolides A and B from *Aspergillus fumigatus* Freseniu, *Tetrahedron Lett*, **2003**, *44*, 941-943, 10.1016/S0040-4039(02)02778-8

162. Singh, L. P., Gill, S. S., Tuteja, N., Unraveling the role of fungal symbionts in plant abiotic stress tolerance. *Plant Signaling Behav*, **2011**, *6*, 175–191, 10.4161/psb.6.2.14146

163. Liu, L., Gao, H., Chen, X., Cai, X., Yang, L., Guo, L., Yao, X., Che, Y., Brasilamides A–D: Sesquiterpenoids from the Plant Endophytic Fungus *Paraconiothyrium brasiliense*, *EurJOC*, **2010**, *17*, 3302-3306, 10.1002/ejoc.201000284

164. Oh, H., Gloer, J. B., Shearer, C. A., Massarinolins A-C: new bioactive sesquiterpenoids from the aquatic fungus massarina tunicata, *J Nat Prod*, **1999**, *62*, 497-501, 10.1021/np980447+

165. Che, Y., Gloer, J. B., Koster, B., Malloch, D., Decipinin A and decipienolides A and B: new bioactive metabolites from the coprophilous fungus *Podospora decipiens*, *J Nat Prod*, **2002**, *65*, 916-919, 10.1021/np010575p

166. Zhao, Z. Z., Zhao, K., Chen, H. P., Bai, X., Zhang, L., Liu, J. K., Terpenoids from the mushroom-associated fungus Montagnula donacina, *Phytochemistry*, **2018**, *147*, 21-29, 10.1016/j.phytochem.2017.12.015

167. Lazary, S., Stähelin, H., Immunosuppressive Effect of a New Antibiotic: Ovalicin, *Antibiot Chemother*, **1969**, *15*, 177-181, 10.1159/000386780

168. Bailey, L. Effect of Fumagillin upon *Nosema apis* (Zander). Nature, **1953**, *171*, 212–213, 10.1038/171212a0

169. Didier, P. J., Phillips, J. N., Kuebler, D. J., Nasr, M., Brindley, P. J., Stovall, M. E., Bowers, L. C., Didier, E. S., Antimicrosporidial activities of fumagillin, TNP-470, ovalicin, and ovalicin derivatives in vitro and in vivo. Antimicrobial agents and chemotherapy, **2006**, *50*, 2146–2155, 10.1128/AAC.00020-06

170. Griffith, E. C., Su, Z., Niwayama, S., Ramsay, C. A., Chang, Y.-H., Liu, J. O., Molecular recognition of angiogenesis inhibitors fumagillin and ovalicin by methionine aminopeptidase 2, *PNAS*, **1998**, *95*, 15183-15188, 10.1073/pnas.95.26.15183

171. Willis, K.J. Definition and Diversity. In State of the World's Fungi 2018, **2018**, p 9.

172. Lok, C. Nature, **2015**, *522*, 270–273.

173. Ahrendt, S. R.; Quandt, C. A.; Ciobanu, D.; Clum, A.; Salamov, A.; Andreopoulos, B.; Cheng, J.-F.; Woyke, T.; Pelin, A.; Henrissat, B.; Reynolds, N. K.; Benny, G. L.; Smith, M. E.; James, T. Y.; Grigoriev, I. V. Nat Microbiol, **2018**, *3*, 1417–1428.

174. Grossart, H.-P. Wurzbacher, C.; James. T. Y.; Kagami, M. *Fungal Ecol*, **2016**, *19*, 28-38.

175. Hawksworth, D. L., Rossman, A. Y., *Phytopathology*, **1997**, *87*, 888–891.

176. Schulz, B., Sucker, J., Aust, J. H., A.-K., Krohn, Ludewig, K., Jones, P.G., Döring, D., *Mycol Res*, **1995,** *99*, 1007–1015, 10.1017/s0953756202006342

177. Meliani, A., Bensoltane, A., Mederbel, K., *Am J Plant Nutr Fert Technol,* **2012,** *2,* 10–18., 10.3923/ajpnft.2012.10.18

178. Bressan,M.; Trinsoutrot Gattin, I.; Desaire, S.; Castel, L.; Gangneux, C.; Laval, K. *Appl. Soil Ecol.,* **2015 ,** *88,* 60–68, 10.1016/j.apsoil.2014.12.007

179. Camacho-Fernández, C.; Hervás, D.; Rivas-Sendra, A.; Marín, M. P.; Seguí-Simarro, J. M. *Plant Methods*, **2018,** *14,* No. 30, 10.1186/s13007-018-0297-4

180. Jedicke, E. *Böden - Entstehung, Ökologie, Schutz;* O. Maier: Ravensburg, Germany, **1989**

181. Gaertner, A. *Plant Biol.* **1969,** *82,* 287–306.

182. Gaertner, A. Veroeff. Inst. Meeresforsch. Bremerhaven **1968,** 3, 75–92.

183. Crow, S. A.; Ahearn, D. G.; Cook, W. L., Bourquin, A. W. *Limno Oceanogr* **1975,** *20,* 644–646. 10.4319/lo.1975.20.4.0644

184. Thuan, N. H., An, T. T., Shrestha, A., Canh, N. X., Sohng, J. K., Dhakal, D., Recent Advances in Exploration and Biotechnological Production of Bioactive Compounds in Three Cyanobacterial Genera: *Nostoc*, *Lyngbya*, and *Microcystis*, *Frontiers in chemistry*, **2019**, *7*, 604, 10.3389/fchem.2019.00604

185. Guigo, R., & de Hoon, M., Recent advances in functional genome analysis. *F1000Research*, **2018**, *7*, F1000 Faculty Rev-1968, 10.12688/f1000research.15274.1

186. Blin, K., Kim, H. U., Medema, M. H., & Weber, T., Recent development of antiSMASH and other computational approaches to mine secondary metabolite biosynthetic gene clusters, *Briefings in bioinformatics*, **2019**, *20*, 1103–1113, 10.1093/bib/bbx146

187. Gacek, A., Strauss, J., The chromatin code of fungal secondary metabolite gene clusters, *Appl Microbiol Biotechnol*, **2012**, *95*, 1389-404, 10.1007/s00253-012-4208-8

188. Brakhage, A. A., Schroeckh V., Fungal secondary metabolites - strategies to activate silent gene clusters, *Fungal Genet Biol*, **2011**, *48*, 15-22, 10.1016/j.fgb.2010.04.004

189. Baral, B., Akhgari, A., Metsä-Ketelä, M., Activation of microbial secondary metabolic pathways: Avenues and challenges. *Synth Sys Biotechnol*, **2018**, *3*, 163–178, 10.1016/j.synbio.2018.09.001

190. Romano, S., Jackson, S. A., Patry, S., Dobson, A., Extending the "One Strain Many Compounds" (OSMAC) Principle to Marine Microorganisms. *Marine drugs*, **2018**, *16*, 244, 10.3390/md16070244

191. Leuchtmann, A., Clémençon, H., The taxonomic position of the genus *Heydenia* (Pyronemataceae, Pezizales) based on molecular and morphological data, *Mycol Progress*, **2012**, *11*, 699–710, 10.1007/s11557-011-0779-5

192. Dix, N. J., Webster, J., Fungi of Extreme Environments. In: Fungal Ecology. Springer, Dordrecht, 1995, 322-340

193. Seyedmousavi, S., Bosco, S. M. G., de Hoog, S., Ebel, F., Elad, D., Gomes, R. R., Jacobsen, I. D., Jensen, H. E., Martel, A., Mignon, B., Pasmans, F., Piecková, E., Rodrigues, A. M., Singh, K., Vicente, V. A., Wibbelt, G., Wiederhold, N. P., Guillot, J., Fungal infections in animals: a patchwork of different situations, *Med Mycol*, **2018**, *56*, e4, 10.1093/mmy/myy028

194. Wang, M., Carver, J. J., Phelan, V. V., Sanchez, L. M., Garg, N., Peng, Y., Nguyen, D. D., Watrous, J., Kapono, C. A., Luzzatto-Knaan, T., Porto, C., Bouslimani, A., Melnik, A. V., Meehan, M. J., Liu, W. T., Crüsemann, M., Boudreau, P. D., Esquenazi, E., Sandoval-Calderón, M., Kersten, R. D., Pace, L. A., Quinn, R. A., Duncan, K. R., Hsu, C. C., Floros, D. J., Gavilan, R. G., Kleigrewe, K., Northen, T., Dutton, R. J., Parrot, D., Carlson, E. E., Aigle, B., Michelsen, C. F., Jelsbak, L., Sohlenkamp, C., Pevzner, P., Edlund, A., McLean, J., Piel, J., Murphy, B. T., Gerwick, L., Liaw, C. C., Yang, Y. L., Humpf, H. U., Maansson, M., Keyzers, R. A., Sims, A. C., Johnson, A. R., Sidebottom, A. M., Sedio, B. E., Klitgaard, A., Larson, C. B., P., C. A. B., Torres-Mendoza, D., Gonzalez, D. J., Silva, D. B., Marques, L. M., Demarque, D. P., Pociute, E., O'Neill, E. C., Briand, E., Helfrich, E. J. N., Granatosky, E. A., Glukhov, E., Ryffel, F., Houson, H., Mohimani, H., Kharbush, J. J., Zeng, Y., Vorholt, J. A., Kurita, K. L., Charusanti, P., McPhail, K. L., Nielsen, K. F., Vuong, L., Elfeki, M., Traxler, M. F., Engene, N., Koyama, N., Vining, O. B., Baric, R., Silva, R. R., Mascuch, S. J., Tomasi, S., Jenkins, S., Macherla, V., Hoffman, T., Agarwal, V., Williams, P. G., Dai, J.,

Neupane, R., Gurr, J., Rodríguez, A. M. C., Lamsa, A., Zhang, C., Dorrestein, K., Duggan, B. M., Almaliti, J., Allard, P. M., Phapale, P., Nothias, L. F., Alexandrov, T., Litaudon, M., Wolfender, J. L., Kyle, J. E., Metz, T. O., Peryea, T., Nguyen, D. T., VanLeer, D., Shinn, P., Jadhav, A., Müller, R., Waters, K. M., Shi, W., Liu, X., Zhang, L., Knight, R., Jensen, P. R., Palsson, B. O., Pogliano, K., Linington, R. G., Gutiérrez, M., Lopes, N. P., Gerwick, W. H., Moore, B. S., Dorrestein, P. C., Bandeira, N., Sharing and community curation of mass spectrometry data with Global Natural Products Social Molecular Networking. *Nat Biotechnol*, **2016**, *34***,** 828–837, 10.1038/nbt.3597

195. Yang, J. Y., Sanchez, L. M., Rath, C. M., Liu, X., Boudreau, P. D., Bruns, N., Glukhov, E., Wodtke, A., de Felicio, R., Fenner, A., Wong, W. R., Linington, R. G., Zhang, L., Debonsi, H. M., Gerwick, W. H., Dorrestein, P. C., Molecular networking as a dereplication strategy. *J Nat Prod*, **2013**, *76*, 1686-1699, 10.1021/np400413s

196. Wüllems, K., Kölling, J., Bednarz, H. Niehaus, K., Hans, V. K., Nattkemper, T. W., *BMC Bioinformatics*, **2019**, *20*, 303, doi.org/10.1186/s12859-019-2890-6

197. Ernst, M., Kang, K. B., Carabello-Rodriguez, A. M., Nothias, L.-F., Wandy, J., Wang, M., Rogers, S., Medema, M. H., Dorrestein, P. C., van der Hooft, J. J. J., MolNetEnhancer: enhanced molecular networks by integrating metabolome mining and annotation tools, *bioRxiv*, **2019**, 654459, 10.1101/654459

198. van der Hooft, J. J., Wandy, J., Barrett, M. P., Burgess, K. E., Rogers, S., Topic modeling for untargeted substructure exploration in metabolomics, *Proc Natl Acad Sci U S A*, **2016**, *113*, 13738–13743, 10.1073/pnas.1608041113

199. Mohimani, H., Gurevich, A., Mikheenko, A., Garg, N., Nothias, L. F., Ninomiya, A., Takada, K., Dorrestein, P. C., Pevzner, P. A., Dereplication of peptidic natural products through database search of mass spectra. *Nat chem biol*, **2017**, *13*, 30–37, 10.1038/nchembio.2219

200. Nguyen, D. D., Wu, C. H., Moree, W. J., Lamsa, A., Medema, M. H., Zhao, X., Gavilan, R. G., Aparicio, M., Atencio, L., Jackson, C., Ballesteros, J., Sanchez, J., Watrous, J. D., Phelan, V. V., van de Weil, C., Kersten, R. D., Mehnaz, S., De Mot, R., Shank, E. A., Charusanti, P., Nagarajan, H., Duggan, B. M., Moore, B. S., Bandeira, N., Palsson, B. Ø.,

Pogliano, K., Gutiérrez, M., Dorrestein, P. C., MS/MS networking guided analysis of molecule and gene cluster families. *Proc Natl Acad Sci U S A*, **2013**, *110*, E2611-20, 10.1073/pnas.1303471110

201. Djamshidian, A., Bernschneider-Reif, S., Poewe, W., & Lees, A. J., *Banisteriopsis caapi*, a Forgotten Potential Therapy for Parkinson's Disease?, *Mov Disord Clin Pract*, **2015**, *3*(1), 19–26, 10.1002/mdc3.12242

202. Patel, K., Gadewar, M., Tripathi, R., Prasad, S. K., & Patel, D. K., A review on medicinal importance, pharmacological activity and bioanalytical aspects of beta-carboline alkaloid "Harmine", *Asian Pac J Trop Biomed*, **2012**, *2*, 660–664, 10.1016/S2221-1691(12)60116-6

203. Wrońska, A. K., Boguś, M. I., Kaczmarek, A., & Kazek, M., Harman and norharman, metabolites of entomopathogenic fungus Conidiobolus coronatus (Entomopthorales), disorganize development of Galleria mellonella (Lepidoptera) and affect serotonin-regulating enzymes, *PloS one*, **2018**,*13*(10), e0204828, 10.1371/journal.pone.0204828

204. Moloudizargari, M., Mikaili, P., Aghajanshakeri, S., Asghari, M. H., & Shayegh, J., Pharmacological and therapeutic effects of Peganum harmala and its main alkaloids. *Pharmacogn rev*, **2013**, *7*, 199–212. 10.4103/0973-7847.120524

205. Shaaban, M. , Schröder, D. , Shaaban, K. A. , Helmke, E. , Grün-Wollny, I. , Wagner-Döbler, I. and Laatsch, H., Flazin, Perlolyrin, and other ß-Carbolines from marine derived Bacteria, *Rev Latinoam Quím*, **2007**, 35, 58-67

206. Nakatsuka S, Feng B, Goto T, Kihara K., Structures of flazin and YS, highly fluorescent compounds isolated from Japanese soy sauce, *Tetrahedron Lett*, **1986**, *27*, 3399–3402

207. Shiomi, K., Hatae, K., Hatano, H., A New Antibiotic, Antimycin A_9, Produced by *Streptomyces* sp. K01-0031. *J Antibiot* **58,** 74–78 (2005) doi:10.1038/ja.2005.10

208. Hanh, T. T., Hang, D. T., Van Minh, C., Dat, N. T., Anti-inflammatory effects of fatty acids isolated from Chromolaena odorata, *Asian Pac J Trop Med*, **2011**, *4*, 760-763, 10.1016/S1995-7645(11)60189-2.

209. Tanvir, R., Javeed, A., Rehman, Y., Fatty acids and their amide derivatives from endophytes: new therapeutic possibilities from a hidden source, *FEMS Microbiology Letters*, **2018**, *365*, fny114, 10.1093/femsle/fny114

210. Tohge, T., Fernie, A. R. An Overview of Compounds Derived from the Shikimate and Phenylpropanoid Pathways and Their Medicinal Importance, *Mini Rev Med Chem*, **2017**, *17*, 1013-1027, 10.2174/1389557516666160624123425

211. Falcone Ferreyra, M. L., Rius, S. P., Casati, P., Flavonoids: biosynthesis, biological functions, and biotechnological applications. *Frontiers in plant science*, **2012**, *3*, 222, 10.3389/fpls.2012.00222

212. Garrido-Arandia, M., Silva-Navas, J., Ramírez-Castillejo, C., Cubells-Baeza, N., Gómez-Casado, C., Barber, D., Pozo, J. C., Melendi, P. G., Pacios, L. F1., Díaz-Perales, A., Characterisation of a flavonoid ligand of the fungal protein Alt a 1, *Scientific reports*, **2016**, *6*, 33468, 10.1038/srep33468

213. Austin, M. B., Noel, J. P., The chalcone synthase superfamily of type III polyketide synthases, *Nat Prod Rep*, **2003**, *20*, 79-110, 10.1039/b100917f

214. Jung, W., Yu, O., Lau, S., O'Keefe, D. P., Odell, J., Fader, G., McGonigle, B., Identification and expression of isoflavone synthase, the key enzyme for biosynthesis of isoflavones in legumes. *Nat Biotechnol*, 2000, **18,** 208–212, doi:10.1038/72671

215. Juvvadi, P. R., Seshime, Y., Kitamoto, K., Genomics reveals traces of fungal phenylpropanoid-flavonoid metabolic pathway in the f ilamentous fungus Aspergillus oryzae, *J Microbiol*, **2005**, *43*, 475-486, 10.1039/c4np00096j

216. Umezawa, H., Tobe, H., Shibamoto, N., Nakamura, F., Nakamura, K., Isolation of isoflavones inhibiting DOPA decarboxylase from fungi and streptomyces, *J Antibiot*, **1975**, *28*, 947-52, 10.7164/antibiotics.28.947

217. Burns, M.K., Coffin, J. M., Kurobane, I., Vining, L. C., McInnes, A. G., Smith, D. G., Walter, J. A., Biosynthesis of chlorflavonin in Aspergillus candidus. 13C- and 14C-labelling evidence for a new route to the flavonoid structure, *J Chem Soc*, **1981**, *1*, 1411-1416, 10.1039/P19810001411

218. Hashimoto, M., Nonaka, T., Fujii, I., Fungal type III polyketide synthases, *Nat Prod Rep*, **2014**, *31*, 1306-1317, 10.1039/c4np00096j

219. Nakata, R., Yoshinaga, N., Teraishi, M., Okumoto, Y., Huffaker, A., Schmelz, E. A., Mori, N., A fragmentation study of isoflavones by IT-TOF-MS using biosynthesized isotopes, *Biosci Biotechnol Biochem*, **2018**, *82*, 1309-1315, 10.1080/09168451.2018.1465810

220. Mabry T. J., Markham K. R., Mass Spectrometry of Flavonoids. In: Harborne J. B., Mabry T. J., Mabry H. (eds) The Flavonoids. Springer, Boston, MA, **1975**, p 78-121, 10.1007/978-1-4899-2909-9_3

221. Ma, Y. L., Li, Q. M., van den Heuvel, H., Claeys, M., Characterization of flavone and flavonol aglycones by collision-induced dissociation tandem mass spectrometry, *Rapid Commun Mass Spectrom*, **1997**, *11*, 1357-1364, 10.1002/(SICI)1097-0231(199708)11:12<1357::AID-RCM983>3.0.CO;2-9

222. Shankar, T., Muthusubramanian, S., Gandhidasan, R., Newer Constituents of *Derris Indica* Stem, *Nat Prod Commun*, 2008, *3*, doi.org/10.1177/1934578X0800300818

223. Weltring, K.-M., Mackenbrock, K., Barz, W., Demethylation, Methylation and 3'-Hydroxylation of Isoflavones by *Fusarium* Fungi, *Z Naturforsch*, **1982**, *37c*, 570-574

224. Murphy, P. A., Hendrich, S., Phytoestrogens in foods, *Adv Nutr*, **2002**, *44*, 195–246, 10.1016/s1043-4526(02)44005-3

225. Mazur, W., 11 Phytoestrogen content in foods. *Baillieres Best Pract Res Clin Endocrinol Metab*, **1998**, *12*, 729–742. *1*0.1016/s0950-351x(98)80013-x

226. Bistline {jr.}, R. G., Maurer, E. W., Smith, F. D., Linfield, W. M., Fatty acid amides and anilides, syntheses and antimicrobial properties. *J Am Oil Chem Soc*, **1980**, *53*, 98–103, 10.1007/BF02674376

227. Kitahara, T., Koyama, N., Matsuda, J., Aoyama, Y., Hirakata, Y., Kamihira, S., Kohno, S., Nakashima, M., Sasaki, H., Antimicrobial activity of saturated fatty acids and fatty amines against methicillin-resistant Staphylococcus aureus, *Biol Pharm Bull*, **2004**, *27*,1321-1326, 10.1248/bpb.27.1321

228. Pretsch, E.; Bühlmann, P.; Badertscher, M. *Spektroskopische Daten zur Strukturaufklärung organischer Verbindungen*, 5th ed.; Springer: Berlin, Germany, **2010**; p 289. doi:10.1007/978-3-540-76866-1

229. Jacobsen, N. E. Chirality and Stereochemistry: Natural Products. *NMR Data Interpretation Explained: Understanding 1D and 2D NMR Spectra of Organic Compounds and Natural Products;* John Wiley and Sons, Inc.: Hoboken, NJ, U.S.A., **2017**; pp 294–297.

230. Wu, Z.-Y.; Wu, Y.; Chen, G.-D.; Hu, D.; Li, X.-X.; Sun, X.; Guo, L.-D.; Li, Y.; Yao, X.-S.; Gao, H. *RSC Adv.* **2014,** *4*, 54144–54148. doi:10.1039/c4ra10365c

231. Tanaka, Y.; Sato, H.; Kageyu, A.; Tomita, T., Separation of geranylgeraniol isomers by high-performance liquid chromatography and identification by 13C nuclear magnetic resonance spectroscopy, *J. Chromatogr.* **1985,** *347*, 275–283, 10.1016/s0021-9673(01)95493-7

232. Hufendiek, P. (2016). Enzyme-inhibitory secondary metabolites and their exudation in the marine-derived fungus *Epicoccum Nigrum* Link (Doctoral dissertation, University of Bonn, Bonn, Germany). Retrieved from Universitäts- und Landesbibliothek Bonn. (urn: 5n-46742)

233. Li, X., Dobretsov, S., Xu, Y., Xiao, X., Shing Hung, O., Qian, P., Antifouling diketopiperazines produced by a deep-sea bacterium, *Streptomyces fungicidicus*, *Biofouling*, **2006**, *22*, 187-194, 10.1080/08927010600780771

234. He, J., Fan, P., Feng, S., Shao, P., Sun, P., Isolation and Purification of Two Isoflavones from Hericium erinaceum Mycelium by High-Speed Counter-Current Chromatography. *Molecules*, **2018**, *23*, 560, 10.3390/molecules23030560

235. Scott, C. W., Peters, M. F., Label-free whole-cell assays: expanding the scope of GPCR screening, *Drug Discov Today*, **2010**, *15*, 704-16, 10.1016/j.drudis.2010.06.008.

236. Schröder, R., Janssen, N., Schmidt, J., Kebig, A., Merten, N., Hennen, S., Müller, A., Blättermann, S., Mohr-Andrä, M., Zahn, S., Wenzel, J., Smith, N. J., Gomeza, J., Drewke, C., Milligan, G., Mohr, K., Kostenis, E., Deconvolution of complex G protein-coupled receptor

signaling in live cells using dynamic mass redistribution measurements, *Nat Biotechnol*, **2010**, *28*, 943-949, 10.1038/nbt.1671

237. Zhang, C., Idelbayev, Y., Roberts, N. *et al.* Small Molecule Accurate Recognition Technology (SMART) to Enhance Natural Products Research. *Sci Rep*, **2017**, *7*, 14243, 10.1038/s41598-017-13923-x

238. Demain, A., Sanchez, S., Microbial drug discovery: 80 years of progress. *J Antibiot*, **2009**, *62*, 5–16, 10.1038/ja.2008.16

239. Imai, Y., Meyer, K.J., Iinishi, A. et al. A new antibiotic selectively kills Gram-negative pathogens. *Nature*, **2019**, *576*, 459–464, 10.1038/s41586-019-1791-1

240. Lin, H. C., Chooi, Y. H., Dhingra, S., Xu, W., Calvo, A. M., Tang, Y., The fumagillin biosynthetic gene cluster in Aspergillus fumigatus encodes a cryptic terpene cyclase involved in the formation of β-trans-bergamotene, *J Am Chem Soc*, *135*, 4616–4619. 10.1021/ja312503y

241. Landmann, C., Fink, B., Festner, M., Dregus, M., Engel, K. H., Schwab, W., Cloning and functional characterization of three terpene synthases from lavender (Lavandula angustifolia), *Arch Biochem Biophys*, **2007**, *465*, 417-29, 10.1016/j.abb.2007.06.011

242. Schewe, H., Holtmann, D., Schrader, J., $P450_{BM-3}$-catalyzed whole-cell biotransformation of α-pinene with recombinant *Escherichia coli* in an aqueous–organic two-phase system. *Appl Microbiol* Biotechnol, **2009**, *83***,** 849–857, 10.1007/s00253-009-1917-8

243. Verbist, L., The antimicrobial activity of fusidic acid, *J Antimicrob Chemother*, **1990**, *25*, 1-5, 10.1093/jac/25.suppl_b.1

244. Chain, E., Florey, H. W., Jennings, M. A., Williams, T. I., Helvolic Acid, an Antibiotic Produced by *Aspergillus fumigatus*, mut. helvola Yuill. *Br J Exp Pathol*, **1943**, *24*, 108–119.

245. O'Neill, A. J., Bostock, J. M., Moita, A. M., Chopra, I., Antimicrobial activity and mechanisms of resistance to cephalosporin P1, an antibiotic related to fusidic acid, *J Antimicrob Chemother*, **2002**, *50*, 839-848, 10.1093/jac/dkf248

8 Appendix

8.1 ITS sequences of isolated strains

8.1.1 Alternaia armoraciae No. 830

>Z1828-4418AI

TCCGTAGGTGAACCTGCGGAGGGATCATTACACAATATGAAGGCGGGCTGGATC
CCTCCTGCTGGGCACTGCTTCACGGCGTGCGCAGTAGGGGCCGGCCCTGCTGAAC
TATTCACCCGTGTCTTTTGCGTACCTCTTGTTTCCTGGGCGGGCTCGCCCGCCACC
AGGACCAACCATAAACCTTTTTGTAATAGCAATCCGCGTCAGTAACAACGTAATT
AATTACAACTTTCAACAACGGATCTCTTGGTTCTGGCATCGATGAAGAACGCAGC
GAAATGCGATACGTAGTGTGAATTGCAGAATTCAGTGAATCATCGAATCTTTGAA
CGCACATTGCGCCCTTTGGTATTCCAAAGGGCATGCCTGTTCGAGCGTCATTTGTA
CCCTCAAGCTTTGCTTGGTGTTGGGCGTCTTTGTCTCCAGCTTGCTGGAGACTCGC
CTTAAAGTCATTGGCAGCCGGCCTACTGGTTTCGGAGCGCAGCACAAGTCGCGCT
CTTCATCCAGCCAAGGTCAGCGTCCAGCAAGCCTTTTTTCAACCTTTGACCTCGGA
TCAGGTAGGGATACCCGCTGAACTTAAGC

>Z1828-4418AEFCL

AGAAGGTACGACATCACTCTTTCTTCCCACATGGGCTGTCGCAACCACCCGGTGC
ATCTCTGAGCGCGCCGCCATTTCTGGCTTATCGCGATGAGGGGCATTTTTGGGTG
GTGGGGTTGTGCGAACTTTTACGCGCTAGCGCTAGTCTGCATGCGGCCTTCGCGA
GCCCCAACACCATGACGCACATCCAATTTCCCCAATTCGGCCACAGCTAACAAGC
CTCACAGGAAGCCGCCGAACTCGGTAAGG

>Z1828-4418BI

TCCGTAGGTGAACCTGCGGAGGGATCATTACACAATATGAAGGCGGGCTGGATC
CCTCCTGCTGGGCACTGCTTCACGGCGTGCGCAGTAGGGGCCGGCCCTGCTGAAC
TATTCACCCGTGTCTTTTGCGTACCTCTTGTTTCCTGGGCGGGCTCGCCCGCCACC
AGGACCAACCATAAACCTTTTTGTAATAGCAATCCGCGTCAGTAACAACGTAATT
AATTACAACTTTCAACAACGGATCTCTTGGTTCTGGCATCGATGAAGAACGCAGC

GAAATGCGATACGTAGTGTGAATTGCAGAATTCAGTGAATCATCGAATCTTTGAA
CGCACATTGCGCCCTTTGGTATTCCAAAGGGCATGCCTGTTCGAGCGTCATTTGTA
CCCTCAAGCTTTGCTTGGTGTTGGGCGTCTTTGTCTCCAGCTTGCTGGAGACTCGC
CTTAAAGTCATTGGCAGCCGGCCTACTGGTTTCGGAGCGCAGCACAAGTCGCGCT
CTTCATCCAGCCAAGGTCAGCGTCCAGCAAGCCTTTTTTCAACCTTTGACCTCGGA
TCAGGTAGGGATACCCGCTGAACTTAAGC

8.1.2 Auxarthron cfr. umbrinum No. 825

>Z1828-4420I

TCCGTAGGTGAACCTGCGGAAGGATCATTAAAGCGTCGAGCCTGCGCCTCCCGGC
GTAGGTGAAACCCCACCCGTGACTACTACACCACATGTTGCTTTGGCGGGCCCGC
CTCTGGCTGCCGGGGTTTCTCTGGATAGCGCCCGCCAAAGATACACTGAACTTCT
GTGAAACTGGATGTCTGAGTTGATATCAATCATTAAAACTTTCAACAATGGATCT
CTTGGTTCCGGCATCGATGAAGAACGCAGCGAAATGCGATAAGTAATGTGAATTG
CAGAATTCCGTGAATCATCGAATCTTTGAACGCACATTGCGCCCTCTGGTATTCCG
GAGGGCATGCCTGTCCGAGCGTCATTGCAACCTTCAAGCGCGGCTTGTGTGTTGG
GCCTCGTCCCCCGTGGACGGGCCTCAAAGGCAGTGGCGGCGTCCGTTTTGGTGCC
CGAGCGTATGGGAATTCTATACCGCTTCAAGGCCCGGCGGCGCTGGTCAAGACCA
ATTTTTATCGGTTGACCTCGGATCAGGTAGGGATACCCGCTGAACTTAAGCATA

8.1.3 *Cadophora* sp. No. 829

>Z1876-4467I

TCCGTAGGTGAACCTGCGGAAGGATCATTAATAGAGTAAGGGCGAAGCTGTAAA
AGGCCGAGCTCTGACCTCCACCCTTGAATAAACTACCTTCGTTGCTTTGGCGGGTC
GCCTCGTGCCAGCGGCTTCGGCTGTTGAGTACCCGCCAGAGGACCACAACTCTTG
TTTTTAGTGATGTCTGAGTACTATATAATAGTTAAAACTTTCAACAACGGATCTCT
TGGTTCTGGCATCGATGAAGAACGCAGCGAAATGCGATAAGTAATGTGAATTGC
AGAATTCAGTGAATCATCGAATCTTTGAACGCACATTGCGCCCTCTGGTATTCCG
GGGGGCATGCCTGTTCGAGCGTCATTATAACCACTCAAGCTCTCGCTTGGTATTG
GGGTTCGCGTCTTCGCGGCCTCTAAAATCAGTGGCGGTGCCTGTCGGCTCTACGC

GTAGTAATACTCCTCGCGATTGAGTTCCGGTAGGTTTACTTGCCAACAACCCCCA
ATCTTTTAAGGTTGACCTCGGATCAGGTAGGGATACCCGCTGAACTTAAGCATAT
CAT

>Z1876-4467VS

GTAACGGCGAGTGAAGCGGTAACAGCTCAAATTTGAAAGCTAGCTCTTTTAGGGT
TCGCATTGTAATTTGTAGAAGATGCTTCGGGTGTGGCCCCGGTCTAAGTTCCTTGG
AACAGGACGTCATAGAGGGTGAGAATCCCGTATGTGACTGGGTGCTTTCGCTCAT
GTGAAGCTCTTTCGACGAGTCGAGTTGTTTGGGAATGCAGCTCAAAATGGGTGGT
AAATTTCATCTAAAGCTAAATATTGGCCAGAGACCGATAGCGCACAAGTAGAGT
GATCGAAAGATGAAAAGCACTTTGGAAAGAGAGTTAAACAGTACGTGAAATTGT
TGAAAGGGAAGCGCTTGCAACCAGACTTGCGCGTAGTTGATCATCCGAGCTTCTG
TTTGGTGCACTCTGCTACGCTCAGGCCAGCATCGGTTTCGGTGGTGGGATAAAGG
CCTTGGGAATGTAGCTCCTCTCGGGGAGTGTTATAGCCCTCGGTGCAATGCCGCC
TATCGGGACCGAGGACCGCGCTTCGGCTAGGATGCTGGCGTAATGGTTGTAAGCG
ACCCGTCTTGAAACACGGACCAAGGAGTCTAACATCTATGCGAGTGTTTGGGTGT
CAAACCCATACGCGTAATGAAAGTGAACGGAGGTGAGAACCCTTAAGGGTGCAT
CATCGACCGATCCTGATGTCTTCGGATGGATTTGAGTAAGAGCATAGCTGTTGGG
ACCCGAAAGATGGTGAACTATGCGTGAATAGGGTGAAGCCAGAGGAAACTCTGG
TGGAGGCTCGCAGCGGTTCTGACGTGCAAATCGATCGTCAAATTTGCGTATAGGG
GCGAAAGACTAATCGAACCATCTAGTAGCTGGTTCCTGCCGAAGTTTCCCTCAGG
ATAGCAGTGTTGAATTCAGTTTTATGAGGTAAAGCGAATGATTAGAGGCCTTGGG
GTTGAAACAACCTTAACCTATTCTCAAACTTTAAATATGTAAGAAGTCCTTGTTAC
TTAATTGAACG

8.1.4 Chaetomium globosum No. 827

>Z1828-4417BT

GGTGCTGCTTTCTGGTACGTCCCAGCAAAGCAAACACTCTTGGCTGATGACAATC
GAGACTGACTTCTTTTCAGGCAGACCATCTCTGGCGAGCACGGCCTCGACAGCAA
TGGCGTGTATGTGGGCATGACAGTTCCCAACCGATAAATCCCCGCTCACCGCTTC
GATAGGTACAACGGCACCTCCGAGCTCCAGCTCGAGCGTATGAACGTGTACTTCA

ACGAGGTCAGTCGGGTCAAATAATTTTACACGACCGAGTGATGGCGTGCTCACAG
TATTATACAGGCTTCCGGCAACAAGTATGTTCCTCGCGCTGTCCTCGTCGACTTGG
AGCCCGGCACCATGGATGCCGTCCGTGCCGGCCCCTTCGGCCAGCTCTTCCGCCC
GGACAACTTCGTCTTCGGCCAGTCGGGTGCCGGCAACAACTGGGCCAAGGGTC

>Z1828-4417RPB2

GCTGAGACCCCGAAGGCCAGGCTGCGGTCTCGTCAAAAACTTGTCACTGATGTGC
TACGTCAGTGTGGGCACCCCGCGGACCCGATCGTTGAGTTCATGATCGCCCGAGG
TATGGAAGTGCTCGAGGAGTACGAACCACTCCGATATCCGAACGCCACCAAGGT
GTTCGTAAACGGCACTTGGGTGGGTGTTCACCAAGACCCAAAGCATCTTGTCACG
CTGGTTCAGGGGCTGCGGAGAAAGAACGTTATCTCGTTTGAGGTTTCGCTCGTTA
GAGACATCCGCGACCGTGAGTTCAAGATCTTTTCAGATGCGGGTCGGGTGATGAG
GCCGCTGTTCACGGTGGAGCAAGAACCGAATGGCGAGAGCGGCGCTGAGATGGG
CGCACTGATCCTGAATAAGGATCATATTGGGCGCCTGAAGATGGACGCAGAGCT
GGGCAAATACCACCCGGACTACTGGGGCTGGCAAGGCCTGTTGAAGTCGGGCGC
TATTGAGTATCTTGATGCTGAGGAGGAGGAGACGGTCATGATCTGCATGACCCCC
CAGGATCTTGATCAGTTCCGTGCCCGCAAGATGGGAAGGATCGAGCCGGACAAC
TCCGGGTTGGGCAATAACCGGATCAAGACGAAACCAAATCCGACAACTCACATG
TACACGCACTGCGAGATCCATCCGAGCATGCTCCTCGGCATCTGCGCAAGCATCA
TCCCCTTTCCTGATCATAACCAATCGCCCAGGAACACATACCAGTCCGCTAT

8.1.5 Chrysosporium sp. No. 831

>Z1876-4466I

TCCGTAGGTGAACCTGCGGAAGGATCATTACAGTGTCTGGAGGCCGACCGGCGG
CGTTTCCCTCACGGGGAGCGTCGTGGCTCGTGCCCCCCCCCACACGTGTTTACTAC
ACCCTGTTGCCTTGGTGGGTCTGCCCTTGTGGCTGCCGGGGGTCACCGCGTGTGCC
CCGGGCCCGTACCCACCGATGGACACCCTGAACTCTTTATGAATATAGTGTTGTC
TGAGCGTTTAGCAAATTAAACAAAACTTTCAACAATGGATCTCTTGGTTCTGGCA
TCGATGAAGAACGCAGCGAAATGCGATAAGTAATGTGAATTGCAGAATTCCGTG
AATCATCGAATCTTTGAACGCACATTGCGCCCTCTGGTATTCCGGGGGGCATGCC
TGTTCGAGCGTCATTGCAACCCCTCAAGCACAGCTTGTGTGTTGGGCTCTCGTCCC

CTGTGGACGGGCCTGAAATGCAGTGGCAGCACCGAGATACCGGTGTCTGAGTGT
ATGGGCATTGATCATCACTCGATAGACCCGATCGGCGCTGACCGTCAAACCACGA
TTCCTCGGAATCATCCAGTTTTGACCTCGGATCAGGTAGG

8.1.6 Cladosporium allicinum No. 823

>Z1378-2864EF

TCATCGAGAAGTTCGAGAAGGTGAGCACTCTTCCGGCGCCTTGTTGTCTGGTCAT
CGATGCAATCTCTTCGCCCCACCAAGCCACCCCGCCTCGTCGCAATCTGCGATAA
GGTGTCTGACGCCTGGCTTGGCGAAGAACTTGTCTCTCGAGGGACAGACAGCACG
CCACCCACTCCTACCTGAACACATCACTGACAATTCACCACAGGAAGCCGCCGAG
CTCGGTAAGGGTCCTTCAAGTAA

>Z1378-2864ITS

TTACAAGAACGCCCGGGCTTCGGCCTGGTTATTCATAACCCTTTGTTGTCCGACTC
TGTTGCCTCCGGGGCGACCCTGCCTTCGGGCGGGGGCTCCGGGTGGACACTTCAA
ACTCTTGCGTAACTTTGCAGTCTGAGTAAACTTAATTAATAAATTAAAACTTTTAA
CAACGGATCTCTTGGTTCTGGCATCGATGAAGAACGCAGCGAAATGCGATAAGTA
ATGTGAATTGCAGAATTCAGTGAATCATCGAATCTTTGAACGCACATTGCGCCCC
CTGGTATTCCGGGGGGCATGCCTGTTCGAGCGTCATTTCACCACTCAAGCCTCGCT
TGGTATTGGGCAACGCGGTCCGCCGCGTGCCTCAAATCGTCCGGCTGGGTCTTCT
GTCCCCTAAGCGTTGTGGAAACTATTCGCTAAAGGGTGTTCGGGAGGCTACGCCG
TAAAACAACCCCATTTCTAAGGTTGACCTCGGATCAGGTAGGGATACCCGCTGAA
CTTAAGCATATCATA

8.1.7 Clonostachys rosea No. 821

>Z2328-2172 ITS

TCCGTTGGTGAACCAGCGGAGGGATCATTACCGAGTTTACAACTCCCAAACCCAT
GTGAACATACCTACTGTTGCTTCGGCGGGATTGCCCCGGGCGCCTCGTGTGCCCC
GGATCAGGCGCCCGCCTAGGAAACTTAATTCTTGTTTTATTTTGGAATCTTCTGAG

TAGTTTTTACAAATAAATAAAAACTTTCAACAACGGATCTCTTGGTTCTGGCATCG
ATGAAGAACGCAGCGAAATGCGATAAGTAATGTGAATTGCAGAATTCAGTGAAT
CATCGAATCTTTGAACGCACATTGCGCCCGCCAGTATTCTGGCGGGCATGCCTGT
CTGAGCGTCATTTCAACCCTCATGCCCCTAGGGCGTGGTGTTGGGGATCGGCCAA
AGCCCGCGAGGGACGGCCGGCCCCTAAATCTAGTGGCGGACCCGTCGTGGCCTCC
TCTGCGAAGTAGTGATATTCCGCATCGGAGAGCGACGAGCCCCCTGCCGTTAAAC
CCCCCAACTTTTCCAAGGT

8.1.8 Heydenia cf. alpina No. 824

>Z2259-3333ITS

TCCGTAGGTGAACCTGCGGAAGGATCATTAAAAAATATAGAATTAATCTTCTGTA
AACCCAATCTGCGTATTTCTACCTGTTGCTTTCGTGAGACTGTGAACGCAAGTTCC
CTCTGGCGCTGTTTTTAGGAACAGCTGTTGGGGAGTGCTCACGGGAGGTAATTAT
AAACTCTGTTTTTTTTGAATTTTGTCTGAATATTGTTTATACATAAACTTTAAAACT
TTCAACAACGGATCTCTTGGTTCTCGCATCGATGAAGAACGCAGCGAAATGCGAT
AAGTAGTGTGAATTGCAGAATTCAGTGAATCATCGAATCTTTGAACGCACATTGC
GCCTCCTGGTATTCCGGGAGGCATGCCTGTTCGAGCGTCATTAAAATCACTCAAG
CTTAGGTTTACCTATTGCTTGGTCTTGGAGATGGAAGCCAATTTATTGGAATCCTC
TTCGAAATTCAATGGCGAAGACCCTTGCTCTCCCAAGTGTAGTAATAACTTATGT
CACTGAAGGAAGCGAGAAATCTTCTGCCGTAACCCCCATATTTTCTATGATTGAC
CTCGGATCAGGTAGGGATACCCGCTGAACTTAAGCAT

8.1.9 Ilyonectria europaea No. 822

>Z2328-2173BL ITS

TCCGTTGGTGAACCAGCGGAGGGATCATTACCGAGTTTACAACTCCCAAACCCCT
GTGAACATACCATATTGTTGCCTCGGCGGTGCCTGTTTCGGCAGCCCGCCAGAGG
ACCCAAACCCTAGATTACATTAAAGTATCTTCTGAGTCAATGATTAAATCAATCA
AAACTTTCAACAACGGATCTCTTGGTTCTGGCATCGATGAAGAACGCAGCGAAAT
GCGATAAGTAATGTGAATTGCAGAATTCAGTGAATCATCGAATCTTTGAACGCAC
ATTGCGCCCGCCAGTATTCTGGCGGGCATGCCTGTCCGAGCGTCATTTCAACCCTC

AAGCCCCCGGGCTTGGTGTTGGAGATCGGCGAGCCCTCCGGGGCGCGCCGTCTCC
CAAATATAGTGGCGGTCCCGCTGTAGCTTCCTCTGCGTAGTAGCACACCTCGCAC
TGGGAAACAGCGTGGCCACGCCGTGAAACCCCCCACTTCTGAAAGGTTGACCTCG
GATCAGGTAGGAATACCCGCTGAACTTAAGCATAT

8.1.10 *Leucothecium* sp. No. 828

>Z1876-4468I

TCCGTAGGTGAACCTGCGGAAGGATCATTATCGAGCCGCCGACGCGGGCCCGCG
GTACTTCGGTGCCGTTGGGTCCCGTAGGCAAATGGCCCAACCCTTGCTTCTTGAC
AACCATTGTCTCGGCGGTACCGCGCCTTTCGGGGCCAGCTGGATTCATTCCGGCTT
GTGTCCGCCAGAGAACCATTAAAAATCGTTTATCAGATCGTCTAAGAATGAAATA
ATTCAATAAAACTTTCAACAACGGATCTCTTGGTTCCGGCATCGATGAAGAACGC
AGCGAAATGCGATAACTAATGTGAATTGCAGAATTCCGTGAATCATCGAGTCTTT
GAACGCACATTGCACCCTCTGGTATTCCGGGGGGTATATCTGTCCGAGCGTCATT
ACAACCTTAAAGCACGGCTTTTTATTGGATTCTAGTTCTGCTTCGGCGGGACAGGT
CCGAAATGGATTAATGACGTCGCGATTACCACGGAATCGAGCGAATGGAATCATT
AACGCTCTGATTTGAAGTGGCCGACGGTCTTCTGAAGCGGTCCTTTTGGATCGTCT
TTTTAACGGTTGACCTCGG

8.1.11 Metarhizium carneum No. 826

>Z1876-4469I

TCCGTTGGTGAACCAGCGGAGGGATCATTACCGAGTTTACAACTCCCAAACCCCC
TGTGAACTTATACCATTTACTGTTGCTTCGGCGGGTCATGGCCCCGGGGAAGGAC
AGCGGTCGCCGTCAGGCCTCAGCTGCCCGCCCCCGGAAACAGGCGCCCGCCGGG
GAACTCAAACTCTTCTGTATTTCTTTATCTAATATATACTGTCTGAGTAAAAACTA
AAATGAATCAAAACTTTCAACAACGGATCTCTTGGTTCTGGCATCGATGAAGAAC
GCAGCGAAATGCGATAAGTAATGTGAATTGCAGAATTCAGTGAATCATCGAATCT
TTGAACGCACATTGCGCCCGCCAGTATTCTGGCGGGCATGCCTGTTCGAGCGTCA
TTTCAACCCTCAAGTCCCCTGTGGACTCGGTGTTGGGGACCGGCGAGACAGCCGC
GGATCTTCTTCCGCAGCGAGTCGCCGCCCCCCAAATGACTTGGCGGCCTCGTCGC

GGCCCTCCTCTGCGTAGTATAGCACACCTCGCAACAGGAGCCCGGCGAATGGCCA
CTGCCGTAAAACCCCCCAACTTTTTCAGAGTTGACCTCGAATCAGGTAGGAATAC
CCGCTGAACTTAAGCATATA

8.1.12 Scopulariopsis brevicaulis No. 832

>Z1828-4419I

TCCGTTGGTGAACCAGCGGAGGGATCATTACCGAAGTTACTCTTCAAAACCCATT
GTGAACCTTACCTCTTGCCGCGCGTTGCCTCGGCGGGGAGGCGGGGTCTGGGTCG
GCGCGCCCCTCACCGGGCCGCCGTCCCCGTCCCCGTCCCCGCCGGCCGCGCCAAA
CTCTAAATTTGAAAAAGCGTACTGCACGTTCTGATTCAAAACAAAAAACAAGTCA
AAACTTTTAACAACGGATCTCTTGGTTCTGGCATCGATGAAGAACGCAGCGAAAT
GCGATAAGTAATGTGAATTGCAGAATTCAGTGAATCATCGAATCTTTGAACGCAC
ATTGCGCCCGGCAGCAATCTGCCGGGCATGCCTGTCCGAGCGTCATTTCTTCCCTC
GAGCGCGGCTAGCCCTACGGGGCCTGCCGTCGCCCGGTGTTGGGGCTCTACGGGT
GGGGCTCGTCCCCCCCGCAGTCCCCGAAATGTAGTGGCGGTCCAGCCGCGGCGCC
CCCTGCGTAGTAGATCCTACATCTCGCATCGGGTCCCGGCGAAGGCCAGCCGTCG
AACCTTTTATTTCATGGTTTGACCTCGGATCAGGTAGGGTTACCCGCTGAACTTAA
GC

>Z1828-4419EF2

GCGCCATTCTCATCATTGCTGCCGGTACTGGTGAGTTCGAGGCTGGTATCTCCAA
GGATGGCCAGACTCGTGAGCACGCTCTCCTCGCCTTCACCCTCGGTGTCAAGAAC
CTCATTGTCGCCATCAACAAGATGGACACTGCCAAGTGGTCCGAGGACCGCTACA
GGGAGATCATCAAGGAGACCTCCAACTTCATCAAGAAGGTCGGCTACAACCCTA
AGGCTGTTGCCTTCGTCCCCATCACTGGTTTCCACGGCGACAACATGATCCACGC
CTCCACCAACTGCCCCTGGTACAAGGGCTGGGAGCGTGAGGTCAAGTCGGGCAA
GCTCACCGGCAAGACCCTCCTCGAGGCCATCGACTCCATCGAGCCCCCCAAGCGT
CCTACCGAGAAGCCCCTCCGTCTTCCCCTCCAGGATGTCTACAAGATCGGTGGTA
TTGGCACGGTGCCCGTCGGCCGTATTGAGACCGGTGTCATCAAGCCCGGCATGGT
CGTCACCTTCGCCCCCTCCAACGTCACCACTGAGGTCAAGTCCGTCGAGATGCAC
CACGAGCAGCTTCCCGAGGGTGTCCCCGGTGACAACGTTGGTTTCAACGTGAAGA

ACGTCTCCGTCAAGGACATTCGCCGTGGTAACGTTGCCGGTGACTCCAAGAACGA
CCCCCCTATGGGCGCCGCGTCGTTCCAGGCTCAGGTCATCGTCCTCAACCACCCT
GGTCAGATCGGCGCCGGCTACGCGCCCGTTCTTGACTGCCACACTGCCCACATTG
CTTGCAAGTTCTCCGAGCTCCTTGAGAAGATCGACCGCCGTACCGGTAAGTCGGT
TGAGAACAACCCCAAGTTCGTCAAGTCGGGTGACGCTGCCATCGTCAAGATGGTT
CCCTCCAAGCCCATGTGCGTTGAGGCCTTCACCGAGTACCCCC

8.2 ^{1}H and ^{13}C NMR data of isolated metabolites

8.2.1 1D and 2D NMR spectra of Heydenoic acid A (1)

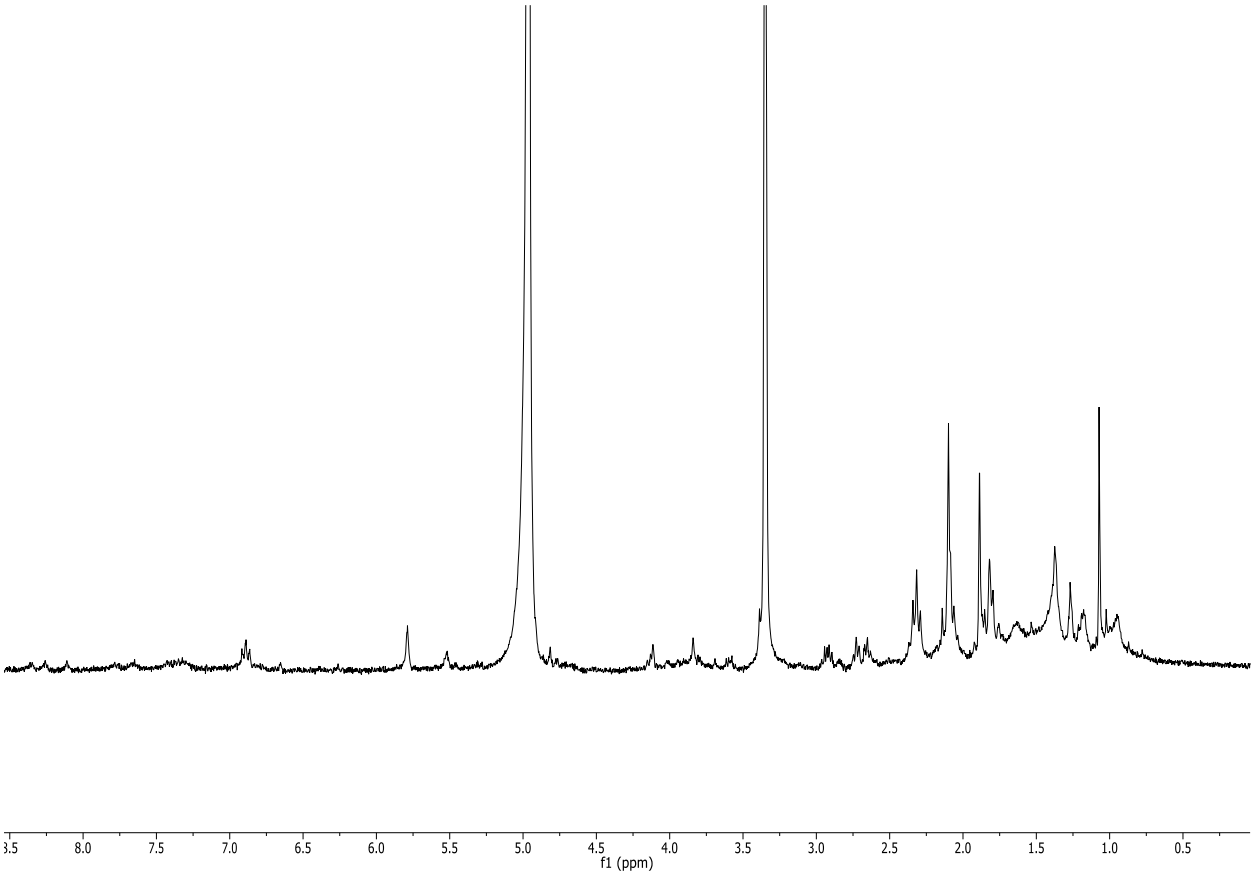

Figure 8.1 ^{1}H NMR of Heydenoic acid A (1) (300MHz, in MeOD).

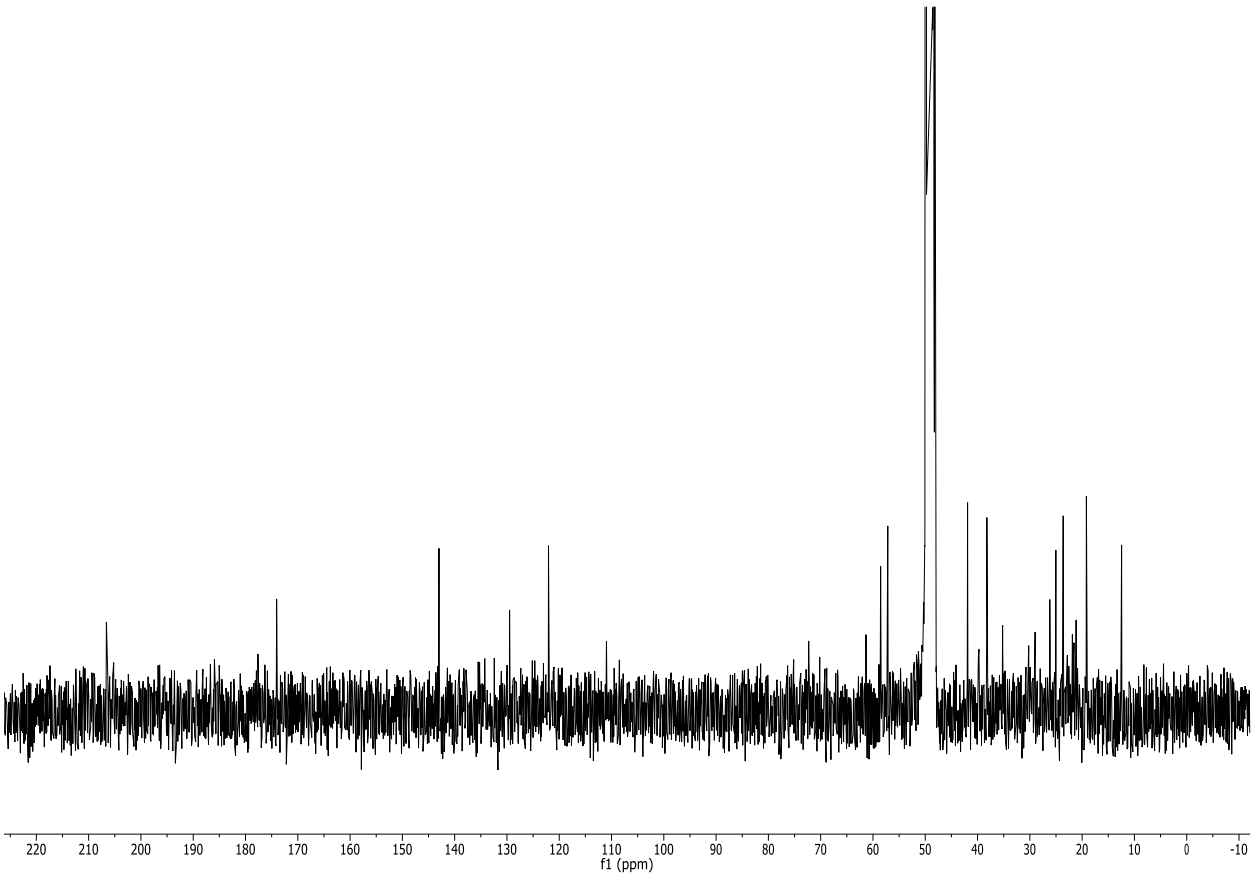

Figure 8.2 ^{13}C NMR of Heydenoic acid A (1) (75MHz, in MeOD)

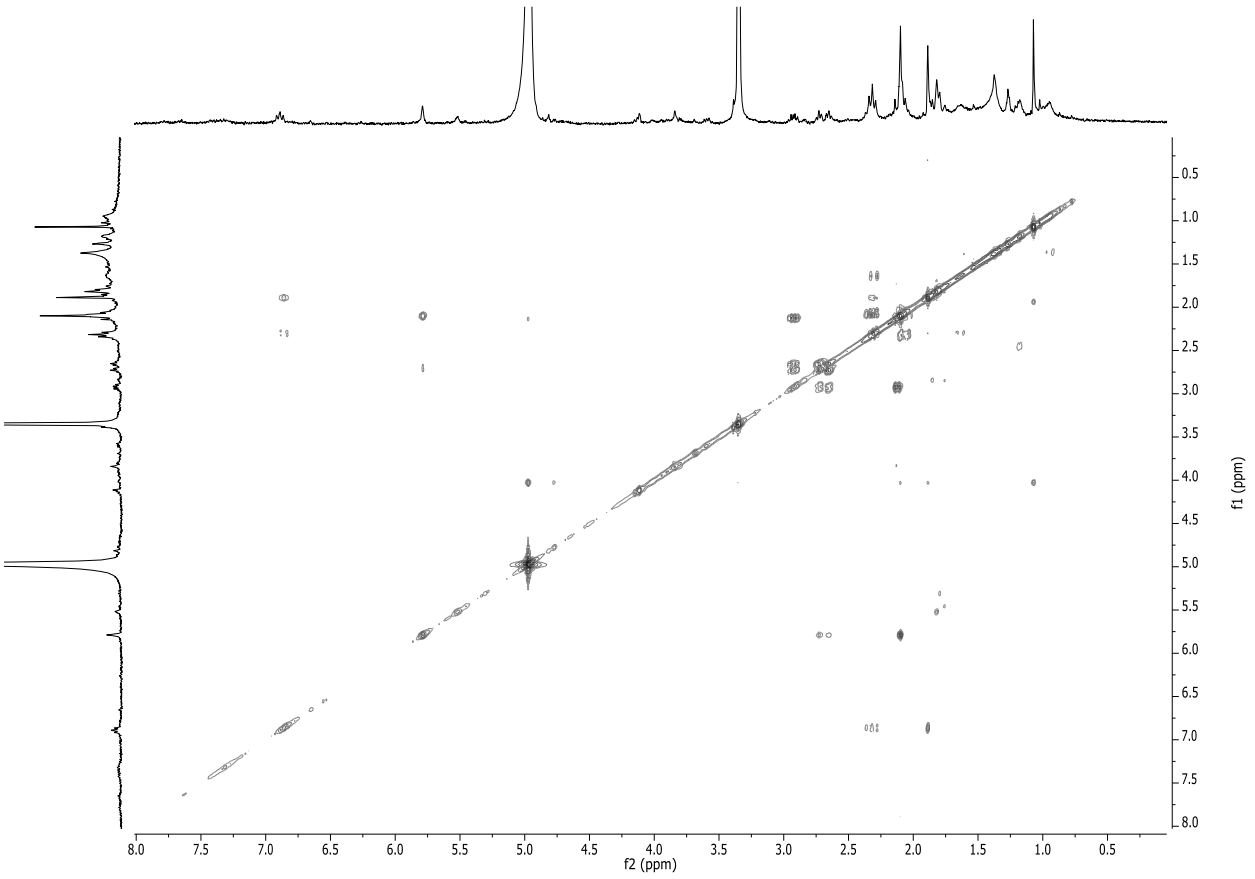

Figure 8.3 ^{1}H- ^{1}H COSY spectrum for Heydenoic acid A (1) in MeOD

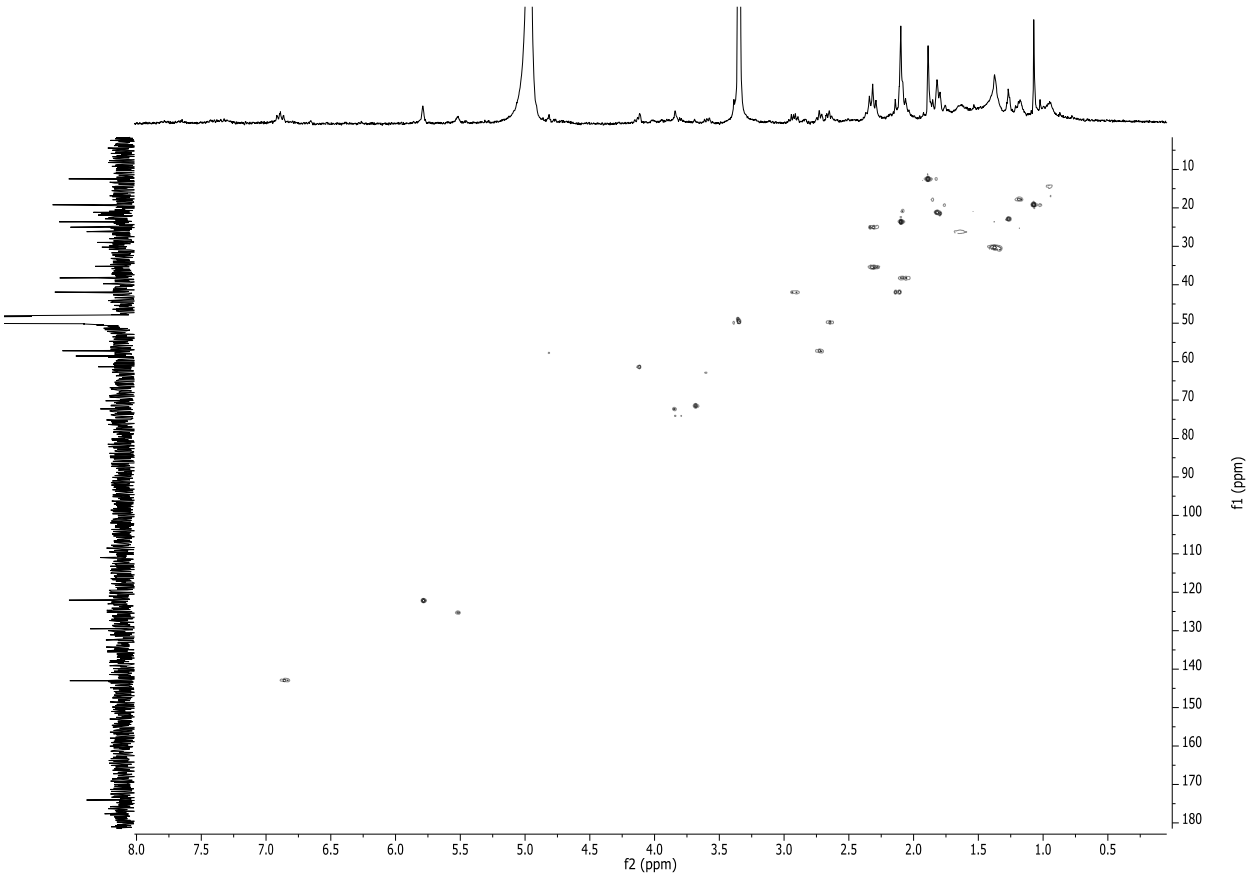

Figure 8.4 HSQC spectrum for Heydenoic acid A (1) in MeOD

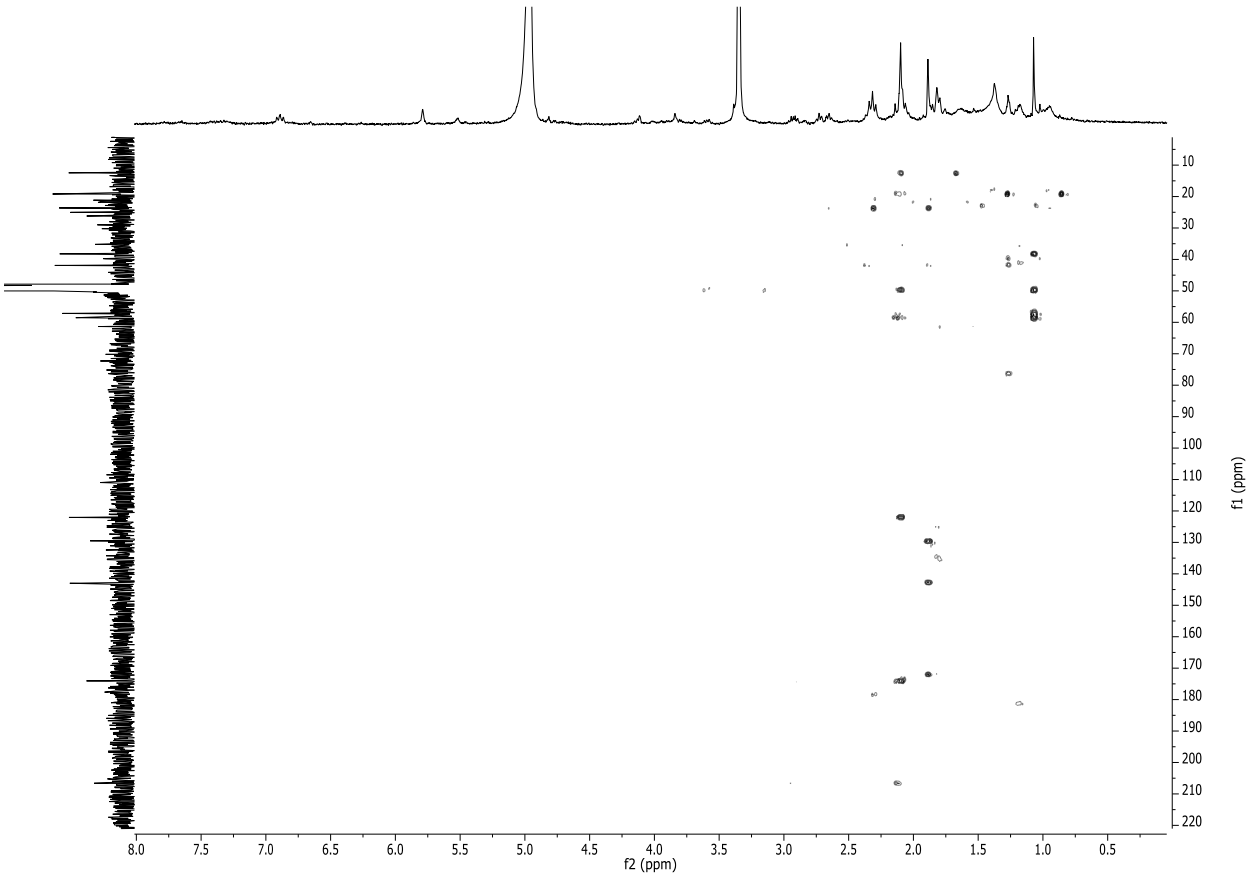

Figure 8.5 HMBC spectrum for Heydenoic acid A (1) in MeOD

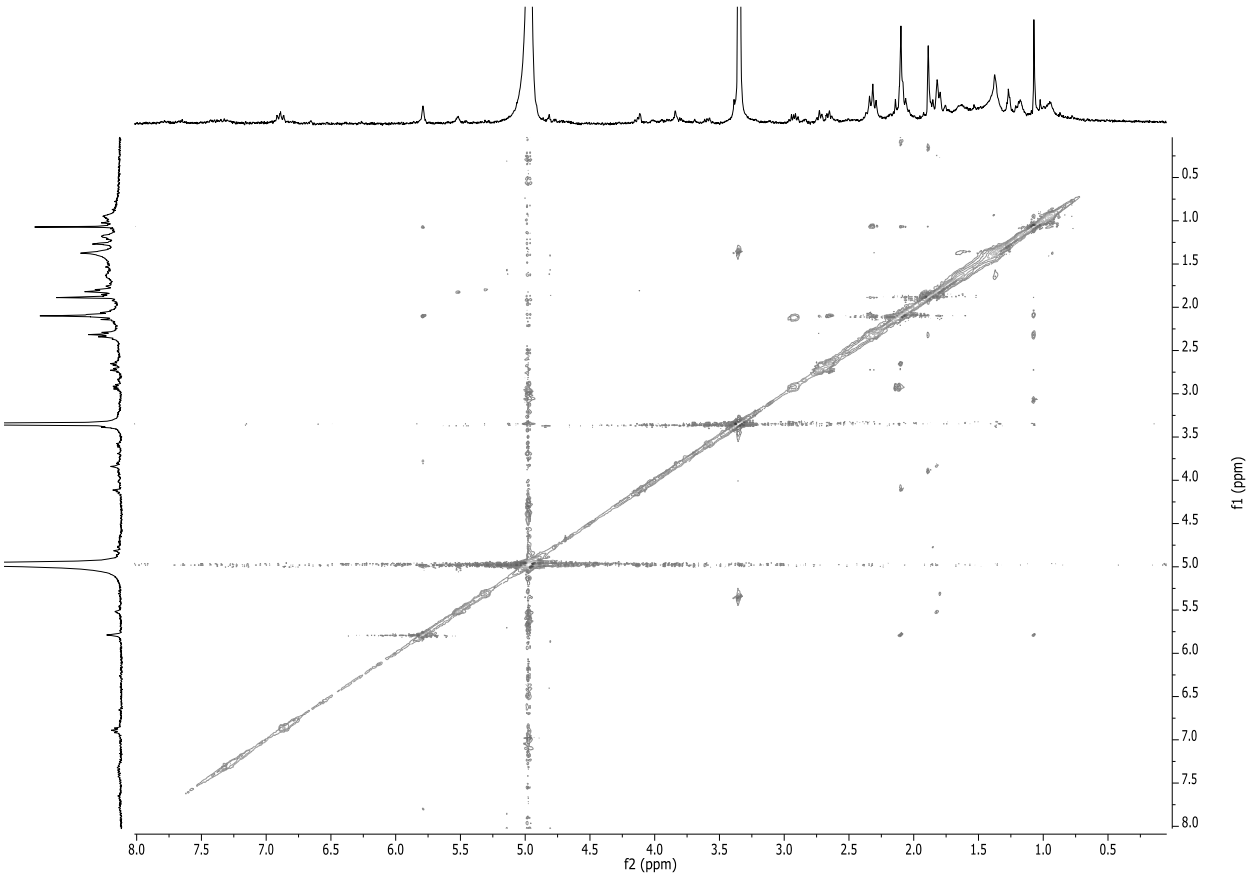

Figure 8.6 NOESY spectrum for Heydenoic acid A (1) in MeOD

8.2.2 1D and 2D NMR spectra of Heydenoic acid B (2)

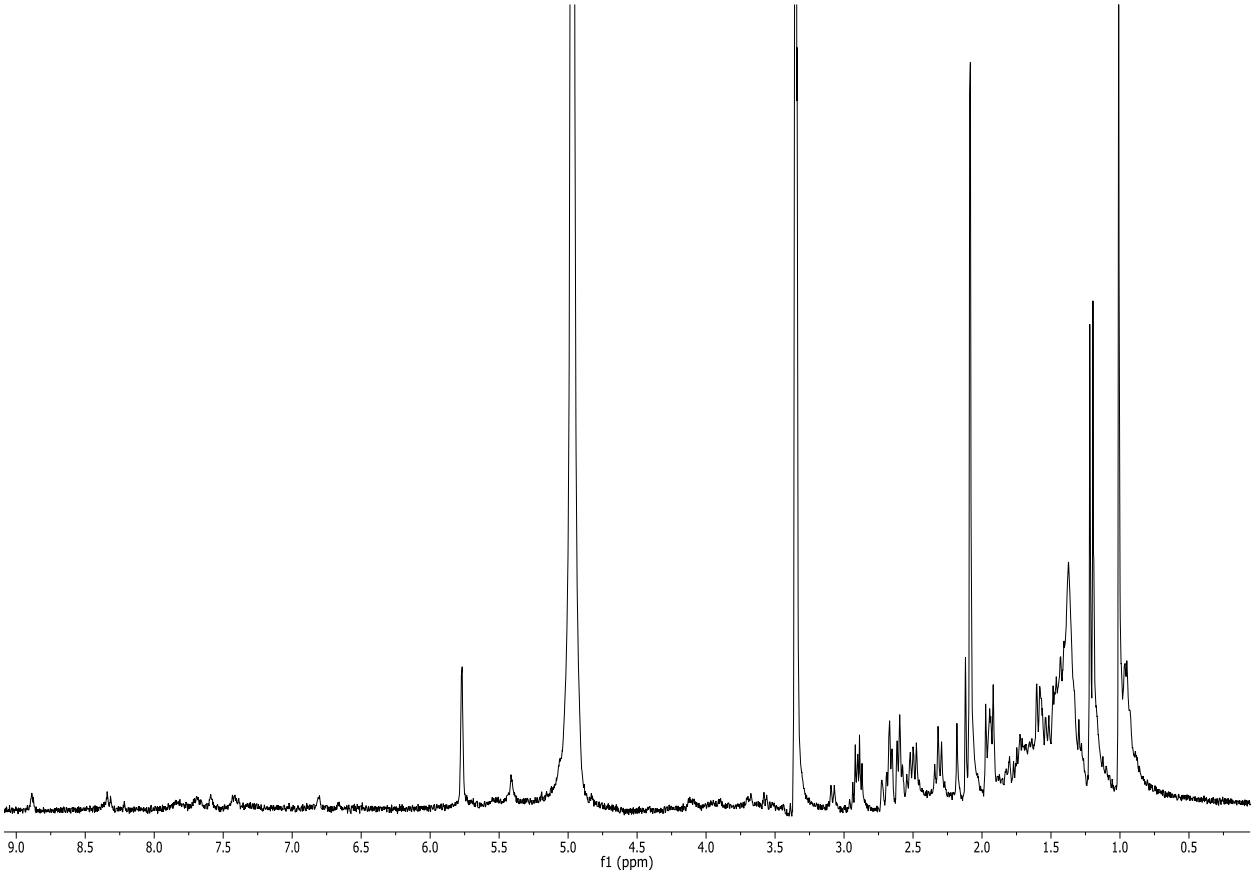

Figure 8.7 ^{1}H NMR of Heydenoic acid B (2) (300MHz, in MeOD)

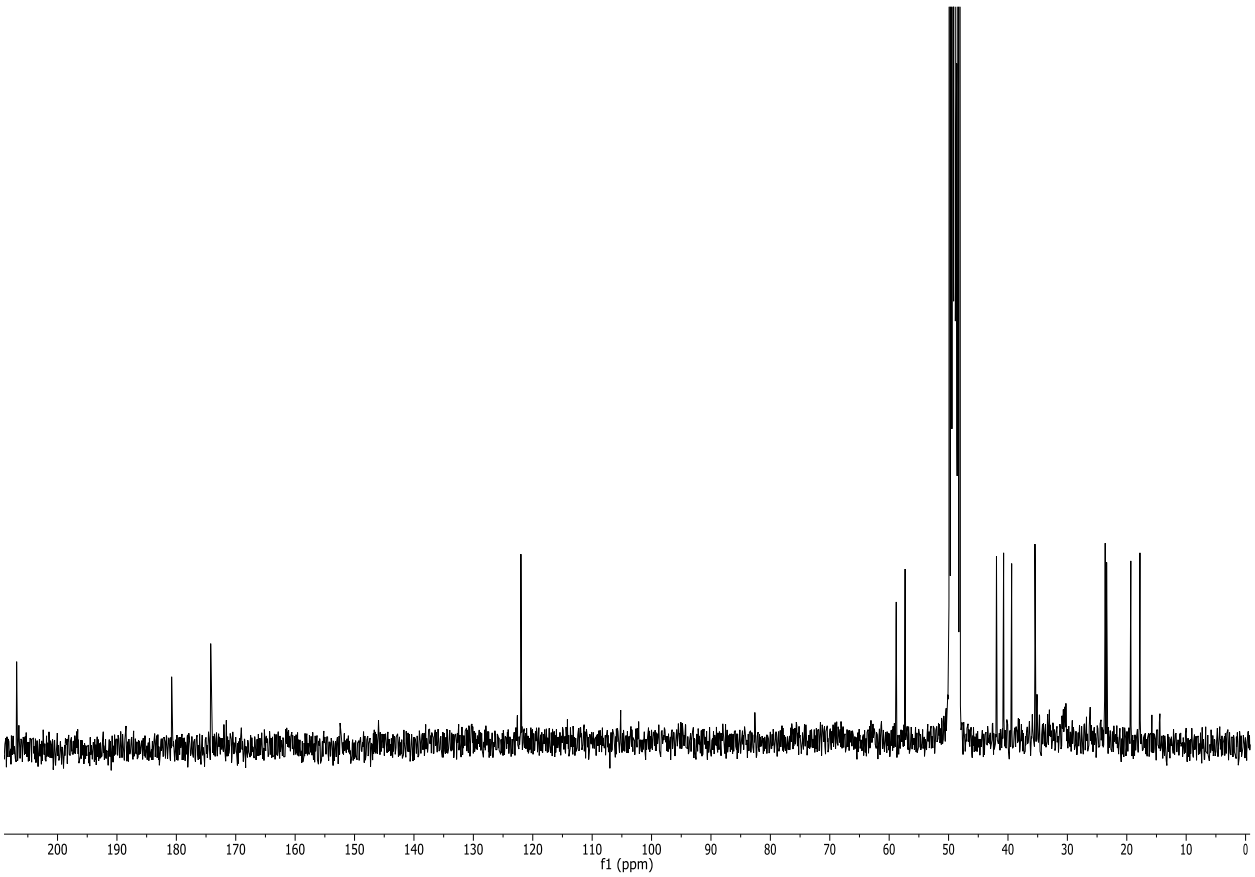

Figure 8.8 ^{13}C NMR of Heydenoic acid B (2) (75MHz, in MeOD)

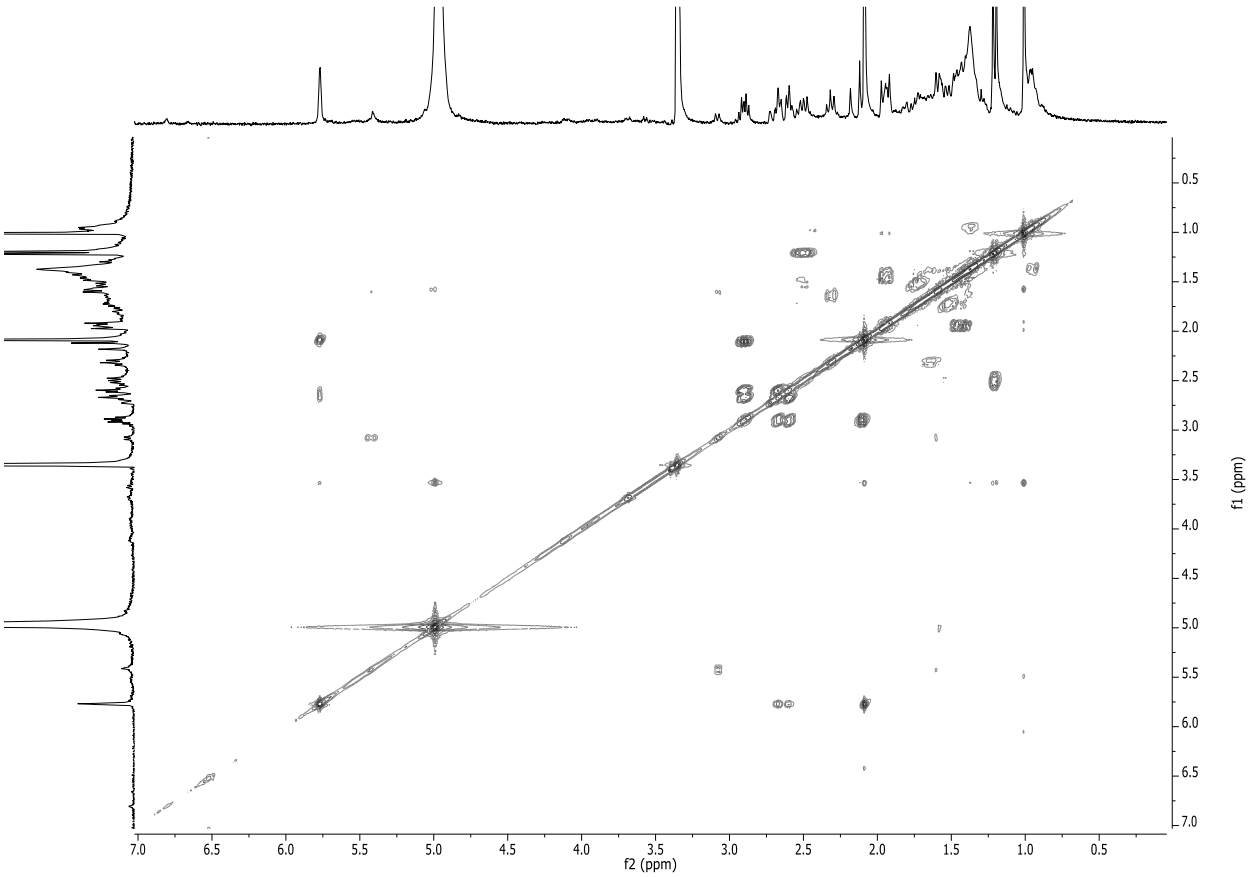

Figure 8.9 ^{1}H- ^{1}H COSY spectrum for Heydenoic acid B (2) in MeOD

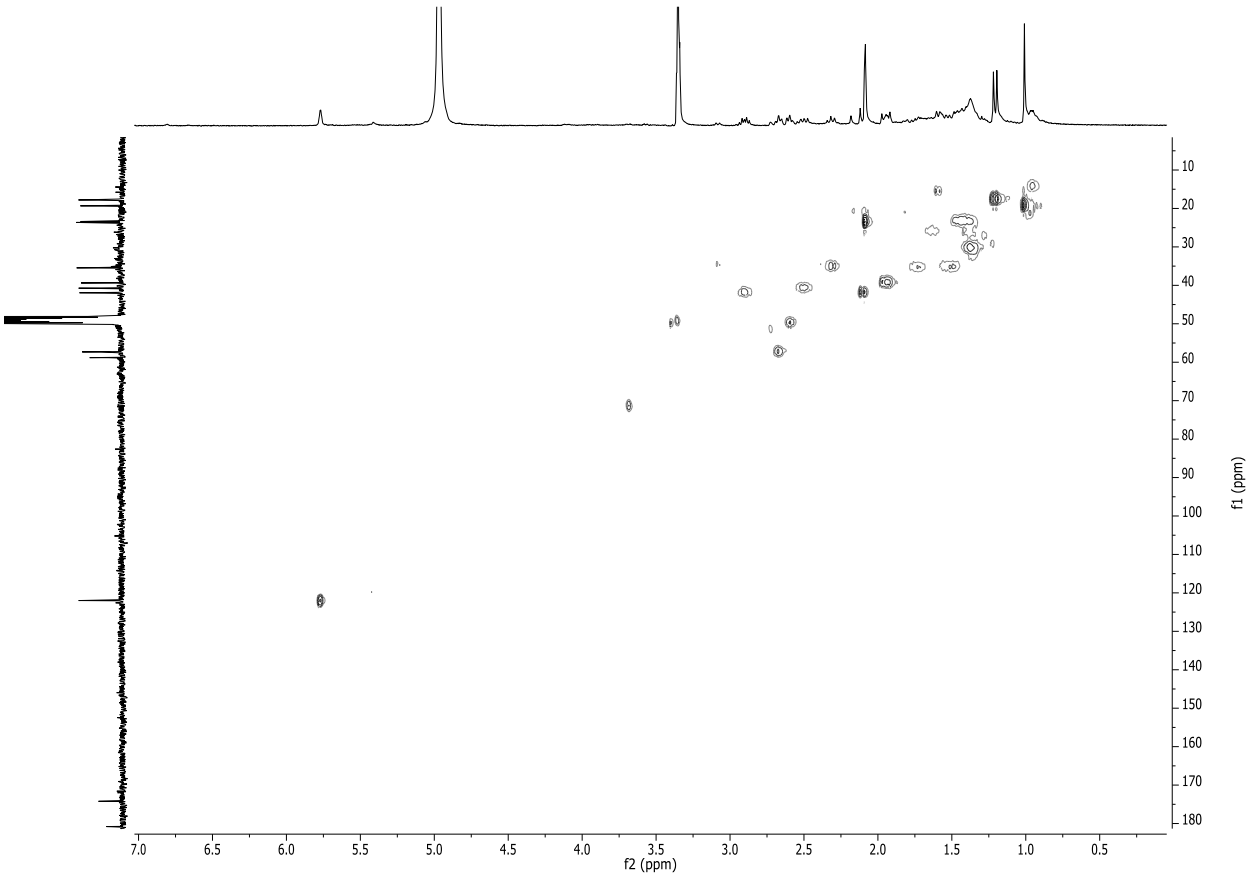

Figure 8.10 HSQC spectrum for Heydenoic acid B (2) in MeOD

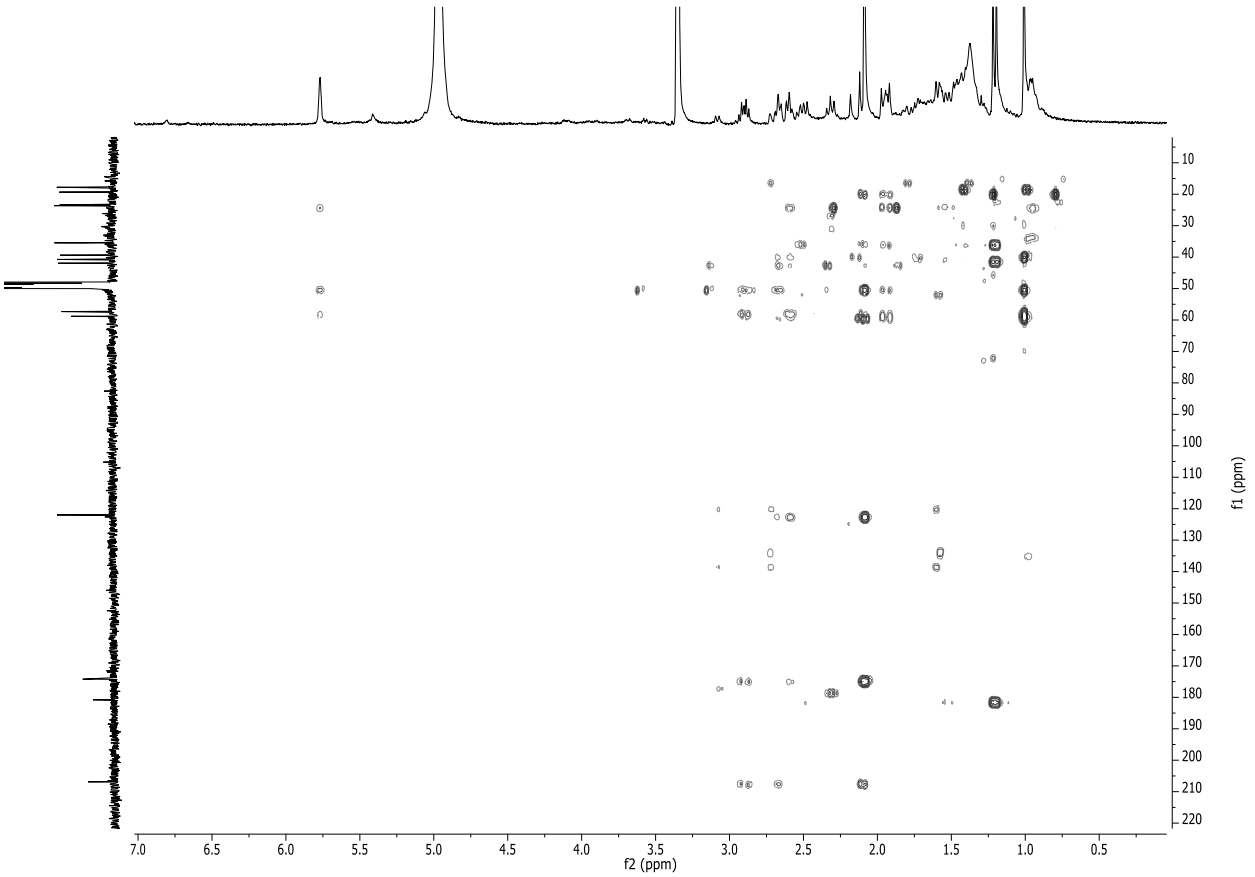

Figure 8.11 HMBC spectrum for Heydenoic acid B (2) in MeOD

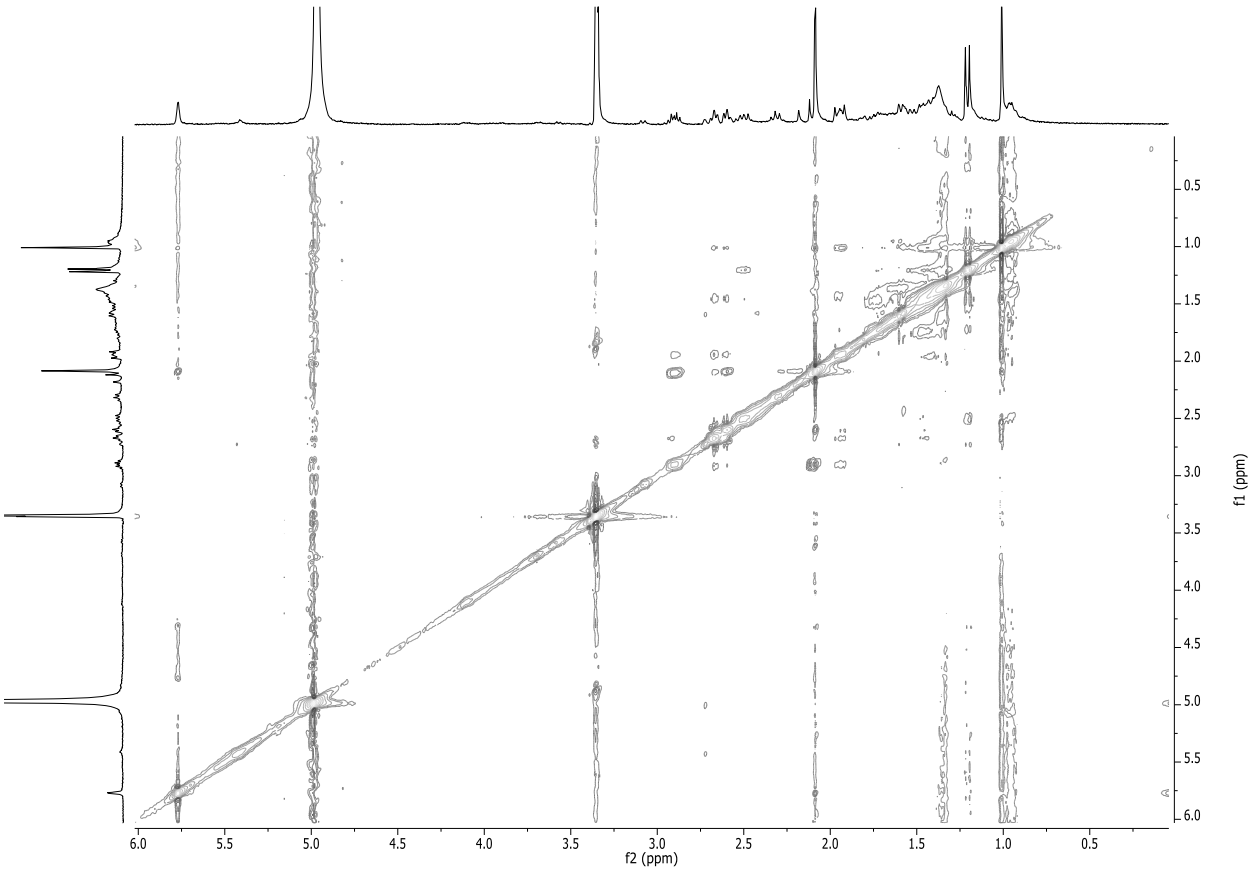

Figure 8.12 NOESY spectrum for Heydenoic acid B (2) in MeOD

8.3 Tables from salinity dependency experiments

Table 8.1 Salinity dependency of the growth of *Cladosporium allicinum* on agar plates.

	colony diameter after 14 days [mm]					
Salinity	plate 1	plate 2	plate 3	$\bar{x}$	σ^2	σ
0‰	55	53	54	54	1	±1
7‰	74	71	71	72	2	±1
14‰	90	87	89	89	2	±1
21‰	94	92	89	92	4	±2
28‰	106	106	108	106	1	±1
35‰	107	108	111	109	3	±2

Table 8.2 Salinity dependency of the growth of *Heydenia* cf. *alpina* on agar plates.

	colony diameter after 14 days [mm]					
Salinity	plate 1	plate 2	plate 3	$\bar{x}$	σ^2	σ
0‰	68	66	67	67	1	±1
7‰	123	125	123	124	1	±1
14‰	130	130	130	130	0	±0
21‰	130	130	130	130	0	±0
28‰	130	130	130	130	0	±0
35‰	130	130	130	130	0	±0

σ = standard deviation